Belg. J. Zool. - Volume 127 (1997) - issue 1 - pages 3-11 - Brussels 1997

THE 37 LRP/P40 POLYPEPTIDE: A MULTIFUNCTIONAL PLEIOTROPIC MOLECULE INVOLVED IN TUMORIGENESIS AND METASTASIS

A REVIEW

NATHALIE CLAUSSE, PASCALE JACKERS AND VINCENT CASTRONOVO

Metastasis Research Laboratory, University of Liège,
Tour de Pathologie 1-B23, Sart Tilman, B-4000 Liège (Belgium)
e-mail: vcastronovo@chu.ulg.ac.be

Key words: metastasis, multifunctional protein, laminin receptor, ribosomal protein.

Abstract. A cDNA coding for a 37 kDa polypeptide has been the center of major interest since it is consistently up-regulated in several cancers in association with the metastatic phenotype of the lesion. Furthermore, this polypeptide displays intriguing multifunctional properties as it has been cloned both as the metastasis-associated 67kD membrane-associated laminin receptor precursor (37 LRP) but also as a cytoplasmic ribosomal-associated protein p40. Isolation of the gene coding for the 37 LRP/p40 peptide in humans and birds, analysis of their structures and extensive amino-acid comparison between available species sequences have brought new topological arguments in favor of a multifunctional role for this protein in cells. Indeed, both genes display characteristics of house-keeping genes and in particular of ribosomal protein -encoding genes. Comparison between all 37LRP/p40 amino-acid sequences identifies a particularly well conserved region in the center of the protein in all organisms. This central part of the protein is the only region similar to the parentally linked RS2 prokaryotic ribosomal protein. In contrast, the carboxy terminal end of the protein is highly variable in all organisms until the vertebrates appear. As vertebrates are the only organisms in which a 67 LR molecule has been clearly described, it is suggested that this region of the molecule supports a new function *i.e* the ability to be included into the 67 kD cell surface laminin receptor. This hypothesis is further sustained by the fact that the carboxy-terminal end of the protein is precisely encoded by the last two exons. An evolutionary scenario is proposed in which the 37 LRP/p40 molecule has always had a function as a ribosome-associated protein, encoded by the central highly conserved region. In the course of evolution, an additional function linked to the carboxy terminal end of the protein would have developed in organisms in which cell-matrix interactions became more complex.

Cancer, metastasis and the 67 kDa laminin receptor

Metastasis is the major cause of mortality and morbidity in cancer. Metastasis formation is a process which involves complex interactions between metastatic cells and the sur-

Invited contribution to the 3th Benelux Congress of Zoology, Namur, November 1996.

rounding tissue. Indeed, in order to metastasize cancer cells have to aquire the ability to leave the initial tumor, migrate into the surrounding tissue, enter a blood or lymphatic vessel, survive in the blood stream or lymph and finally leave the vessel again to invade and proliferate within a target organ (Fig. 1). In the course of this process, metastatic cells have to several times cross the physiological inter-tissue barriers called basement membranes (CASTRONOVO,1993; FLUG & KÖPF-MAIER,1995). Therefore understanding of the interactions between basement membranes and cancer cells is of major interest since inhibiting this process could potentially lead to efficient treatment against this critical step in cancer development.

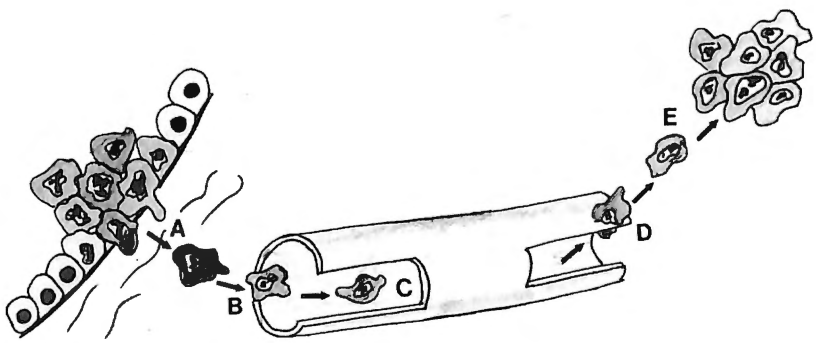

Fig. 1. – Schematic representation of the metastatic cascade. Cancer cells have to leave the initial tumor and migrate into the surrounding tissue (a), enter blood or lymphatic vessels (b), survive into the blood or lymph stream (c), leave the vessel (d), migrate to the target organ (e) and form a secondary colony.

Crossing of basement membranes by cancer cells has been schematically divided into three steps: attachment, degradation and migration (LIOTTA *et al.*,1986). Several laboratories have searched for cellular receptors which could play a role in the initial attachment step of cancer cells to one of the major components of basement membrane, laminin. The first molecule isolated which was able to bind to laminin is a molecule of 67 kD thereafter named the 67kD laminin receptor (67LR) (LESOT *et al.*,1983; MALINOFF & WICHA,1983; RAO *et al.*,1983). Since that time, several other molecules able to bind laminin have been isolated such as members of the integrin family and lectins (CASTRONOVO,1993). However, the 67 LR remains the center of major interest since it has been shown to be over-expressed in several solid tumors such as breast, colo-rectal, gastric and cervical carcinoma in correlation with the invasive and metastatic phenotype (CAMPO *et al.*,1992; CASTRONOVO *et al.*,1992; CIOCE *et al.*, 1991; GASPARINI *et al.*,1995; KONDOH *et al.*,1992; MARTIGNONE *et al.*,1992, 1993; PELLEGRINI *et al.*,1995; SOBEL,1993). The association between 67LR over-expression and cancer progression suggests that the 67 LR might play a role in tumor progression. Therefore, isolation and cloning of the 67LR coding gene and cDNA became a priority.

Cloning of the 37 kDa laminin receptor precursor cDNA

Cloning of the 67 LR encoding cDNA was initially performed using an anti-67 LR antibody which has the interesting functional property of blocking the adhesion of laminin onto the surface of cancer cells. This antibody has been used to screen a human umbilical vein cDNA expression library and led initially to isolation of an incomplete cDNA (WEWER *et al.*,1986). Further work resulted in isolation of a complete cDNA sequence from both mice and humans (RAO *et al.*,1989; YOW *et al.*,1988). Intriguingly, the length of this cDNA allows to encode a polypeptide of a deduced molecular weight of only 37 kD. This discrepancy between the size of the 67 LR and the size of the product encoded by its putative cDNA suggested post-translational modifications. The absence of potential N-glycosylation sites in the cDNA sequence as well as failure to stain the 67 LR with PAS and the maintenance of the 67 kD size of the molecule after neuraminidase, o-glycanase or Endo-F glycosidase treatment allow a glycosylation step to be eliminated as the major cause of size increase (CIOCE *et al.*,1993; LANDOWSKI *et al.*,1995). On the other hand, treatment of the 67 LR by reducing agents does not lead to a diminution of the 67 LR size, eliminating the hypothesis of a possible non-covalent multimeric molecule. Recently, it has been suggested that the 67 LR might be acylated by the fatty acids palmitate, oleate and stearate (LANDOWSKI *et al.*,1995). These fatty acid could be covalently associated with the protein via ester linkage suggesting that the 37 LRP can dimerize with itself or with another peptide to form the 67 LR. However, such suggestions still need further experimental evidence and the molecular mechanisms responsible for the increase in size of the 37 kD molecule into a 67 kD molecule remain unclear so far. Nevertheless, several experiments suggest a precursor/product relationship between the 37 kD molecule encoded by the cDNA and the 67 kD laminin receptor. Indeed, immunoprecipitation with antibodies directed against synthetic peptides derived from the 37 kD encoding cDNA allow precipitation of both the 37 kD and the 67 LR molecules. Further, pulse-chase experiments reveal the disappearance of a 37 kD polypeptide concomitant with appearance of the 67 LR (CASTRONOVO *et al.*,1991). Microsequencing of two peptides from the 67 LR gave a sequence of eight amino-acids identical to a portion of the 37 kD molecule (WEWER *et al.*, 1986). Finally, transfection of the 37 kD cDNA tagged with 6 additional histidines and with an artificially added phage epitope led to the recovery of a tagged 67 kD molecule which is able to bind laminin and is localized at the cell surface (MONTUORI *et al.*, pers. comm.). These observations are all consistent with a precursor/product relationship between the two molecules and led to the 37 kD molecule being called the laminin receptor precursor (37 LRP).

Interestingly, the cDNA coding for this 37 LRP molecule has been cloned by others as a cytoplasmic protein, in particular as the mouse ribosome-associated protein p40 (MAKRIDES *et al.*,1988; ROSENTHAL & WORDEMAN,1995; TOHGO *et al.*, 1994). In addition, search for homology between sequences from an archebacterium and all published sequences reveals that the 37 LRP deduced amino-acid sequence is homologous at 40% with the prokaryotic ribosomal protein RS2 (OUZONIS *et al.*,1995). This new putative role for the 37 LRP cDNA raises several questions and invites further investigations in order to better understand the role of this intriguing molecule in cells. In that perspective we decided to clone the gene coding for this 37LRP/p40 cDNA in order to better understand

its position either in a house-keeping gene family or as a tightly regulated gene. In addition we have conducted an extensive amino-acid sequence comparison between 37 LRP/p40 cDNA from all species already described and a new sequence that we have recently cloned in the laboratory from chicken spleen cDNA (CLAUSSE *et al.*,1996). This avian sequence is consistant with available mammalian sequences and thus extends the comparison more widely within the vertebrates.

The 37 LRP/p40 gene family

The 37 LRP/p40 gene has been cloned both from human and chicken DNA. The cloning of the human gene has been hampered by the presence in the human genome of around 26 copies of pseudogenes. These pseudogenes have been characterized in our laboratory (JACKERS *et al.*,1996a). They are highly homologous to the active gene but are interrupted by several stop codons. These pseudogenes have no intronic sequence, they are terminated by a polyA-tail and flanked by direct repeated sequences. These characteristics suggest that they probably arose by retroposition events. A PCR-based strategy produced a specific intronic probe and allowed us to specifically isolate the active human gene copy (JACKERS *et al.*,1996b). By contrast, the chicken appears to be the only organism in which the 37LR/p40 gene exists as a single copy. We were therefore able to isolate in parallel by a classical cloning technique the avian version of the 37LRP/p40 active chicken gene (CLAUSSE *et al.*,1996). Both genes are spread onto 6 kb of genomic DNA and are split into 7 exons with an initial short non-coding exon (Fig. 2). They have no classical TATA-box. Rnase protection and primer extension experiments reveal at least two transcriptional start sites located in a pyrimidine-rich tract. These features are characteristic of house-keeping genes and more particularly of genes encoding ribosomal proteins. Interestingly, in the intron 4 the human gene contains a region coding for a small nucleolar RNA E2. Finally, chromosomal hybridization localized the human 37 LRP/p40 gene to 3p21.3 band, a chromosomal locus frequently involved in rearrangements associated with cancer.

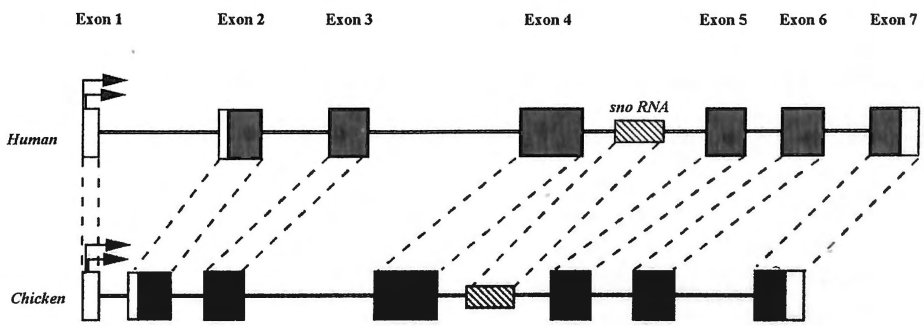

Fig. 2. – Schematic representation of the human (a) and chicken (b) gene structure. Exons are depected by boxes. Mutltiple transcriptional start sites are represented by horizontal arrows. Coding region is hatched. The position of the human encoding small nucleolar RNA sequence is represented by a grey box.

The 37 LRP/p40: a multifunctional protein

The 37 LRP cDNA has been cloned in 17 different species including mammals such as human, rat, bovine, mouse, and hamster, birds, insects, urchin, hydra, higher plant as arabidopsis, fungus and yeast. Comparison of the deduced amino-acid sequences from each cDNA reveals an extremely high degree of conservation throughout evolution. However, when these different sequences are carefully aligned to each other it appears that the conserved region is restricted to the central part of the molecule from amino-acid 20 to amino acid 209 whereas the carboxy-terminal end of the molecule varies between species until the appearance of vertebrates (CLAUSSE *et al.*,1996) (Fig. 3). Indeed, since birds and mammals diverged in evolution, *i.e.* 300 millions years ago, this carboxy-terminal end of the protein has been extremely well conserved. It appears that a high selective pressure has been applied to this region of the protein in vertebrates only. It is therefore tempting to speculate that, in vertebrates, a specific function might be located in that region of the protein which would explain this contrasting «sudden» sequence «freezing» arising in vertebrates. As a 67LR molecule related to the 37LRP/P40 has been clearly described in vertebrates only, we suggest that this carboxy-terminal end of the molecule would be responsible for the yet undefined post-translational events leading to the 67 LR. In favor of this hypothesis is the alignment of the gene structure with sequence comparison. Indeed, this superposition reveals that this vertebrate conserved carboxy-terminal region corresponds exactly to exons 6 and 7 (Fig. 4). The existence in vertebrates of a specific function in that particlar region would be in accordance with the widely held theory that exons are function depositary elements serving as basic building blocks to diversify and modulate protein function during evolution (BLAKE,1979; Blake,1983). To go further in this analysis, we have aligned the parentally linked prokaryotic RS2 ribosomal protein sequences with the 37 LRP/p40 amino-acids deduced sequences (DAVIES *et al.*,1992). To our surprise, it appears that although the RS2 proteins are longer in size than the central conserved part of the 37 LRP/p40 (257 and 209 amino-acid respectively), the best alignment was obtained by creating a gap of 49 amino-acids in the 37LRP/P40 in order to confine the entire RS2 sequence in this central conserved region (Fig.4). Moreover, it appears that the two consensus RS2 motif signatures described in RS2 proteins are present in all 37LRP/P40 sequences available with the only exception of one tryptophane. These observations led us to suggest that the 37LRP/P40 molecule might play two functions in cell: a cytoplasmic ribosomal-associated function played by the central part of the protein, conserved since archebacteria and efficient in all organisms, and since vertebrates, a cell surface role as a laminin receptor when incorporated into the 67 kD laminin receptor via its carboxy terminal end. We proposed an evolutionary scenario for this molecule: originally involved in translation, a vital function for cell biology, the protein could have aquired new properties *i.e.* as a building block of a receptor, in the course of evolution to accomodate the new extracellular matrix protein, laminin. This potential multifunctional role for a protein is not unique. Indeed, a rather similar situation has been described for eye lens crystalline in which one gene product has either a sructural role in the refractive properties of the lens or a house-keeping enzyme role when associated in dimeric molecule (HENDRICKS *et al.*,1988; WISTOW *et al.*,1988). Other examples illustrate possible multiple functions for ribosomal protein. Indeed, when associated in a multimeric protein by trans-

glutamination, the S19 ribosomal protein would play the role of a chemotactic agent for macrophages at the site of inflamation (NISHIURA *et al.*,1996). In the same perspective, galectin-3 a human lectin originally isolated as a cell surface laminin binding protein has lately been described as a nuclear protein involved in mRNA splicing mechanism (DAGHER *et al.*,1995). Such a dual fate for a single gene product might constitute a parsimonious means of protein function diversification during evolution.

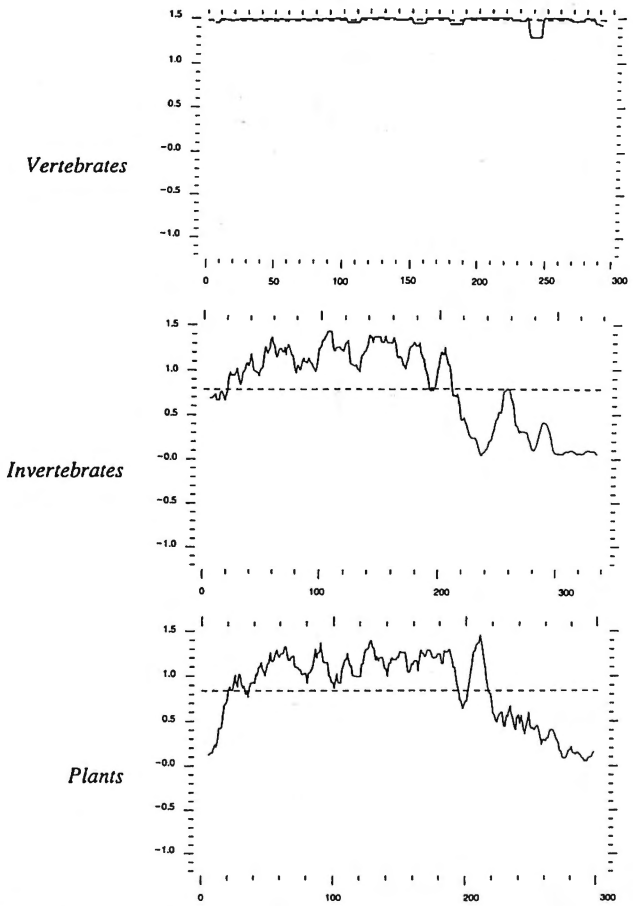

Fig. 3. – Amino acid similarity between all 37 LRP/p40 cDNA protein sequences deduced from all species described. Similarity between amino-acis (vertical axis) has been calculated for each amino-acid position (horizontal axis) according to the Burgess table by the GCG programm using the Plotsimilarity function after alignment with Pileup function (DEVEREUX *et al.*,1984). Maximum similarity of 1.5 represents identical amino-acids. The mean value is represented by a dotted line crossing the graph. Homology is therefore significant when the line is above the mean value whereas no significant homology is when the value is below the mean value. The vertebrate group includes chicken, bovine, mouse, hamster, rat and human sequences. Invertebrates include the insect *Drosophila*, two urchin species *Urechis caupo* and *Tripneustes gratilla*, the hydra *Chlorohydra viridissima* and the cestode *Echinococcus granulosus* sequences. Plants include the higher plant *Arabidopsis thaliana*, the fungus *Pneumocystis carinii*, and the yeast *Saccharomyces cerevisiae.*

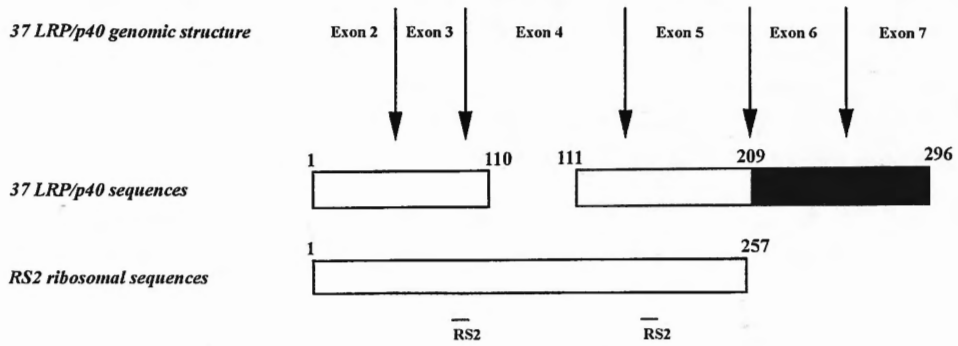

Fig. 4. – Schematic alignment of 37 LRP/p40 sequences with parentally linked RS2 ribosomal protein sequences. Position of the exons are shown at the top of the figure relative to the deduced amino-acids sequences from 37 LRP/p40 sequences. The hatched box represents the region conserved only in vertebrates. The gap in the 37 LRP/p40 sequences is created to obtain the best alignment with RS2 sequences shown below. RS2 signature positions are represented by horizontal lines under the scheme. Numbers on top of each sequence reflect amino-acid positions.

REFERENCES

BLAKE, C. (1979) – Exons encode protein functional units. *Nature,* **277**: 598-600.

BLAKE, C. (1983) – Exons-present from the beginning. *Nature*, **306**: 535-537.

CAMPO, E., C. MONTEAGUDO, V. CASTRONOVO, A.P. CLAYSMITH, P.L. FERNANDEZ & M.E. SOBEL (1992) – Detection of laminin receptor mRNA in human cancer cell lines and colorectal tissues by in situ hybridization. *Am J Pathol.*, **141**: 1073-83.

CASTRONOVO, V. (1993) – Laminin receptors and laminin-binding proteins during tumor invasion and metastasis. *Invasion and metastasis,* **13**: 1-30.

CASTRONOVO, V., E. CAMPO, F. VAN DEN BRULE, A.P. CLAYSMITH, V. CIOCE, F.-T. LIU, P.L. FERNANDEZ & M. E. SOBEL (1992) – Inverse modulation of steady-state messenger RNA levels of two non-integrin laminin-binding proteins in human colon cancer. *J. Natl.Cancer Inst.,* **84**: 1161-1169.

CASTRONOVO, V., A. P. CLAYSMITH, K.T. BARKER, V. CIOCE, H.C. KRUTZSCH & M.E. SOBEL (1991) – Biosynthesis of the 67 kDa high affinity laminin receptor. *Biochem Biophys Res Commun*, **177**: 177-83.

CIOCE, V., V. CASTRONOVO, B.M. SHMOOKLER, S. GARBISA, W.F. GRIGIONI, L.A. LIOTTA & M.E. SOBEL (1991) – Increased expression of the laminin receptor in human colon cancer. *J Natl Cancer Inst.*, **83**: 29-36.

CIOCE, V., I. M. MARGULIES, S. M.E. & V. CASTRONOVO (1993) – Interaction between the 67kDa laminin receptor and laminin. *Kidney Int.,* **43**: 30-37.

CLAUSSE, N., P. JACKERS, P. JARES, B. JORIS, S. M.E. & V. CASTRONOVO (1996) – Identification of the active gene coding for the metastasis-associated 37 LRP/p40 multifunctional protein. *DNA and Cell Biology*, **15**: 1009-1023.

DAGHER, S.F., J.L. WANG & R.J. PATTERSON (1995) – Identification of galectin-3 as a factor in pre-mRNA splicing. *Proc. Natl. Acad. Sci.*, **92**: 1213-1217.

DAVIES, S.C., A. TZAGOLOFF & S.R. ELLIS (1992) – Characterization of a yeast mitochondrial ribosomal protein structurally related to the mammalian 68-kDa high affinity laminin receptor. *The Journal of Biological Chemistry*, **267**: 5508-5514.

DEVEREUX, J., P. HAERBERLI & O. SMITHIES (1984) – A comprehensive set of sequence analysis programm for the VAX. *Nucl. Acid Res.*, **12**: 387-395.

FLUG, M. & P. KÖPF-MAIER (1995) – The basement membranes and its involvment in carcinoma cell invasion. *Acta Anat (Basel)*, **152**: 69-84.

GASPARINI, G., M. BARBARESCHI, P. BORACCHI, P. BEVILACQUA, P. VERDERIO, P. DALLA PALMA & S. MÉNARD (1995) – 67-kDa laminin-receptor expression adds prognostic information to intratumoral microvessel density in node negative breast cancer. *Int. J. Cancer*, **60**: 604-610.

HENDRICKS, W., J.W. MULDERS, M.A. BIBBY, C. SLINGSBY & H. BLOEMENDAL (1988) – Duck lens ecrytallin and lactate dehydrogenase B4 are identical: A single gene product with two distinct functions. *Proc. Natl. Acad. Sci.*, **85**: 7118-7144.

JACKERS, P., N. CLAUSSE, M.T. FERNANDEZ, A. BERTI, F. PRINCEN, U. WEWER, M.E. SOBEL & V. CASTRONOVO (1996a) – Seventeen copies of the human 37 kDa laminin receptor precursor/p40 ribosome-associated protein gene are processed pseudogenes arisen from retropositional events. *Biochem. Biophys. Acta*, **1305**: 98-104.

JACKERS, P., F. MINOLETTI, D. BELOTTI, N. CLAUSSE, G. SOZZI, S.M.E. & V. CASTRONOVO (1996b) – Isolation from a multigene family of the active human gene for the metastasis-associated multifunctional protein 37 LRP/p40 at chromosome 3p21. *Oncogene*, **13**: 495-503.

KONDOH, N., C.W. SCHWEINFEST, K.W. HENDERSON & T.S. PAPAS (1992) – Differential expression of S19 ribosomal protein, laminin-binding protein, and human lymphocyte antigen class I messenger RNAs associated with colon carcinoma progression and differentiation. *Cancer research*, **52**: 791-796.

LANDOWSKI, T.H., E.A. DRATZ & J.R. STARKEY (1995) – Sudies of the structure of the metastasis-associated 67 kDa laminin binding protein: fatty acid acylation and evidence supporting dimerization of the 32 kDa gene product to form the mature protein. *Biochemistry*, **34**: 11276-11287.

LESOT, H., U. KUHL & K. VON DER MARK (1983) – Isolation of laminin-binding protein from muscle cell membrane. *EMBO.*, **2**: 861-865.

LIOTTA, L.A., C.N. RAO & U.M. WEWER (1986) – Biochemical interactions of tumor cells with the basement membrane. *Annu Rev Biochem*, **55**: 1037-57.

MAKRIDES, S., S.T. CHITPATIMA, R. BANDYOPADHYAY & G. BRAWERMAN (1988) – Nucleotide sequence for a major messenger RNA for a 40 kilodalton polypeptide that is under translational control in mouse tumor cells. *Nucleic Acid Research*, **16**: 2349.

MALINOFF, H.L. & M.S. WICHA (1983) – Isolation of cell surface receptor protein for laminin from murine fibrosarcoma cells. *J. Cell Biol.*, **96**: 1475-1479.

MARTIGNONE, S., S. MÉNARD, R. BUFALINO, N. CASCINELLI, R. PELLEGRINI, E. TAGLIABUE, S. ANDREOLA, F. RILKE & M.I. COLNAGHI (1993) – Prognostic significance of the 67-Kilodalton laminin receptor expression in human carcinomas. *J. Natl. Cancer Inst.*, **85**: 398-402.

MARTIGNONE, S., R. PELLEGRINI, E. VILLA, N.N. TANDON, A. MASTROIANNI, E. TAGLIABUE, S. MÉNARD, R. BUFALINO & M.I. COLNAGHI (1992) – Characterization of two monoclonal antibodies directed against the 67kDa high affinity laminin receptor and application for the study of breast carcinoma progression. *Clin. Exp. Metast.*, **10**: 379-386.

NISHIURA, H., Y. SHIBUYA, S. MATSUBARA, S. TANASE, T. KAMBARA & T. YAMAMOTO (1996) – Monocyte chemotactic factor in rheumatoid arthritis synovial tissue. Probably a cross-linked derivative of S19 ribosomal protein. *J. Biol. Chem.*, **271**: 878-882.

OUZONIS, C., N. KYRIPIDES & C. SANDER (1995) – Novel families in archean genomes. *Nucleic Acids Research*, **23**: 565-570.

PELLEGRINI, R., S. MARTIGNONE, E. TAGLIABUE, D. BELOTTI, R. BUFALINO, N. CASCINELLI, S. MÉNARD & M.I. COLNAGHI (1995) – Prognostic significance of laminin production in relation with its receptor expression in human breast carcinomas. *Breast cancer Research and Treatment*, **35**: 195-199.

RAO, C. N., V. CASTRONOVO, M.C. SCHMITT, U.M. WEWER, A.P. CLAYSMITH, L.A. LIOTTA & M.E. SOBEL (1989) – Evidence for a precursor of the high-affinity metastasis-associated murine laminin receptor. *Biochemistry*, **28**: 7476-86.

RAO, N.C., S.H. BARSKY, V. P. TERRANOVA & L.A. LIOTTA (1983) – Isolation of a tumor cell laminin receptor. *Biochem Biophys Res Commun*, **111**: 804-8.

ROSENTHAL, E.T. & L. WORDEMAN (1995) – A protein similar to the 67 kDa laminin binding protein and p40 is probably a component of the translational machinery in Urechis caupo oocytes and embryos. *Journal of Cell Science*, **108**: 245-256.

SOBEL, M.E. (1993) – Differential expression of the 67 kDa laminin receptor in cancer. *Cancer Biol.*, **4**: 311-317.

TOHGO, A., S. TAKASAWA, H. MUNKATA, H. YONEKURA, N. HAYASHI & H. OKAMOTO (1994) – Structural determination and characterization of a 40 kDa protein isolated from rat 40S ribosomal subunit. *FEBS letters*, **340**: 133-138.

WEWER, U.M., L.A. LIOTTA, M. JAYE, G.A. RICCA, W.N. DROHAN, A.P. CLAYSMITH, C.N. RAO, P. WIRTH, J. E. COLIGAN, R. ALBRECHTSEN (1986) – Altered levels of laminin receptor mRNA in various human carcinoma cells that have different abilities to bind laminin. *Proc Natl Acad Sci U S A*, **83**: 7137-41.

WISTOW, G.J., T. LIETMAN, L.A. WILLIAMS, S.O. STAPPEL, W.W. DE JONG, J.HORWITZ & J. PIATIGORSKY (1988) – t-crystallin/a-enolase: one gene encodes both an enzyme and a lens structural protein. *J; Cell. Biol.*, **107**: 2729-2736.

YOW, H., J.M. WENG, H.S. CHEN, C. LEE, G.D.J. STEEL & L.B. CHEN (1988) – Increased mRNA expression of a laminin-binding protein in human color carcinoma:complete sequence of a full-lenght cDNA encoding the protein. *Proc natl aca sci USA*, **85**: 6394-6398.

Belg. J. Zool. - Volume 127 (1997) - issue 1 - pages 13-33 - Brussels 1997

NITRIC OXIDE SYNTHASE IN THE BRAIN OF THE CLAWED TOAD *XENOPUS LAEVIS*: IS THERE A RELATIONSHIP WITH THE VISUAL SYSTEM?

WILFRIED ALLAERTS, RIENK TUINHOF, RUUD UBINK AND ERIC W. ROUBOS

Department of Cellular Animal Physiology, University of Nijmegen, Nijmegen Institute for Neurosciences, Toernooiveld 1, 6525 ED Nijmegen, The Netherlands.

Abstract. Nitric oxide (NO), a free radical, has emerged as an intracellular and intercellular messenger molecule with many biological functions, including a role in memory. The neuroanatomical distribution of the enzyme nitric oxide synthase (NOS) is described in the brain and pituitary of *Xenopus laevis*, using immunohistochemistry with a polyclonal antiserum against human brain NOS, and using the nicotinamide adenine dinucleotide phosphate – diaphorase (NADPH-d) histochemical staining. NOS-containing neurons were found in the telencephalon, the diencephalon, the mesencephalon and the metencephalon, and were especially numerous in the pars lateralis of the amygdala, the lateral and dorsal pallium, the deep periventricular layers of the optic tectum and the locus coeruleus. The distribution of NOS-containing neurons in *Xenopus* is very similar to the distribution of NOS-immunopositive neurons as reported in several amphibian and reptilian species, and is also very reminiscent of the distribution of targets of the visual input system in amphibians. Therefore, a literature survey of tract tracing studies of the visual system in amphibians was performed, particularly referring to the thalamo-tectal, thalamo-telencephalic and crossed tecto-bulbar pathways. Beside a possible role of NO in the control of background adaptation in *Xenopus*, the present data, in combination with data reported in literature, suggest that NOergic neurotransmission is involved in the processing of visual information in amphibians.

Key-words: Nitric oxide synthase immunoreactivity, NADPH-diaphorase activity, neuroanatomy, amygdala, optic tectum, locus coeruleus, *Xenopus laevis*.

INTRODUCTION

Among the many proposed functions of nitric oxide (NO) in biological systems and especially in the central nervous system (GARTHWAITE & BOULTON, 1995), the role of NO as a «retrograde messenger» in memory (BARINAGA, 1991) remains elusive. This elusiveness is reflected for instance in the question of how the macroscopic phenomenon of memory is realized at the microscopic and/or molecular level. Different models for memory as well as for the role of NO in memory have been suggested. According to SCHUMAN &

Contribution to the 3th Benelux Congress of Zoology, Namur, November 1996.

MADISON (1991) NO signaling is required to activate the process of long-term potentiation (LTP) underlying memory, whereas others have demonstrated an involvement of NO in memory through the process of long-term depression (LTD) (GARTHWAITE *et al.*, 1988; SHIBUKI & OKADA, 1991). Also in astrocytes cultured *in vitro*, it was shown that long-lasting changes of calcium oscillation frequency, induced by repeated glutamate stimulation, depended on the activity of nitric oxide synthase (NOS) (PASTI *et al.*, 1995), and these authors proposed this effect as a cellular model for LTP. On the other hand, NO was called a less specific and less controllable chemical compound than most neurotransmitters or hormones (ANBAR, 1995). Nevertheless, the ubiquitous presence of NO in many organs and also in many taxonomic groups, points to a remarkable function well conserved in evolution (ANBAR, 1995) and to unique chemical properties of this free radical (BUTLER *et al.*, 1995). Given the low molecular weight, neutral electric charge and limited interaction with water, ANBAR (1995) concluded that NO diffuses rapidly through cytoplasm and biomembranes. Through this ability to affect many biochemical functions simultaneously, NO was suggested to act primarily as an intracellular synchronizing chemical messenger (ANBAR, 1995). Thus, an ultra-fast messenger for function synchronization, and a messenger for long-lasting response modulation (in the brain), were two basic molecular mechanisms inferred to explain some of the actions of NO at the macroscopic level.

We recently suggested also a role for NO signaling in the brain of the clawed toad *Xenopus laevis* in the process of skin colour adaptation to background light intensity (ALLAERTS *et al.*, 1997). This conclusion was primarily based on two observations: (**1**) the ability of NO to modulate a-MSH secretion from the pituitary pars intermedia (PI), and (**2**) the presence of NOS in neurons of the locus coeruleus. This area of the hindbrain is supposed to be involved in the control of background adaptation in *Xenopus* (TUINHOF *et al.*, 1994). We identified NOS activity in this brain area using immunocytochemistry with a polyclonal anti-human brain NOS (bNOS) and using the nicotinamide adenine dinucleotide phosphate-diaphorase (NADPH-d) histochemical reaction on brain sections. According to DAWSON *et al.* (1991) a close relationship, if not an identity, exists beween NADPH-diaphorase and bNOS. We also found NOS-immunopositive neurons in the optic tectum and NADPH-d reactivity in the amygdala (ALLAERTS *et al.*, unpublished), two brain areas which have not been implicated in the light mediated control of background adaptation. On the other hand, recent neuroanatomical and neuropharmacological studies have demonstrated the involvement of NOS in the visual system of birds (WILLIAMS *et al.*, 1994) and mammals (CUDEIRO *et al.*, 1994).

In the present study, we closely examine the neuroanatomical distribution of NADPH-d positive neurons in *Xenopus laevis*. Since the distribution of NADPH-d positive neurons was very reminiscent of the distribution of the targets of visual inputs for the brain of amphibians, the question was raised whether a relationship exists between the NOergic neurons and the visual system in such animals. Following a literature survey of tract tracing studies of the visual system in amphibians (see discussion), the distribution of NOS-containing neurons (NOS-immunoreactive and/or NADPH-d reactive) is compared with the functional brain areas in orientation and in visual recognition, two functions that appear to be related in amphibians (NORTHCUTT & KICLITER, 1980). The amphibian brain, and especially the telencephalon, reflects a primitive level of organization compared to all

amniota and even some of the anamniote classes, as shown for instance by the brain-body and telencephalon-body ratios which are similar to *Latimeria*, the sole living crossopterygian (NORTHCUTT & KICLITER, 1980; BUTLER & HODOS, 1996). During the evolution of the tetrapods, the amphibian telencephalic ground form, the so-called laminar organization, has served as a base form for several radiations of telencephalic hypertrofy and differentiation (BUTLER & HODOS, 1996). Despite their relative primitivism, it appears that amphibian mechanisms of orientation and visual recognition are not well understood. And, similar to the existing discrepancy between different paradigms for memory (see above), a unifying theory of the operation of the amphibian visual system has not been formulated*.

MATERIAL AND METHODS

Abbreviations used in text and figures

A	anterior thalamic nucleus
ac	anterior commissure
Ad	nucleus anterodorsalis tegmenti
Apl	amygdala, pars lateralis
Apm	amygdala, pars medialis
Av	nucleus anteroventralis tegmenti
BN	bed nucleus of the pallial commissure
bNOS	brain nitric oxide synthase
C	central thalamic nucleus
Cb	cerebellum
cbn	cerebellar nucleus
DA	dopamine
dp	dorsal pallium
eNOS	endothelial nitric oxide synthase
GABA	γ-aminobutyric acid
Hd	dorsal habenula
HRP	horseradish peroxidase
Hv	ventral habenula
Ip	interpeduncular nucleus
Is	nucleus isthmi
LA	lateral thalamic nucleus, pars anterior
LC	locus coeruleus
lfb	lateral forebrain bundle
lp	lateral pallium
Lpd	lateral thalamic nucleus, pars posterodorsalis
Lpv	lateral thalamic nucleus, pars posteroventralis
LTD	long-term depression
LTP	long-term potentiation
mfb	medial forebrain bundle
Mg	magnocellular nucleus
mp	medial pallium
a-MSH	α-melanophore-stimulating hormone
NADPH-d	nicotinamide adenine dinucleotide phosphate - diaphorase
NB	nucleus of Bellonci
NPv	nucleus of the paraventricular organ
NPY	neuropeptide Y

*After the first submission of the present manuscript, our attention was called to some recent publications that had not yet been listed in the medline bibliographical system at that moment. These publications describe the neuroanatomical distribution of NADPH-d reactive and/or immunoreactive neurons in the urodele amphibian *Pleurodeles waltl* (GONZÁLEZ *et al.*, 1996), in the frog *Rana perezi* (MUÑOZ *et al.*, 1996), in the clawed toad *Xenopus laevis* (BRÜNING & MAYER, 1996) and in the lizard *Gekko gecko* (SMEETS *et al.*, 1997). These studies largely are in line with our own observations in *Xenopus laevis*, and are schematically represented in Table 1.

NO	nitric oxide
NOS	nitric oxide synthase
nIII	nervus oculomotorius
nV	nervus trigeminus
ON	nervus opticus
OT	olfactory tubercle
P	posterior thalamic nucleus
pc	posterior commissure
pd	hypophysis, pars distalis (in text: PD)
pi	hypophysis, pars intermedia (in text: PI)
PLP	periodate-lysine-paraformaldehyde (fixative)
pn	hypophysis, pars nervosa
POa	anterior preoptic nucleus
Rad	dorsal raphe nucleus
Rm	nucleus reticularis medius
SC	suprachiasmatic nucleus
Str	striatum
TE	thalamic eminence
tect	tectum mesencephali
tegm	tegmentum mesencephali
TH	tyrosine hydroxylase
Tor	torus semicircularis
TP	posterior tubercle
VH	ventral hypothalamic nucleus
VM	ventromedial thalamic nucleus
III	nucleus nervi oculomotorius
Vm	nucleus motorius nervi trigemini
Vpr	nucleus princeps nervi trigemini

Animals

Adult male and female *Xenopus laevis* were obtained from our laboratory stock. Animals were fed beef heart and trout pellets (Trouvit, Trouw, Putten, The Netherlands) once a week. To study a possible effect of background light condition on NOS expression, the toads were kept under constant illumination on either a black or a white background for at least three weeks, at 22 °C.

Immunohistochemistry and enzyme histochemistry

Toads were anaesthetized by immersion in 0.1 % tricaine methane sulfonate (MS 222, Sandoz, Basle, Switzerland) and perfused via the aorta with ice-cold 0.6 % Ringer's solution for 3 min, followed for 15 min with either Bouin-Hollande, Zamboni's fixative (for paraffin immunohistochemistry) or with periodate-lysine-paraformaldehyde (PLP) fixative after McLean & Nakane (1974) (for cryo-immunohistochemistry and cryo-enzyme histochemistry). Brains and pituitaries were dissected and postfixed for 2-3 hr in the same fixative. For paraffin immunohistochemistry, brains and pituitaries were dehydrated with an ethanol series (Merck, Darmstadt, Germany), isopropanol (Merck) and finally xylol (Janssen Chimica, Geel, Belgium), and embedded in paraplast. For cryo-histochemistry, brains and pituitaries were immersed in 10 % (w:v) sucrose in 0.15 M sodium phosphate buffer and after saturation frozen at -70 °C. From both paraffin-embedded and cryo-protected material we cut sagittal and transversal sections of 10-20 µm, which were transferred to poly-L-lysine-coated slides (Sigma, St Louis, MO, USA).

Sections were stained following the ABC immunostaining procedure (Hsu *et al.*, 1981) and the βNADPH-d procedure (Dawson *et al.*, 1991). Technical details of these staining procedures are described elsewhere (Allaerts *et al.*, unpublished). Antisera used in this study were a polyclonal anti-human bNOS serum (Transduction Laboratories,

Lexington, KY, USA; diluted 1:100) and a monoclonal antiserum against tyrosine hydroxylase (TH) (Instar Corporation, Stillwater, MN, USA). Sections were evaluated using bright field and epi-fluorescence microscopy with a Leitz DM RB/E microscope equipped with a Leica Vario Orthomat E camera system.

RESULTS

An overview of the brain and pituitary areas studied is represented in Figs 1 and 2. Line drawings of transverse projections are shown in Fig. 2 corresponding to the levels indicated in Fig. 1. The nomenclature follows that previously used (TUINHOF *et al.*, 1994). Figs 3 to 5 show photomicrographs of some of the transversal and also of some sagittal sections taken laterally to the medial plane (Fig. 3a, b). Results from anterograde fil-ling of the optic nerve with horseradish peroxidase (HRP) are adapted from TUINHOF *et al.* (1994).

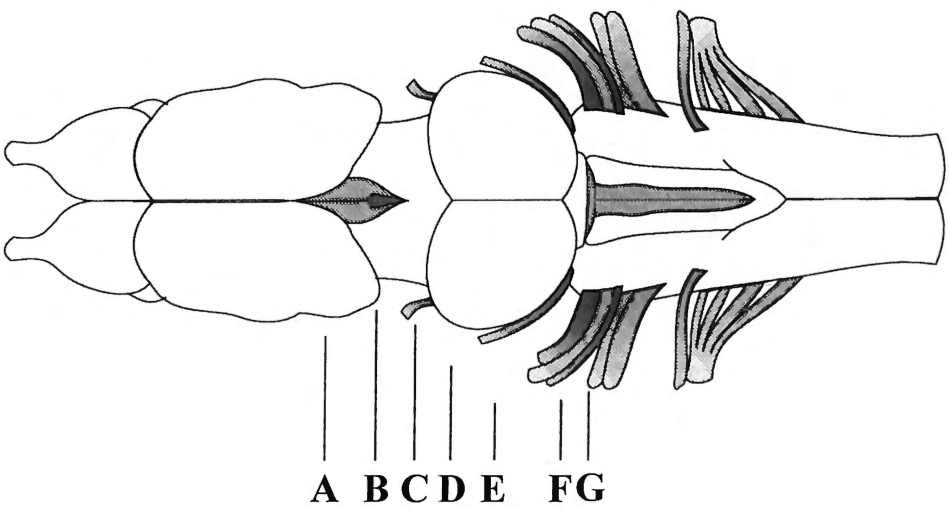

Fig. 1. – Schematic representation of the brain of the South African clawed toad *Xenopus laevis* (dorsal view), indicating the levels at which transversal sections have been presented in Fig. 2.

Telencephalon

The most rostral population of NADPH-d$^+$ neurons is found in the olfactory tubercle (OT) (Fig. 3a). In the telencephalon proper we found small populations of NADPH-d$^+$ cell bodies in the dorsal (dp) and lateral pallium (lp) (Figs 2, 4d-e). In the caudal telencephalon very strong NADPH-d reactivity is found in neurons of the amygdala pars lateralis (Apl) (Fig. 4a-c). Somata and fibers were darkly stained. Fibers from these somata cross the anterior commis-

sure to innervate the contralateral amygdala (Fig. 4c). According to NORTHCUTT & KICLITER (1980) the Apl can be regarded as an elongation of the lp, thus forming a C-shaped nucleus. The relevance of the amygdala with respect to the amphibian visual system is discussed below.

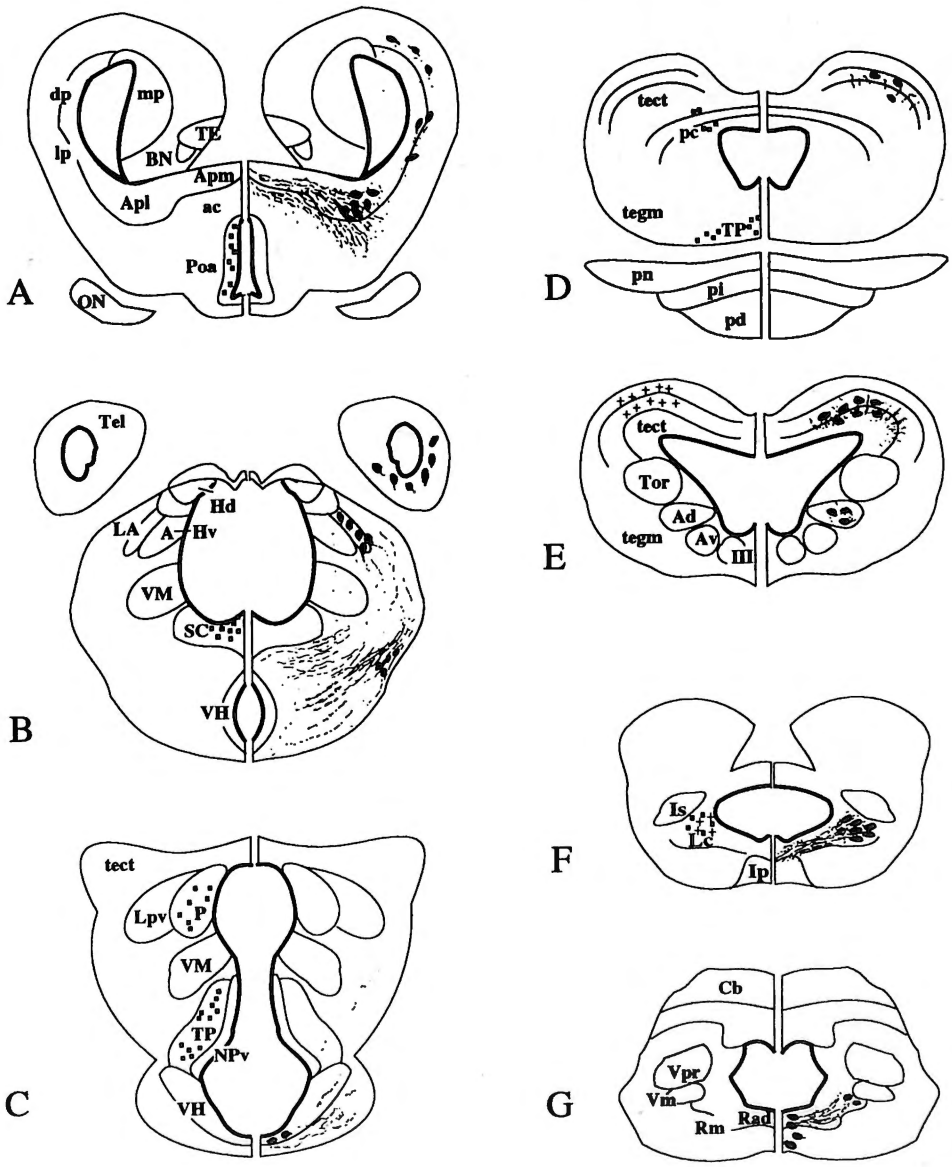

Fig. 2. – Diagram of transverse sections through the brain of *Xenopus laevis*, at levels indicated in Fig. 1. Dots and curved lines on the right indicate NADPH-d reactive neuron somata and NADPH-d reactive fibers, respectively. Plus signs on the left indicate bNOS-immunoreactive neuron somata. Squares on the left indicate TH-immunoreactive neurons (TUINHOF *et al.*, 1994).

Diencephalon

Following anterograde labeling of the optic nerve with HRP, we previously described HRP-reactive fibers contacting neuropeptide Y (NPY)-immunoreactive neurons in the nucleus suprachiasmaticus (TUINHOF *et al.*, 1994). Moreover, we found bundles of HRP-reactive fibers running parallel to the geniculate body and the neuropil of Bellonci, whereas terminal fields were observed in the optic tectum (see below). In the present study, NADPH-d$^+$ neurons were present in the pars anterior of the lateral thalamic nucleus (LA), medio-dorsal to the neuropil of Bellonci (NB), and in the ventral hypothalamic nucleus (VH) (Fig. 2). NADPH-d reactivity was absent from the magnocellular (Mg) and suprachiasmatic nuclei (SC). Furthermore, NADPH-d$^+$ fibers and small NADPH-d$^+$ cells occurred at the ventromedial edge of the optic tract (Fig. 5a). Some of the NADPH-d$^+$ fibers ran similar to the course of NOergic fibers observed at the edge of the optic tract in the turtle *Pseudemys scripta*, which would correspond to tectothalamic and thalamotectic fibers (BRÜNING *et al.*, 1994).

Mesencephalon

Using both immunostaining with anti-bNOS and the NADPH-d reaction we found NOS-reactive neurons in the optic tectum (tect) (Fig. 3c-d). NADPH-d reactivity was localized in somata of deep tectal neurons and also in some fibers projecting towards the superficial tectal layers (Fig. 3c). The NADPH-d$^+$ somata occurred mostly in layer 6 and also in layer 4 (see also HUGHES, 1990a,b and discussion). bNOS-like immunoreactivity was present in some of the neuron somata within the same layers and also in some fibers travelling across the deep medullary layer (POTTER, 1969) towards the superficial tectum and in fibers projecting to the posteroventral tegmentum (Fig. 2). Some NADPH-d$^+$ neurons, moreover, were found in the nucleus anterodorsalis tegmenti (Ad) (Figs 2 and 5b).

Metencephalon

In sagittal (Fig. 3b and inset) and coronal (Fig. 5c) cryo-sections, we encountered a dense cluster of NADPH-d$^+$ neurons (somata and fibers) in the isthmic area corresponding topographically to the locus coeruleus (LC). Paraffin sections of this area also show bNOS-immunoreactive neurons. The locus coeruleus was also identified immunohistochemically using anti-TH. Moreover, using double labeling with TH antiserum and the NADPH-d reaction we demonstrated intermingling and also close juxtaposition of TH$^+$ and NADPH-d$^+$ neurons, but no double-labeled cells. NADPH-d$^+$ neurons in the LC send fibers into a rostroventral direction (Fig. 3b: inset) towards the ventral tegmental area. Other LC neurons have axons that follow more medial and caudal directions and seem to innervate the anterior part of the dorsal raphe nucleus (Rad) (Fig. 5c).

Pituitary

We did not find bNOS-immunoreactivity in paraffin sections of the pituitary of *Xenopus laevis* fixed with Zamboni, whereas in PLP-fixed cryo-sections some NADPH-d activity occurred in endothelia of the pars intermedia (PI) and pars distalis (PD), probably corresponding to endothelial NOS (eNOS).

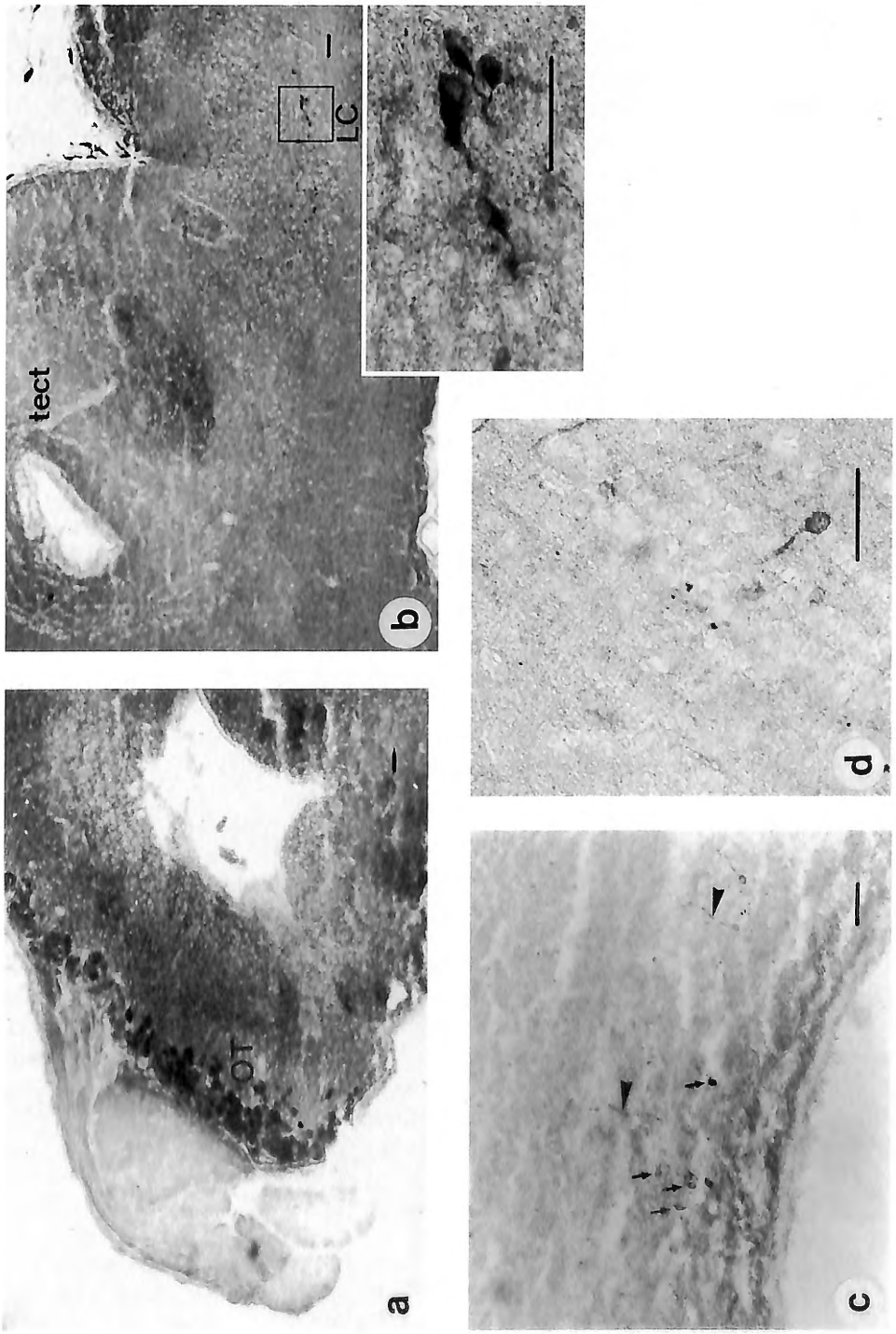

Fig. 3

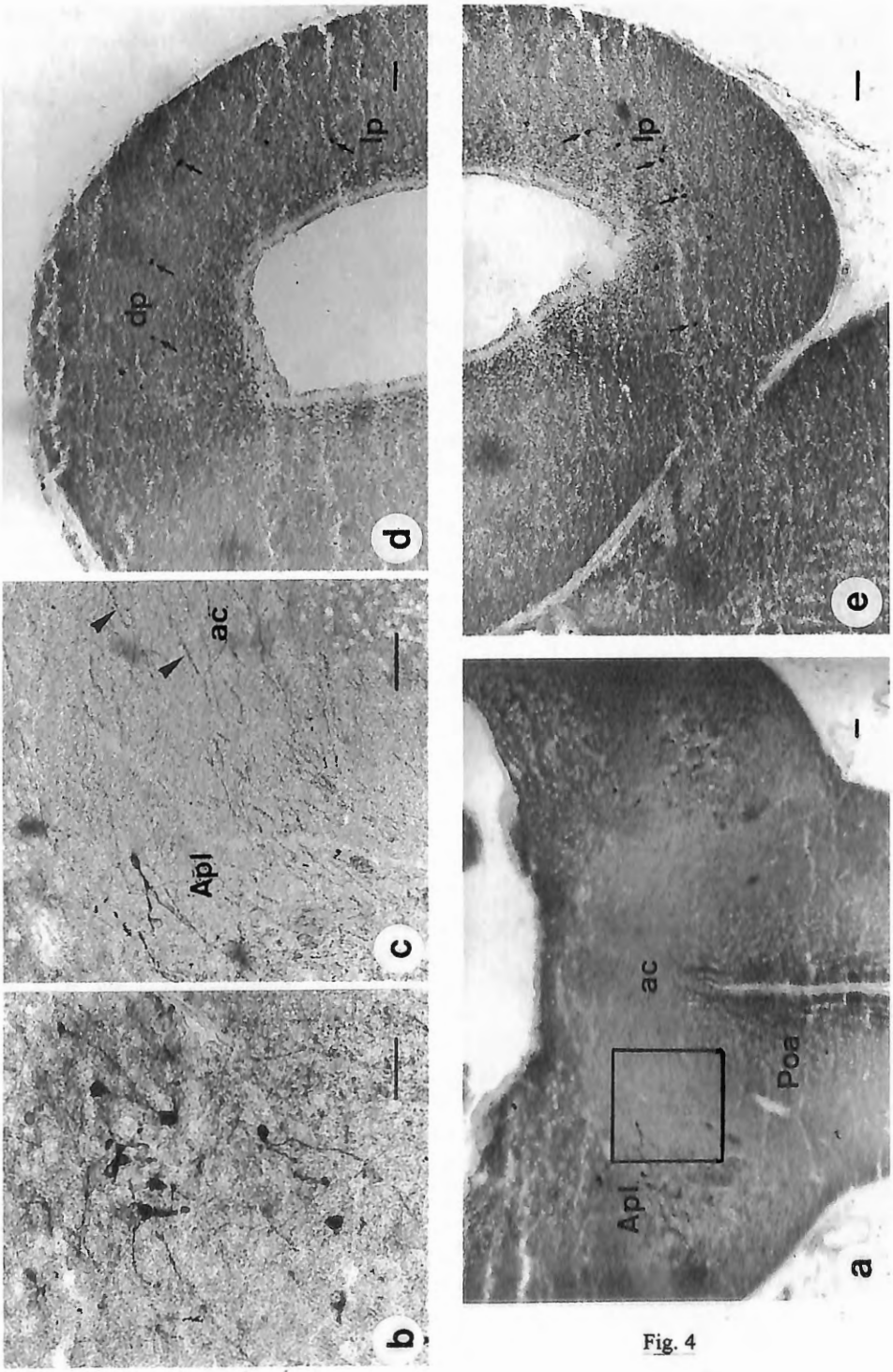

Fig. 4

Fig. 3. – Cryo-sections of *Xenopus laevis* brain fixed with PLP and stained with the NADPH-d histochemical reaction **(a-c)** and detail of a paraffin section of Zamboni-fixed *Xenopus* brain immunostained with polyclonal anti bNOS serum **(d)**. **a:** Sagittal section through the rostral telencephalon, indicating NADPH-d$^+$ somata in the olfactory tubercle (OT)(x50). **b:** Sagittal section through mesencephalon and methencephalon, showing NADPH-d$^+$ neurons in the optic tectum (tect) and the locus coeruleus (LC)(x50). A higher magnification of the framed region in the locus coeruleus is shown in the inset (x400). **c:** Transversal section of the periventricular layers of the optic tectum (x126). Note the NADPH-d$^+$ neurons (small arrows) in the deep tectal layers, and some projections towards the superficial tectal layers (arrowheads). **d:** Detail of sagittal section of optic tectum showing bNOS-immunoreactive neuron in deep tectal layer (x320). All sections are from *Xenopus* adapted to black background. (Scale bars = 50 μm).

Fig. 4. – Transversal cryo-sections of *Xenopus laevis* brain (PLP fixation) stained with the NADPH-d histochemical reaction: **(a-c)** through the telencephalon at the level of the anterior commissure (ac); **(d-e)** low magnification of lateral telencephalic wall at the level of the preoptic area (Poa). **a:** Overview of basal telencephalon (x50). **b:** Detail of amygdala pars lateralis (Apl) showing dense cluster of NADPH-d$^+$ neurons (x200). **c:** Higher magnification of frame in **(a)** showing Apl and anterior commissure (ac), with NADPH-d$^+$ fibers coursing through the ac (arrowhead) (x200). **d:** NADPH-d+ neuron somata (arrows) in the dorsal (dp) and lateral pallium (lp)(x80). **e:** NADPH-d$^+$ neuron somata (arrows) in ventral part of lp (x80). All sections are from *Xenopus* adapted to a white background. (Scale bars = 50 μm).

Fig. 5. – Transversal cryo-section of *Xenopus laevis* brain (PLP fixation) stained with NADPH-d histochemical reaction: **a:** Low magnification of the optical tract in the diencephalon: NADPH-d reactivity is found in fibers of the optical tract and in small cells at the ventromedial edge of the optical tract (arrowheads)(x80). **b:** Detail of the lateral thalamus showing NADPH-d$^+$ neurons in the nucleus anterodorsalis tegmenti (Ad)(x200). **c:** Cluster of NADPH-d$^+$ neurons in the locus coeruleus (LC) and NADPH-d$^+$ fibers projecting towards the dorsal raphe (arrowhead)(x140). Sections in **a** and **b** are from white-adapted, the section in **c** is from a black-adapted *Xenopus*.(Scale bars = 50 μm).

DISCUSSION

On the basis of NADPH-d histochemistry and bNOS immunohistochemistry we here present a neuroanatomical description of the NOergic neurons in the brain of *Xenopus laevis*. NADPH-d positive neurons were found in several nuclei of the telencephalon, diencephalon, mesencephalon, and metencephalon. These data largely confirm previous neuroanatomical descriptions in *Xenopus laevis* (BRÜNING & MAYER, 1996; ALLAERTS *et al.*, unpublished) and in other amphibian and reptile species (BRÜNING *et al.*, 1994; GONZÁLEZ *et al.*, 1996; MUÑOZ *et al.*, 1996; SMEETS *et al.*, 1997) (see Table 1 for comparison of the descriptions in the amphibian species). DAWSON *et al.* (1991) have shown that in the rat NADPH-d activity correlates to NOS activity both in the brain and in peripheral tissues, although some tissues like the adrenal cortex and the liver display NADPH-d activity in the absence of NOS. Also in *Xenopus laevis* (BRÜNING & MAYER, 1996) and in the urodele amphibian *Pleurodeles waltl* (GONZÁLEZ *et al.*, 1996) a close correlation was found between NADPH-d activity and NOS immunoreactivity except for the olfactory nerve (NADPH-d activity in the absence of NOS immunoreactivity). Using Western blotting of *Xenopus* hindbrain homogenates, we previously demonstrated an approximately 150 kDa

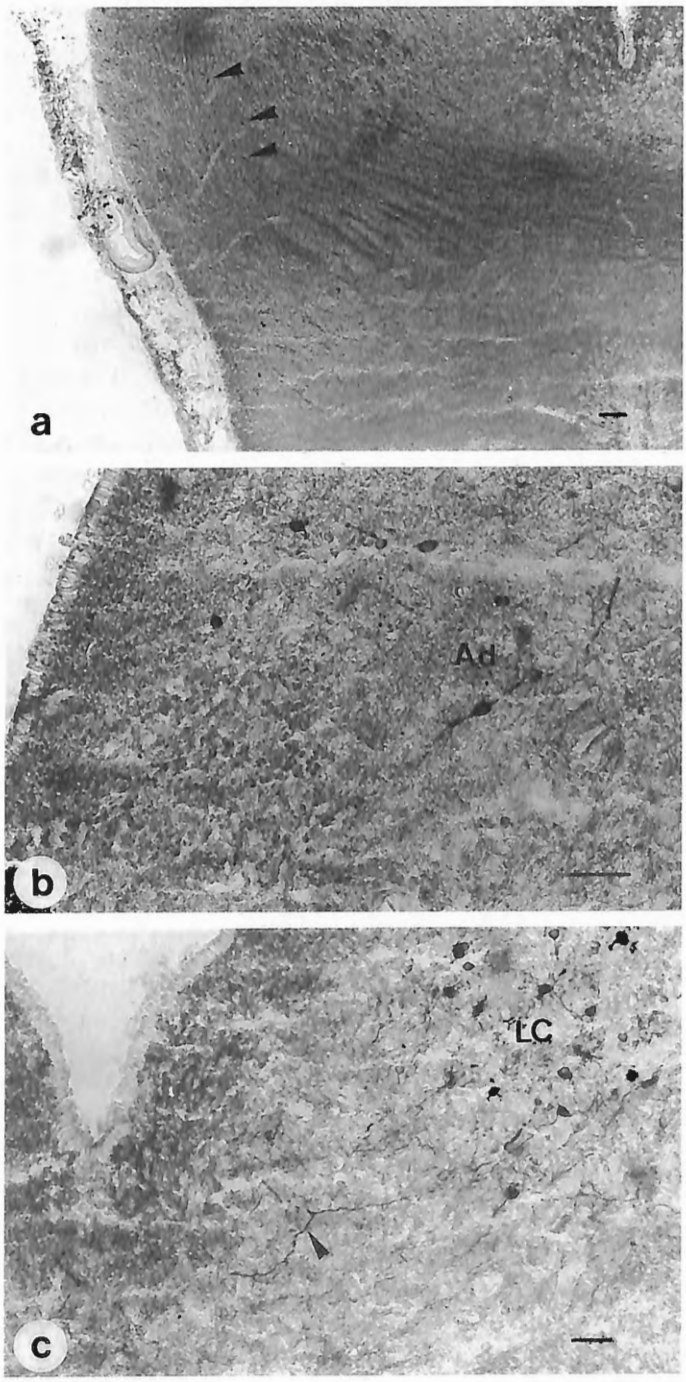

Fig. 5

band immunostained with a polyclonal bNOS antiserum, confirming the presence of bNOS in *Xenopus* hindbrain (ALLAERTS *et al.*, 1997).

Functional relevance of a brain NOergic system in Xenopus?

Previously we have shown differences in activity of hypothalamic nuclei under different conditions of background light intensity (TUINHOF *et al.*, 1993,1994). On the basis of a variety of methods (immunocytochemistry, retrograde labeling, etc.) we proposed that a small number of brain centers was responsible for the regulation of melanotrope activity in the process of background adaptation. In our view the most important regulatory mechanism is provided by the inhibition of α-MSH secretion via the hypothalamic suprachiasmatic nucleus (SC) (TUINHOF *et al.*, 1993), which contains neurons that simultaneously produce NPY, dopamine (DA) and γ-aminobutyric acid (GABA) (DE RIJK *et al.*, 1992). Another important hypothalamic centre is the magnocellular nucleus (Mg) that may have a mild stimulatory effect on the melanotropes through the release of thyrotropin-releasing hormone (TRH) and corticotropin-releasing hormone (CRH) (TUINHOF *et al.*, 1994). The third centre involved in background adaptation is the locus coeruleus (LC) in the metencephalon, for it was shown that noradrenaline (NA)-containing fibres innervate the PI, whereas NA-positive neurons are localized in the LC (TUINHOF *et al.*, 1994; JANSEN *et al.*, 1997).

We recently also compared bNOS-activity in the brain and pituitary of *Xenopus laevis* adapted to either a black or a white background (ALLAERTS *et al.*, 1997) and no differences were observed. The occurrence of bNOS activity in neurons of the LC, and the capability of NO to stimulate α-MSH secretion from single melanotrope cells *in vitro*, suggest a role of NO in the control of background adaptation (ALLAERTS *et al.*, 1997). However, our present data show the absence of NOS-activity in the Mg and SC, and especially the SC receives a direct input from the optic nerve (TUINHOF *et al.*, 1994). The intermingling of NOS-containing and TH^+ neurons without a cellular co-localization of bNOS and TH in the LC may also indicate a role in the presumed effect of stress on background adaptation. The involvement of the LC in the regulation of stress-induced responses has been documented in the rat (TILDERS & BERKENBOSCH, 1986). Alternatively, the role of NO may reside in the higher visual centers that regulate background adaptation. In this respect it is interesting to note that CUDEIRO *et al.* (1994) have demonstrated that suppression of the visual responses of relay cells in the dorsal lateral geniculate nucleus of the cat *in vivo* is induced by iontophoretic administration of N^G-nitro-L-arginine, a competitive inhibitor of NOS. This suppression of visually or N-methyl-D-aspartic acid (NMDA) evoked responses thereby seemed independent of an increase of cyclic guanosine-3',5'-mono-phosphate (cGMP), and the function of NO at this level of the visual system was called permissive (CUDEIRO *et al.*, 1994). In another model system, the chicken embryo, WILLIAMS *et al.* (1994) found a correlation of NOS expression with changing patterns of axonal projections in the developing optic tectum. They concluded that NOS is involved in the development and refinement of the proper pattern of connections in the chicken retinotectal system (WILLIAMS *et al.*, 1994).

Comparison of the distribution of NOS-containing neurons in the amphibian brain with literature data of tracing studies of targets of the visual system in amphibians shows a striking overlap between NOergic neurons and parts of the visual system. We here speculate on a possible link between NOergic neurotransmission and the visual system in amphibians. For an overview of this system we refer to NORTHCUTT & KICLITER (1980), who especially document the telencephalic connections of the visual system (see below), as well as to the tracing studies of the optic tract by HERRICK (1925, 1948), LÁZÁR (1969), HUGHES (1990a,b) and to the textbook of *Comparative Vertebrate Neuroanatomy* by BUTLER & HODOS (1996). The suggestion of a role of NOergic transmission in the visual and possibly also orientation systems in the amphibian brain, as for instance suggested by the NOS-containing neurons in the optic tectum (see below), does not preclude other functions of NOergic transmission, such as indicated by the NOS activity in the olfactory tubercle (BRÜNING *et al.*, 1994; Table 1 and present data). BRÜNING *et al.* (1994) have shown that NADPH-d reactivity in the olfactory tubercle is correlated with b-NOS immunoreactivity in the turtle *Pseudemys scripta*, but obviously these NADPH-d$^+$ neurons in the olfactory tubercle have no relationship to the visual system. Also SMEETS *et al.* (1997) remarked that NADPH-d activity and NOS immunoreactivity are not confined to any functional sensorimotor system or neurotransmitter system. Otherwise, at least a permissive role of NOergic transmission in parts of the visual system in mammals (CUDEIRO *et al.*, 1994) and birds (WILLIAMS *et al.*, 1994) has now been functionally demonstrated. However, experimental studies using selective NOS inhibitors will be necessary to substantiate the functional relevance of NOergic neurotransmission in the amphibian brain *in vivo*.

Telencephalic connections relevant to the amphibian visual system

The «classical» viewpoint on the amphibian telencephalic organization, as expressed in *e.g.* HERRICK's monography (1948), considers the amphibian telencephalon as a simple, unspecialized web of nervous tissue that receives mainly secondary or tertiary olfactory connections, and of which the efferents carry primarily olfactory information to the hypothalamus or midbrain, to become integrated with ascending gustatory information (cited in NORTHCUTT & KICLITER, 1980). According to NORTHCUTT & KICLITER (1980) several arguments can be raised against this «classical» viewpoint, favouring an integrative role of the amphibian telencephalon, including the integration of visual, auditory and somatic information. Although some of the references cited in NORTHCUTT & KICLITER (1980) may seem rather old, comparison of these references with recent reviews (*e.g.* BUTLER & HODOS, 1996) strengthens their validity, and moreover, little new information on tracing studies in the amphibian telencephalon has become available since. Below we summarize some of the arguments listed by NORTHCUTT & KICLITER (1980)(see also the schematic illustration in Fig. 6).

1) The medial pallium in amphibians not only receives connections of the lateral pallium (the main target of the olfactory input), but also receives direct thalamic projections carrying visual and somatic information, and afferents from the preoptic area (POa) and ventral thalamus as shown by HRP labeling studies (NORTHCUTT & KICLITER, 1980; BUTLER & HODOS, 1996). The medial pallium is connected via the medial forebrain bun-

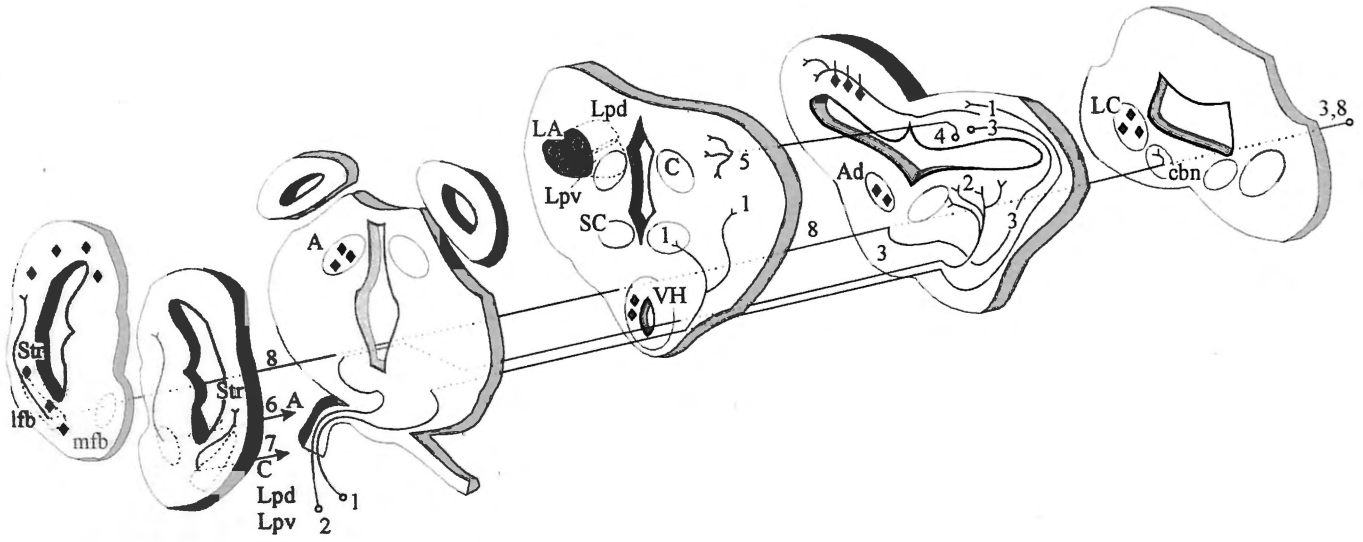

Fig. 6. – Schematic representation of the connections of the visual system in the amphibian brain, adapted from tracing studies by LÁZÁR (1969), SCALIA & GREGORY (1970), KICLITER & NORTHCUTT (1975), KICLITER (1979) (reviewed in NORTHCUTT & KICLITER, 1980). The terminology of diencephalic nuclei follows the terminology of NEARY & NORTHCUTT (1983). The brain is represented by thick sections from rostral to caudal position comparable to thin sections B, C, E, F in Fig. 2 as well as a mid-telencephalic thick section (rostral to Fig.2, A). Black diamonds represent NADPH-d active and/or bNOS immunoreactive neurons as described in this study (see also Fig.2). **1-2:** retino-tectal and retino-thalamic pathways observed following HRP-labeling of the optic nerve; **3-5:** efferent pathways of the optic tectum found by anterograde degeneration studies (e.g. LÁZÁR, 1969): tecto-isthmic connection and crossed tecto-bulbar pathway (**3**), fibers in mesencephalic commissure (**4**) and tecto-diencephalic connection (**5**); **6-7:** connections of mfb (**6**) and lfb (**7**) to dorsal thalamic nuclei (see text) (thalamo-frontal tract, NORTHCUTT & KICLITER, 1980); **8:** telencephalic-medullar connection to the cerebellar nucleus (cbn), as revealed by HRP-labeling (KICLITER, 1979).

dle (mfb) (Fig. 6) to the anterior thalamic nucleus (A) (terminology adapted in NEARY & NORTHCUTT, 1983).

2) The amphibian striatum (str) receives both visual and auditory information from dorsal thalamic centers (already suggested by HERRICK, 1948), as demonstrated by anterograde neuron degeneration studies (KICLITER & NORTHCUTT, 1975). NORTHCUTT & KICLITER (1980) suggest that the amphibian striatum (str) may be linked to the optic tectum via the lateral forebrain bundle (lfb) and ipsilateral relay centers located in the lateral dorsal thalamus (SCALIA & GREGORY, 1970), but not by relay centers in the anterior thalamic nucleus (BUTLER & HODOS, 1996) (Fig. 6).

3) The amphibian amygdala pars lateralis receives projections via the lfb from the hypothalamus and the caudal dorsal thalamus (namely the central nucleus [C] and lateral nuclei [Lpv and Lpd]), which areas in amphibians are linked with the optic tectum (see argument 2) (NORTHCUTT & KICLITER, 1980).

4) HRP labeling studies of the lateral amygdala revealed afferent cell groups of the ipsilateral dorsal thalamic nuclei (connected via the lfb) as well as HRP-labeled cell groups in the ipsilateral rostral medulla of the brainstem (KICLITER, 1979), identified as the cerebellar nucleus (cbn) according to NIEUWENHUYS & OPDAM (1976) and situated immediately caudal to the LC (Fig. 6). The lfb carries visual information to the str and possibly also to the Apl (GRUBERG & AMBROS, 1974), as already shown by tracing studies of LÁZÁR (1969). Interestingly, BRÜNING & MAYER (1996) observed dendrites of NOS-positive neurons in the anterior entopeduncular nucleus (lateral from amygdala) of *Xenopus laevis*, intermingling with fibers of the lfb (see below).

Several lines of evidence, obtained from anatomical, histochemical and embryological studies, have led to NORTHCUTT & KICLITER's conclusion (1980) that the amphibian lateral pallium and pars lateralis of the amygdala (which are topologically contiguous regions of the lateral telencephalic wall) are homologous to the reptilian dorsal ventricular ridge and lateral cortex. However, in sauropsids (reptiles and birds) the different regions of the dorsal ventricular ridge became segregated so that different regions of the primary pallial region received only one single sensory modality, whereas in amphibians several modalities converge on the striatum, i.e., the subpallial region of the lateral telencephalic wall (NORTHCUTT & KICLITER, 1980). Whether the amphibian striatal cells are also multimodal, however, remains to be clarified (NORTHCUTT & KICLITER, 1980). The relevance of the medial telencephalic wall (pallium and striatum) for the amphibian visual system was proven experimentally by showing evoked potentials recorded upon electrical stimulation of the optic nerve (KARAMIAN *et al.*, 1966), but beside visual afferents the medial telencephalic wall also receives auditory and somatosensory afferents (KARAMIAN *et al.*, 1966).

In our study, NADPH-d activity in the telencephalon was found in the pars lateralis of the amygdala, in the lateral and dorsal pallium and in the olfactory tubercle (see Table 1 for comparison with other studies in amphibians). Studies in reptiles (BRÜNING *et al.*, 1994; SMEETS *et al.*, 1997) moreover, have shown bNOS-immunoreactivity in neurons of the basal ganglia complex, the basal amygdaloid nucleus and the dorsal ventricular ridge, and in fibers coursing in a tract connecting the basal amygdaloid nucleus with the hypothalamus, corresponding to the stria terminalis. Besides the homology between amphibian and reptilian subpallial regions, also the NOergic neurotransmission seems to be con-

TABLE 1

Comparison of literature data on the bNOS immunoreactivity and the NADPH-d reactivity in the brain of three amphibian species.

Pleurodeles waltl[1]	*Rana perezi*[2]	*Xenopus laevis*[3]
Telencephalon		
primary olfactory fibers (d)		terminal nerve (d)
olfactory bulb (+)	olfactory bulb (d)	olfactory lobe (-)
pallium (+)	pallium (d)	pallium (+)
septum (+)	septum (d)	septum (very few)
caudal striatum (+)	striatum and nucleus of diagonal band (d)	striatum (+) nucleus accumbens (+)
amygdala (+)	amygdala (d)	amygdala pars lateralis and anterior entopeduncular nucleus (+)
Diencephalon		
preoptic area (+)	preoptic and infundibular recesses of 3rd ventricle (d)	preoptic nucleus (+)
ventral hypothalamus (+)	suprachiasmatic and magnocellular nuclei (d)	ventral hypothalamus (+)
posterior tubercle (+)		posterior tubercle (+)
	ant.,lat., centr. and lateral posteroventral thalamic nuclei (d)	lateral thalamic nuclei (lat., ant. & post. thalamic nucl.) and post.entopeduncular nucl.(+)
Brainstem		
mesencephalic tegmentum (+)	pretectal area (d)	
optic tectum (+)	optic tectum (d)	optic tectum (+)
	torus semicircularis (d)	magnocell.nucl. of torus semicircularis (+)
isthmic-pretrigeminal region (+)		
isthmic region (+)	isthmic nucleus (d)	isthmic nucleus (-)
	locus coeruleus (*)	locus coeruleus (+)
Rhombencephalon		
descending trigeminal tract (+)	sensory trigeminal nuclei (d)	descending nucleus of trigeminal nerve (+)
	octaval area (d)	
solitary tract (+)	nucleus of solitary tract (d)	dorsal to solitary tract (+)
raphe nucleus (+)	raphe nucleus (d)	
mid-caudal reticular formation (+)	reticular nuclei (d)	inferior reticular nucleus (+)
	dorsal column nucleus (d)	

[1] GONZALEZ *et al.*, 1996: distribution of bNOS immunoreactivity and NADPH-d activity.
[2] MUÑOZ *et al.*, 1996: distribution of NADPH-d activity.
[3] BRÜNING & MAYER, 1996: distribution of bNOS immunoreactivity and NADPH-d activity.
+ : bNOS immunoreactivity and NADPH-d activity are co-localized.
d : only NADPH-d activity.
- : reported negative for both NADPH-d and bNOS staining.
* : co-localization of NADPH-d with tyrosine hydroxylase immunoreactivity.

served in both vertebrate groups, indicating a well conserved and important role for NO in the functioning of this brain region. However, the multimodal or multi-functional character of the amphibian medial telencephalic wall may hamper the characterization of individual functional units (NORTHCUTT & KICLITER, 1980), so making the functional characterization of the NOergic transmission in the amphibian telencephalon difficult.

Thalamic connections relevant to the amphibian visual system

The demonstration of two telencephalic visual projections in amphibians according to NORTHCUTT & KICLITER (1980) enables a comparison between the amphibian visual system and that of the sauropsids, which also have a dual telencephalic visual system (HALL & EBNER, 1970; KARTEN & REVZIN, 1966; KARTEN & NAUTA, 1968; KARTEN *et al.*, 1973). This dual system consists of **(a)** the retino-thalamo-telencephalic system (shortly «thalamofugal» system) and **(b)** the retino-tecto-thalamo-telencephalic system (shortly «tectofugal» system) (NORTHCUTT & KICLITER, 1980). Characteristics of sauropsid visual systems provide criteria for proposing homology of the amphibian visual system. When rigidly applying the criteria for homology, according to NORTHCUTT & KICLITER (1980) neither of the two sauropsid visual projection systems is exactly represented in amphibians, although the retino-tecto-thalamo-telencephalic system comes closest to meeting the criteria. SCALIA & GREGORY (1970) already stated that amphibians do possess a well-developed retino-tectal pathway but have a comparatively small retino-thalamic system, whereas anatomical evidence for a thalamo-telencephalic projection is still scarce. RUBINSON (1968) and LÁZÁR (1969) described projections of the optic tectum in *Rana* to a region of the lateral thalamic neuropil, which does not receive direct retinal projections. Post-synaptic cells of fibers in this neuropil are located in the posterocentral and part of the posterolateral nuclei, and project to the striatum via the lfb (SCALIA & GREGORY, 1970). SCALIA & GREGORY (1970) therefore concluded that the latter pathway may represent the amphibian homologue of the geniculo-striate system in mammals, i.e., the mammalian form of the thalamofugal system (BUTLER & HODOS, 1996). A specific problem in the localization of post-synaptic neurons in amphibia, according to SCALIA & GREGORY (1970), is caused by the relatively long dendrites of nuclei with rather distant location compared to the terminal fields of the retinofugal fibers. MUÑOZ *et al.* (1996) observed terminal fields of NADPH-d$^+$ neurons in the visual recipient plexus of Bellonci and in the thalamic geniculate nucleus of the frog *Rana perezi*. A functional role of NOS in the visual relay cells of the geniculate nucleus of the cat was shown by CUDEIRO *et al.* (1994).

In conclusion, the absence of a dorsal ventricular ridge in amphibians tones down any homology between amphibian and higher vertebrate telencephalic systems, unless we may regard the lateral pallium and pars lateralis of the amygdala as a primitive, relatively unspecialized but evolutionary homologue of the dorsal ventricular ridge, as suggested by NORTHCUTT & KICLITER (1980).

NOS and the crossed tecto-bulbar pathway in amphibians

The NOS-immunopositive and NADPH-d reactive neurons were observed in layer 4 and 6 of the optic tectum (terminology according to LÁZÁR, 1969, POTTER, 1969 and

HUGHES 1990a,b). This distribution is reminiscent of the distribution of neurons that give rise to the tecto-bulbar pathway, as demonstrated using HRP-labeling in the frog *Rana pipiens* by HUGHES (1990b). The somata of these neurons according to HUGHES (1990b) are located in the superficial half of layer 6, with some dendrites ascending to the superficial tectal layers, the so-called retino-recipient layers (HUGHES, 1990a). BRÜNING *et al.* (1994) observed NOS-immunopositive neurons in the deep tectal layers of the turtle *Pseudemys scripta*, and suggested that NOS-positive fibers originating from the periventricular gray leave the tectum in a way corresponding to the tecto-bulbar and tecto-thalamic tract. Efferent pathways of the amphibian optic tectum have been demonstrated by LÁZÁR and co-workers (LÁZÁR, 1969; LÁZÁR *et al.*, 1983) and include projections to the ipsilateral dorsal thalamic nuclei and the ipsilateral isthmic nucleus (BUTLER & HODOS, 1996) (Fig. 6). Further labeling and tracing studies are necessary to demonstrate that NOergic neurons indeed are involved in the crossed tecto-bulbar pathway (as suggested by BRÜNING & MAYER, 1994) and also to demonstrate their synaptic input.

In contrast to most mammalian species studied (reviewed in HUGHES, 1990b), in the optic tectum of frogs and turtles the neurons that give rise to the crossed tecto-bulbar pathway have dendrites that extend into the retino-recipient superficial layers of the tectum. This was *e.g.* demonstrated using the HRP-labeling and the cobalt filling technique in the frog (LÁZÁR *et al.*, 1983). The latter finding is consistent with the view that the neurons that give rise to the frog's crossed tecto-bulbar pathway receive a direct retinal input, and also suggests that the neurons may receive this input from more than one type of retinal ganglion cell (HUGHES, 1990b). Moreover, a gradient-like distribution of these neurons with preferential location at the ventrolateral border has been described in many amphibians, reptiles, birds and mammals, although with some dissimilarities, indicating a fundamental role in tectal functioning (HUGHES, 1990b). HUGHES (1990b) suggests that the spatial gradient of these deep tectal neurons underlies the functional gradients in the control of orienting movements, such as demonstrated in the cat (MCILWAIN, 1982).

CONCLUDING REMARKS

In the introduction we referred to some studies suggesting a «macroscopic» role of NO in memory, through processes at a «microscopic» or molecular level, corresponding to long-lasting response modulation (in neurons) and fast function synchronization (in cells in general). When looking at the microscopic neuroanatomy of NOS-containing neurons in *Xenopus laevis*, a complex neuronal web emerges. Comparison of the distribution of bNOS-immunopositive and NADPH-d reactive neurons with the results of a literature survey of tract tracing studies of targets of the visual system in amphibians, shows that NOS is present in many (if not all) tracts and centers involved in orientation and visual information processing. The interrelationship between orientation and visual recognition suggested is based on at least two arguments: **(1)** the anatomy and ultrastructure of the optic tectum (see *e.g.* HUGHES, 1990a,b) and **(2)** the connections between the optic tectum and the pars lateralis of the amygdala, which is the main target of the vomeronasal organ, indicating a possible integration of visual and other sensory input (reviewed in NORTHCUTT & KICLITER, 1980). Despite the multi-functional character and relatively unspecialized

aspect of the amphibian telencephalic lateral wall, the overall simplicity of the amphibian telencephalon may favor both macroscopic and microscopic approaches to the study of the role of NOergic transmission in the vertebrate brain. Pharmacological *in vivo* studies (using NOS inhibitors, guanylate cyclase activators and/or specific phosphodiesterase inhibitors) and also further neuroanatomical tracing studies will be necessary to prove the suggested link between NOergic transmission and the visual system, as already shown in parts of the visual system in birds and mammals (WILLIAMS *et al.*, 1994; CUDEIRO *et al.*, 1994).

ACKNOWLEDGEMENTS

This work was supported by a fellowship from the Human Capital & Mobility (HCM)-network of the European Community (Contract ERBCHRXCT920017), grant number 805-26.241 from the Stichting Levenswetenschappen (subsidized by the Dutch Organization of Scientific Research, NWO) and an NWO/INSERM exchange grant. We thank Dr. Bruce G. Jenks (University of Nijmegen) and Dr. Wil Smeets (Free University of Amsterdam) for critical comments.

REFERENCES

ALLAERTS, W., R. UBINK, M. BUZZI, B.G. JENKS & E.W. ROUBOS (1997) – Role of nitric oxide synthase and nitric oxide in background adaptation in *Xenopus laevis*. *Ann. N.Y. Acad. Sci.*, (in press).

ANBAR, M. (1995) – Nitric oxide: a synchronizing chemical messenger. *Experientia,* **51**: 545-550.

BARINAGA, M. (1991) – Is nitric oxide the «retrograde messenger»? *Science,* **254**: 1296-1297.

BRÜNING, G. & B. MAYER (1996) – Localization of nitric oxide synthase in the brain of the frog, *Xenopus laevis*. *Brain Res.,* **741**: 331-343.

BRÜNING, G., S. WIESE & B. MAYER (1994) – Nitric oxide synthase in the brain of the turtle *Pseudemys scripta elegans*. *J. Comp. Neurol.,* **348**: 183-206.

BUTLER, A.B. & W. HODOS (1996) – *Comparative Vertebrate Neuroanatomy*. New York, Wiley & Sons Publ., 514 pp.

BUTLER, A.R., F.W. FLITNEY & D.L.H. WILLIAMS (1995) – NO, nitrosoniumions, nitroxide ions, nitrosothiols and iron-nitrosyls in biology: a chemist's perspective. *T.I.P.S.,* **16**: 18-22.

CUDEIRO, J., K.L. GRIEVE, C. RIVADULLA, R. RODRIGUEZ, S. MARTINEZ-CONDE & C. ACUNA (1994) – The role of nitric oxide in the transformation of visual information within the dorsal lateral geniculate nucleus of the cat. *Neuropharmacology,* **33**: 1413-1418.

DAWSON, T.M., D.S. BREDT, M. FOTUHI, P.M. HWANG & S.H. SNYDER (1991) – Nitric oxide synthase and neuronal NADPH diaphorase are identical in brain and peripheral tissues. *Proc. Natl. Acad. Sci. USA,* **88**: 7797-7801.

DE RIJK, E.P.C.T., F.J.C. VAN STRIEN & E.W. ROUBOS (1992) – Demonstration of coexisting catecholamine (dopamine), amino acid (GABA), and peptide (NPY) involved in inhibition of melanotrope cell activity in *Xenopus laevis*: a quantitative ultrastructural, freeze-substitution immunocytochemical study. *J. Neurosci.,* **12**: 864-871.

GARTHWAITE, J. & C.L. BOULTON (1995) – Nitric oxide signaling in the central nervous system. *Annu. Rev. Physiol.,* **57**: 683-706.

GARTHWAITE, J., S.L. CHARLES & R. CHESS-WILLIAMS (1988) – Endothelium-derived relaxing factor release on activation of NMDA receptors suggests roles as intercellular messenger in the brain. *Nature,* **336**: 385-388.

GONZÁLEZ, A., A. MUÑOZ, M. MUÑOZ, O. MARÍN, R. ARÉVALO, A. PORTEROS & J.R. ALONSO (1996) – Nitric oxide synthase in the brain of a urodele amphibian (*Pleurodeles waltl*) and its relation to catecholaminergic neuronal structures. *Brain Res.,* **727**: 49-64.

GRUBERG, E.R. & V.R. AMBROS (1974) – A forebrain visual projection in the frog (*Rana pipiens*). *Exp. Neurol.,* **44**: 187-197.

HALL, W.C. & F.F. EBNER (1970) – Thalamotelencephalic projections in the turtle (*Pseudemys scripta*). *J. Comp. Neurol.,* **140**: 187-197.

HERRICK, C.J. (1925) – The amphibian forebrain. III. The optic tracts and centers of *Amblystoma* and the frog. *J. Comp. Neurol.,* **39**: 433.

HERRICK, C.J. (1948) – *The Brain of the Tiger Salamander.* University of Chicago Press, Chicago (*fide* Northcutt and Kicliter, 1980).

HSU, S.M., L. RAIND & H. FANGER (1981) – Use of avidin-biotin-peroxidase complex (ABC) in immunoperoxidase technique. A comparison between ABC and unlabeled antibody (PAP) procedures. *J. Histochem. Cytochem.,* **29**: 577-580.

HUGHES, T. (1990a) – A light- and electron-microscopic investigation of the optic tectum of the frog, *Rana pipiens*, I: The retinal axons. *Visual Neurosci.,* **4**: 499-518.

HUGHES, T. (1990b) – A light- and electron-microscopic investigation of the optic tectum of the frog, *Rana pipiens*, II: The neurons that give rise to the crossed tecto-bulbar pathway. *Visual Neurosci.,* **4**: 519-531.

JANSEN, K., C. FABRO, C. ARTERO, M. FEUILLOLEY, H. VAUDRY, A. FASOLO & M.F. FRANZONI (1997) – Characterization of pars intermedia connections in amphibians by biocytin tract tracing and immunofluorescence aided by confocal microscopy. *Cell Tissue Res.,* **287**: 297-304.

KARAMIAN, A.I., N.P. VESSELKIN, M.G. BELEKHOVA & T.M. ZAGORULKO (1966) – Electrophysiological characteristics of tectal and thalamo-cortical divisions of the visual system in lower vertebrates. *J. Comp. Neurol.,* **127**: 559-576.

KARTEN, H.J. & A.M. REVZIN (1966) – The afferent connections of the nucleus rotundus in the pigeon. *Brain Res.,* **2**: 368-377.

KARTEN, H.J. & W.J.H. NAUTA (1968) – Organization of the retinothalamic projections in the pigeon and owl. *Anat. Rec.,* **160**: 373.

KARTEN, H.J., W. HODOS, W.J.H. NAUTA & A.M. REVZIN (1973) – Neural connections of the «visual wulst» of the avian telencephalon. Experimental studies in the pigeon (*Columba livia*) and owl (*Speotyto cunicularia*). *J. Comp. Neurol.,* **150**: 253-278.

KICLITER, E. & R.G. NORTHCUTT (1975) – Ascending afferents to the telencephalon of ranid frogs: an anterograde degeneration study. *J. Comp. Neurol.,* **161**: 239-253.

KICLITER, E. (1979) – Some telencephalic connections in the frog, *Rana pipiens. J. Comp. Neurol.,* **185**: 75-86.

LÁZÁR, G. (1969) – Efferent pathways of the optic tectum in the frog. *Acta biol. Acad. Sci. hung.,* **20**: 171-183.

LÁZÁR, G., P. TOTH, G. CSANK & E. KICLITER (1983) – Morphology and location of tectal projection neurons in frogs: a study with HRP and cobalt filling. *J. Comp. Neurol.,* **215**: 108-120.

MCILWAIN, J.T. (1982) – Lateral spread of neural excitation during microstimulation in intermediate gray layer of cat's superior colliculus. *J. Neurophysiol.,* **47**: 167-178.

McLEAN, J.W. & P.K. NAKANE (1974) – Periodate-lysine-paraformaldehyde fixative: a new fixative for immunoelectron microscopy. *J. Histochem. Cytochem.,* **22**: 1077-1083.

MUNOZ, M., A. MUÑOZ, O. MARÍN, J.R. ALONSO, R. ARÉVALO, A. PORTEROS & A. GONZÁLEZ (1996) – Topographical distribution of NADPH-diaphorase activity in the central nervous system of the frog, *Rana perezi. J. Comp. Neurol.,* **367**: 54-69.

NEARY, T.J. & R.G. NORTHCUTT (1983) – Nuclear organization of the bullfrog diencephalon. *J. Comp. Neurol.,* **213**: 262-278.

NIEUWENHUYS, R. & P. OPDAM (1976) – Structure of the brain stem. *In*: R. LLINÁS & W. PRECHT (eds.), *Frog Neurobiology.* New York, Springer Verlag: 811-855.

NORTHCUTT R.G. & E. KICLITER (1980) – Organization of the amphibian telencephalon. *In:* S.O.E. EBBESON (Ed.), *Comparative Neurology of the Telencephalon.* New York, Plenum Press: 203-255.

PASTI, L., T. POZZAN & G. CARMIGNOTO (1995) – Long-lasting changes of calcium oscillations in astrocytes. *J. Biol. Chem.,* **270**: 15203-15210.

POTTER, H.D. (1969) – Structural characteristics of cell and fiber populations in the optic tectum of the frog (*Rana catesbeiana*). *J. Comp. Neurol.,* **136**: 203-232.

RUBINSON, K. (1968) – Projections of the tectum opticum of the frog. *Brain Behav. Evol.,* **1**: 529.

SCALIA, F. & K. GREGORY (1970) – Retinofugal projections in the frog: location of the postsynaptic neurons. *Brain Behav. Evol.,* **3**: 16-29.

SCHUMAN, E.M. & D.V. MADISON (1991) – A requirement for the intracellular messenger nitric oxide in long term potentiation. *Science,* **254**: 1503-1506.

SHIBUKI, K. & D. OKADA (1991) – Endogenous nitric oxide release required for long-term synaptic depression in the cerebellum. *Nature,* **349**: 326-328.

SMEETS, W.J.A.J., J.R. ALONSO & A. GONZÁLEZ (1997) – Distribution of NADPH-diaphorase and nitric oxide synthase in relation to catecholaminergic neuronal structures in the brain of the lizard *Gekko gecko. J. Comp. Neurol.,* **377**: 121-141.

TILDERS, F.J. & F. BERKENBOSCH (1986) – CRF and catecholamines; their place in the central and peripheral regulation of stress-response. *Acta Endocrinol. Copenh. (suppl.),* **276**: 63-75.

TUINHOF, R., F.Y.S.C. LAURENT, R.G.E. EBBERS, W.J.A.J. SMEETS, M.C.H.M. VAN RIEL & E.W. ROUBOS (1993) – Immunocytochemistry and *in situ* hybridization of neuropeptide Y in the hypothalamus of *Xenopus laevis* in relation to background adaptation. *Neuroscience,* **55**: 667-675.

TUINHOF, R., C. ARTERO., A. FASOLO, M.F. FRANZONI, H.J. TEN DONKELAAR, P.G.P. WISMANS & E.W. ROUBOS (1994) – Involvement of retinohypothalamic input, suprachiasmatic nucleus, magnocellular nucleus and locus coeruleus in control of melanotrope cells of *Xenopus laevis*: a retrograde and anterograde tracing study. *Neuroscience,* **61**: 411-420.

WILLIAMS, C.V., D. NORDQUIST & S.C. MCLOON (1994) – Correlation of nitric oxide synthase expression with changing patterns of axonal projections in the developing visual system. *J. Neurosci.,* **14**: 1746-1755.

Belg. J. Zool. - Volume 127 (1997) - issue 1 - pages 35-45 - Brussels 1997

RECOMBINANT PROTEIN EXPRESSION IN INSECT CELL SYSTEMS

ROGER HUYBRECHTS, VEERLE VULSTEKE, JEROEN POELS, ERWIN LAUWERS, JOZEF VANDEN BROECK AND ARNOLD DE LOOF

Catholic University of Leuven, Laboratory of Developmental Physiology and Molecular Biology, Zoological Institute, Naamsestraat 59, B-3000 Leuven, Belgium.
e-mail: roger.huybrechts@bio.kuleuven.ac.be

Abstract. Since the introduction of baculovirus expression vectors, the suitability of insect cells for the expression of functionally active genes of eukaryotic origin has been exhaustively documented. Originally realization of a functional viral expression vector was laborious and depended on double homologous *in vivo* recombination success as well as successful purification of recombinant baculovirus by plaque assay. Using the commercial Bac to Bac™ expression system we confirm that transposon-assisted recombination and cloning of recombinant transfectable bacmid DNA in bacteria now allow fast productive expression of a gene of interest.

As an alternative to the expression by infected cells which sometimes suffers from the effects induced by cell lysis, we developed a stable *Drosophila* S-2 cell transformation protocol using the constitutive promoter of the immediate early gene of the silkworm baculovirus (BmNPV). Although baculovirus immediate early gene promoters are reported to be rather weak promoters, we routinely obtain expression levels up to the same range as obtained with the baculovirus system.

Keywords: transient expression, *baculovirus*, stable transformation.

INTRODUCTION

Less than two decades ago knowledge of protein diversity, functionality and structural organization mainly depended on, and was limited by, developments in protein identification, separation and purification technology. Hitherto, proteins of low abundance were only purified and structurally characterized when financial revenues could be *a priori* assured due to specific therapeutic (*e.g.* insulin), enzymatic (*e.g.* hirudin) or antigenetic (*e.g.* viral coat proteins for vaccine production) properties of the protein. Since the introduction of recombinant DNA and bacterial transformation technology it became clear that original limitations such as the need for an abundant natural source of the protein to be purified, were no longer valid. Due to the lack of posttranslational protein processing in bacterial hosts, restriction of expression to a prokaryotic environment in many cases results in the production of functionally inactive and/or structurally changed proteins.

Contribution to the 3th Benelux Congress of Zoology, Namur, November 1996.

Whereas bacterial hosts remain irreplacable for rapid gene cloning, amplification and manipulation, new alternatives for gene expression and mass production of particular recombinant proteins needed to be explored. Among the resulting eukaryotic expression systems those based on yeast cells (*Saccharomyces cerivisiae*, *Pichia pastoris*) are considered to be most efficient and cost effective but they still have peculiar processing properties which make them unsuitable for the expression of particular proteins (HERSCOVICS & ORLEAN, 1993; KALSNER *et al.*,1992). In those situations, the choice of a suitable expression system is mainly limited to either expression in insect (LUCKOW, 1991) or mammalian (JENKINS & CURLING, 1994) cells and, in specific situations, to production in transgenic animals (DAMAK *et al.*, 1996). One major drawback of the mammalian *in vitro* expression systems (*CHO* cells, hybridoma cell lines) is their limited productivity due to the lack of strong promoters. This limitation probably explains the wide range of recombinant proteins of mammalian origin that became preferentially produced in the heterologous insect cell based expression system. The availability of strong promoters for expression in insect cells and the resulting higher yields, together with the functionally active proteins obtained (JARVIS & SUMMERS, 1992) added to the world-wide use of this system which we will further elaborate in this paper.

TRANSIENT EXPRESSION OF RECOMBINANT PROTEINS IN INSECT CELLS USING BACULOVIRUS EXPRESSION VECTORS

Baculoviruses

The term baculovirus designates a particular group of viruses that only replicates in invertebrates and therefore can be considered safe for humans and vertebrates in general. In the context of *baculovirus* expression vectors, only a particular subgroup of so-called nuclear polyhedrosis viruses (NPV's) is considered. These NPV's are characterized by their double life cycle. Early in the infection cycle assembled virions are released by budding from the host cell membrane. Later in the infection cycle virions become enveloped inside the cell nucleus and end up embedded inside a crystalline matrix of viral encoded polyhedrin protein. This embedding results in microscopically visible polyhedrons or occlusion bodies inside the nucleus and an easily recognized cytopathogenic effect which is typical for all nuclear polyhedrosis viruses.

Rapid accumulation of polyhedrin protein late in the infection cycle points towards the presence of a strong promoter controlling this gene. Furthermore, in an *in vitro* situation, only extracellular viruses are needed for re-infection of new cells. These observations suggested the use of the polyhedrin gene as a favoured site for foreign gene insertion. Placing a foreign gene downstream of the strong polyhedrin gene promoter indeed resulted in a recombinant viral expression vector which, once used for insect cell infection, in most cases allowed the production of large amounts (up to µg/ml) of the recombinant protein.

Baculovirus expression in practice

Baculoviruses, having a double stranded circular DNA genome of +/-120 kb, are not suitable *per se* for direct *in situ* cloning of a foreign gene. As explained in Fig. 1 production of a recombinant baculovirus expression vector involves cloning the gene downstream of the polyhedrin promoter present in a so-called transfer plasmid. In this transfer plasmid the polyhedrin expression cassette is flanked at both sides by viral sequences which also flank the polyhedrin gene in the intact wildtype virus. By cotransfecting DNA of the recombinant transfer plasmid together with DNA of wildtype virus into insect host cells (*e.g.* Sf-9 cells) homologous recombination between corresponding flanking sequences present in both DNA's takes place and results in an exchange of the polyhedrin gene of the wildtype virus for the polyhedrin expression cassette. As a result of this cotransfection, within a few days both recombinant virions as well as wildtype virions will start to accumulate in the culture medium of such transfected cells. In a second important step the recombinant viruses need to be cloned from the mainly wildtype virus-contaminated pool by subsequent rounds of so-called plaque purification. Once an inoculum of pure recombinant virus is obtained and following a gradual scaling up of viral progeny by reinfection cycles of increasing cell numbers, the productive infection of insect cells can be started. Since expression of the gene of interest depends upon viral infection, the recombinant protein production though high in relative yield is short in duration due to lysis and death of the host cells. Reinfection of new host cells is the only means of obtaining larger amounts of the desired recombinant protein.

In terms of production it should be mentioned that the lepidopteran host cells can be cultured either in an adhering monolayer, which is most appropriate during transfection and plaques purification cycles, or in suspension cultures allowing higher cell densities. The use of suspension cultures is most suitable for this productive expression.

Pitfalls and improvements in the production of recombinant baculovirus expression vectors

Successful production of a recombinant baculovirus expression vector assumes both experience in insect cell culture technology and in basic viral handling practice. The former should not be a real drawback since culturing insect cells is not as demanding as culturing mammalian cells. Equipment needed is absolutely minimal, except for the summer period when a refrigerated incubator may become necessary since the lepidopteran cells have optimum growth characteristics below 28°C. On the other hand no atmospheric regulation is necessary and insect cells can be cultured in closed culture flasks. Several culture media are commercially available and usually need to be supplemented with 10% of insect cell qualified, heat inactivated, fetal calf serum for optimal growth performance. During productive expression the fetal calf serum supplemented medium can be replaced by serum free media which is also commercially available. Concerning viral handling, at least during the starting period, some practical assistance might be most welcome but it can be learned by trial and error as well. In terms of safety considerations, as mentioned earlier, baculoviruses *per se* are harmless for the experimenter. It should be mentioned however that although the viruses do not replicate in human cells, internalisation by non- permis-

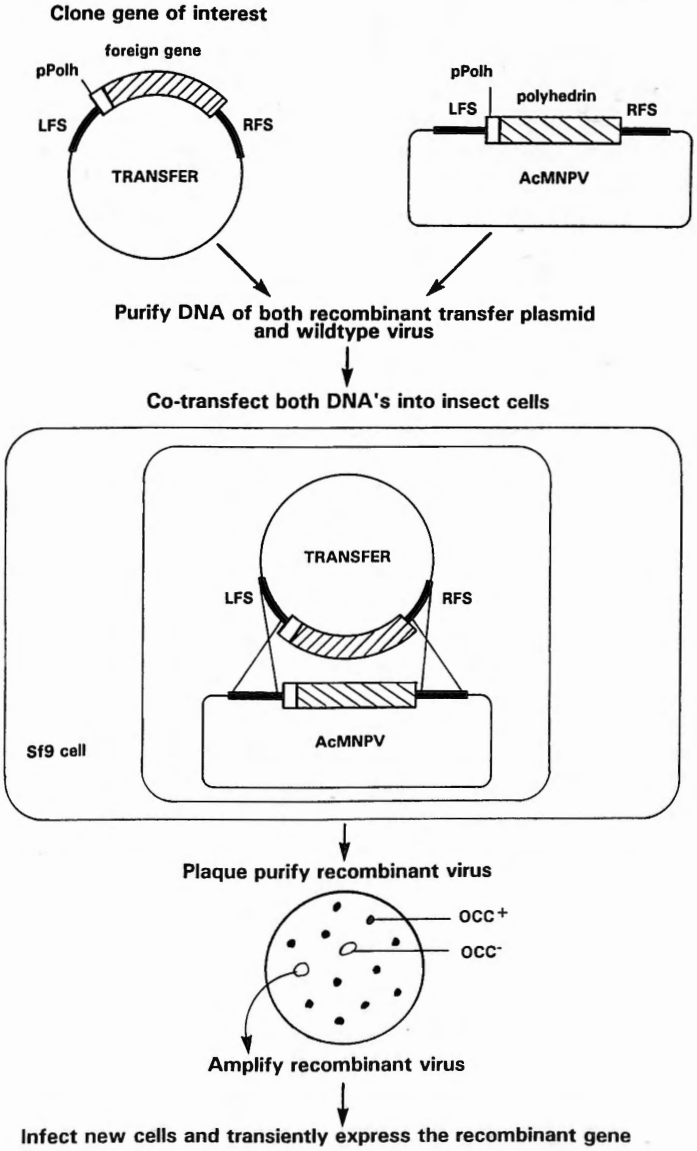

Fig. 1. – Schematic representation of the classical baculovirus expression system: The gene of interest (either gDNA or cDNA) is cloned in a polycloning site downstream of the strong polyhedrin promoter. Upon cotransfection of host cells with both the recombinant transfer plasmid and purified viral DNA, recombinant baculovirus generation is based upon a double homologous recombination event between polyhedrin flanking sequences that are present in both DNA's. In the absence of any recombination event wildtype virus is assembled and released as well. Several rounds of plaque purification are needed to obtain pure recombinant baculovirus suitable for productive expression during subsequent infection rounds.

sive cells is well known and transactivating effects by viral early genes can never be excluded. Especially in those situations in which baculoviruses containing human genes or genes of human pathogens are constructed those viruses should be handled with appropriate care and always in conformance with local biosafety regulations.

One major technical limitation of the classical production of recombinant baculovirus is the dependence upon the success of the double homologous recombination which needs to take place following co-transfection of both viral and recombinant transfer vector DNA. Depending on the DNA quality, the outcome of homologous recombination can result in about 3% of the viruses produced being good recombinants. However in most cases less than 1% of recombinants can be observed during subsequent plaques purification. This cloning of recombinant viruses is most tricky. In the classic situation the difference between wildtype or occlusion body positive plaques and recombinant or occlusion body negative plaques has to be established with the microscope. With a trained eye this is not really difficult. Newcomers are advised to pick-up as many plaque-resembling spots as possible. Following infection of cells in a multiwell plate with viruses present in those plaques, the identity of the plaques can then be simply determined by PCR using a combination of either universal polyhedrin based primers or more specifically using a combination of one gene specific primer with either one of both universal primers.

Suppliers of commercial kits (In Vitrogen, Pharmingen, GibcoBRL-Life Technologies,...) are aware of the inexperience of most researchers trying baculovirus expression. To overcome these difficulties several approaches have been introduced (DAVIES, 1994). Generally the wildtype virus DNA delivered with those kits is linearized by a single digestion in the polyhedrin region. In theory linear viral DNA should not replicate and in theory only recircularisation following recombination can result in virus production. In practice a high number of wildtype plaques is observed due to the need for double homologous recombination, usually preceded by single recombination. Alternatively a marker gene is integrated in either the viral DNA used for cotransfection or, preferably in the transfer vector used for making the desired recombinant construct. In both cases this marker gene helps with the recognition and identification of recombinant plaques. A better alternative is the use of an artificial deletion mutant of wildtype viral DNA for co-transfection. In such a mutant an essential gene is deleted and functionally repaired only in recombinants. As a result only recombinant viral progeny is produced and plaque purification can be omitted.

More recently LUCKOW and co-workers (1993) developed a baculovirus expression system in which most steps up to the production of transfectable recombinant viral DNA are performed in bacteria (see Fig. 2). By making use of the Tn7 bacterial transposase this system became independent of random recombination events. Extension of this system with a traditional blue/white selection of true recombinants makes the conventional cloning of the gene of interest in the donor plasmid the most difficult part of the entire procedure. Most importantly, with this bac to bac™ system a significant time saving is achieved making it the best choice in those situations in which high numbers of recombinant viruses need to be produced within a limited time period. Following some preliminary trials we are now using this bac to bac protocol with good results on a routine basis (POELS, 1996; HUYBRECHTS, unpublished).

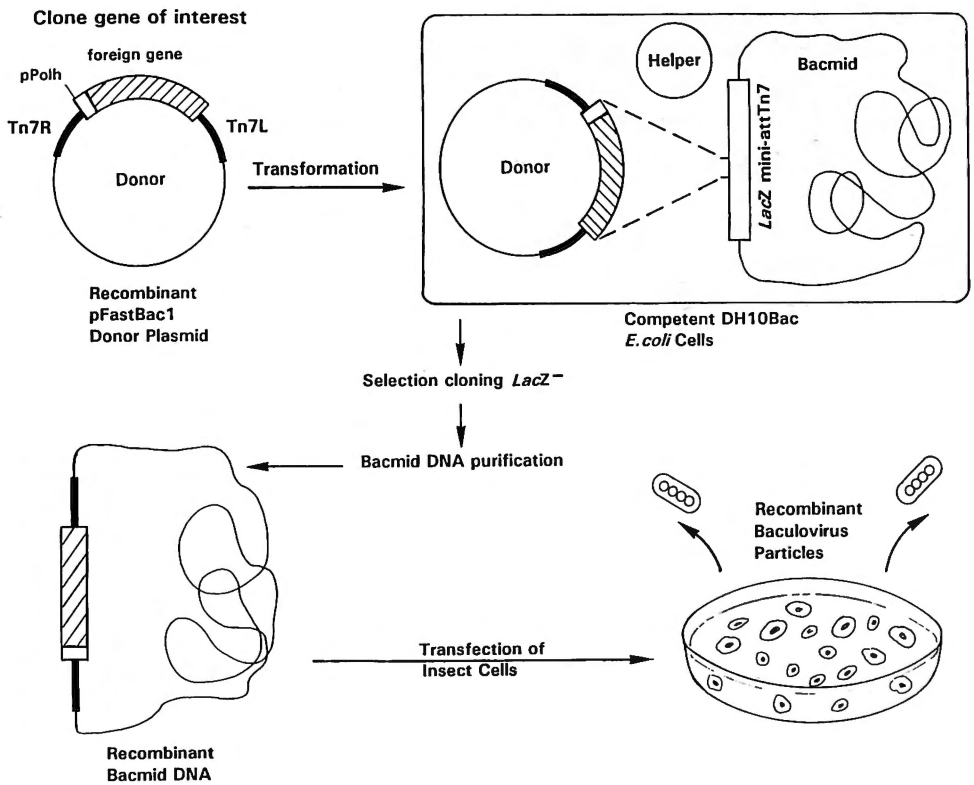

Fig. 2. – Schematic explanation of the Bac to Bac™ protocol for rapid production of recombinant baculovirus: Following cloning of the gene downstream of the polyhedrin promoter present in a donor plasmid, the purified recombinant donor plasmid is used for transformation of DH10 Bac cells. These host cells contain a replicating baculovirus genome having the polyhedrin open reading frame replaced by LacZ and being flanked with Tn7 attachment sites. A helper plasmid delivering the Tn7 transposase in trans is also present in these DH10Bac cells and will transpose the polyhedrin transcription unit of the donor plasmid (*cfr.* presence of flanking Tn7 donor sites) into the attachment site as present in the bacmid. After plating and growing of the transformed bacteria, a white colony is selected and bacmid DNA purified. This recombinant Bacmid DNA once transfected into insect host cells will generate recombinant baculovirus only. Since no contaminating wildtype baculovirus is released no plaque purification is needed and productive infection of host cells can be started immediately. (Bac to Bac™ is distributed by GibcoBRL-Life Technologies).

CONTINUOUS EXPRESSION IN INSECT CELLS FOLLOWING PRODUCTION OF STABLE TRANSFORMED CELL LINES

Although the baculovirus expression system became one of the most widely used methods for the quantitative production of a variety of recombinant proteins, it should be noted that protein expression is maximal in cells near death due to viral infection.

Obviously in many cases this is suboptimal for correct overall processing of the protein of interest and, more importantly may result in high levels of protein degradation due to the release of proteolytic enzymes during lysis of infected cells. On the other hand the advantage of high expression levels due to the functioning of strong extra late viral promoters (cfr. supra polyhedrin promoter but equally the well known P10 promoter) can still not be realized outside an intact viral and *in se* lytic environment.

In practice, good alternative expression using the advantages of an insect cell based expression environment can be realized making use of early baculovirus promoters for driving the expression of the gene of interest in a constitutive and therefore continuous way. In contrast to the extra late viral gene promoters which need a cascade of transactivating

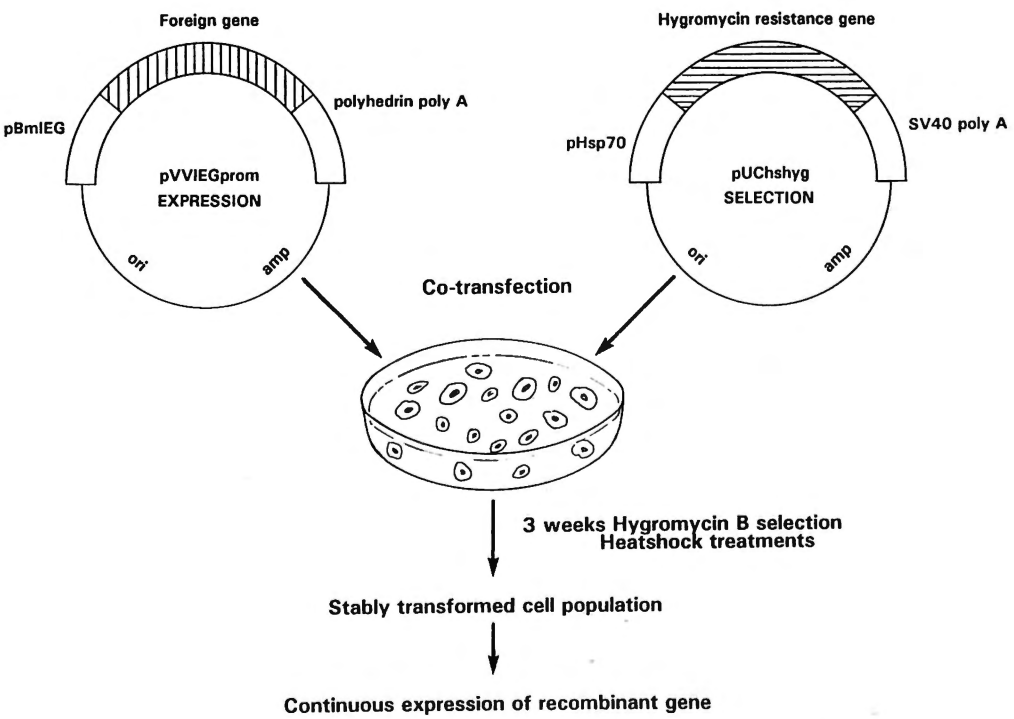

Fig. 3. – Overview of the protocol for the production of stable transformed insect cell lines for constitutive expression of a gene of interest. The gene to be expressed is inserted into a polycloning site downstream of the pBMIEG promoter present in the expression plasmid which contains appropriate transcription termination and poly-adenylation signals originating from the polyhedrin gene. When *Drosophila* S-2 cells are used as expression environment, selection for true chromosomal integration is best accomplished by cotransfection of the expression plasmid and a Hygromycin-B resistance gene containing plasmid (*e.g.* pUChshyg). Since here the resistance gene is situated downstream of the inducible *Drosophila* heatshock hsp70 promoter, repeated heatshock treatments are necessary as long as cells are grown in Hygromycin-B (240 µg/ml) containing medium. Usually a three week selection period is sufficient for obtaining stable transformed cells that contain both the selection and expression plasmid.

events by a still obscure array of viral encoded proteins in order to become functional, these early baculoviral genes use the host cells own polymerase II transcription activation machinery. As a consequence, simple plasmid constructs containing the gene of interest cloned downstream of an immediate early baculovirus gene promoter will, upon simple transfection into insect cells, even those originating from insects of non-lepidoperan orders, result in transient production of the corresponding recombinant protein (HUYBRECHTS *et al.*, 1992). Continuous expression can be achieved when transfected cells can be selected for genomic integration of the recombinant expression cassette. As illustrated in Fig. 3 this is realized in practice by cotransfecting a recombinant expression plasmid together with a second selection plasmid carrying an antibiotic resistance gene preferentially placed under control of an inducible promoter. It became empirically evident that selection for integration of the selection plasmid results in a resistant cell population carrying the expression plasmid in their genome as well (see Fig. 4 as well as VULSTEKE *et al.*,1993; VANDEN BROECK *et al.*, 1995; LAUWERS, 1996). It was further evidenced that such transformed cells remained stable even without continued selection. In Fig. 5 it is well documented that in contrast to earlier predictions concerning the rather low strength of such early baculovirus promoters this continuous expression system can become at least as productive as the classic polyhedrin promoter based expression system. In part this is explained by the possibility of obtaining extremely high cell densities with the Schneider S-2 cells compared to the Lepidoptera Sf9 cell line we use in the respective context. Additionally it can be concluded that in the continuous expression system, accumulation

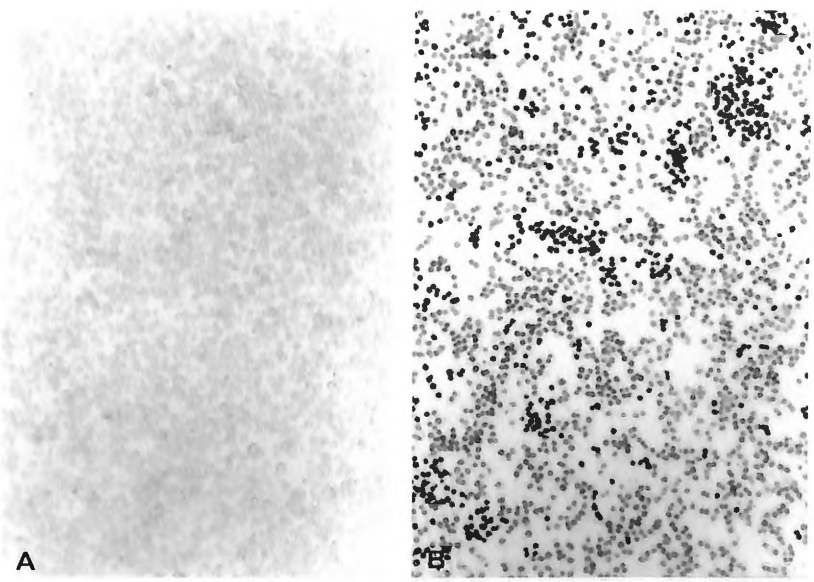

Fig. 4. – Illustration of a typical cotransfection and selection result during production of stable transformed S-2 cells. A lacZ coding sequence was used for constructing the recombinant expression plasmid (*cfr.*VULSTEKE *et al.* 1993 for specific details). Panel B clearly illustrates that all cells of the Hygromycin-B resistant population stain X-gal positive as well. Control cells (panel A) do not show any endogenous galactosidase activity. Differences in staining intensities between individual cells are explained by differences in integrated copy numbers of the expression plasmid.

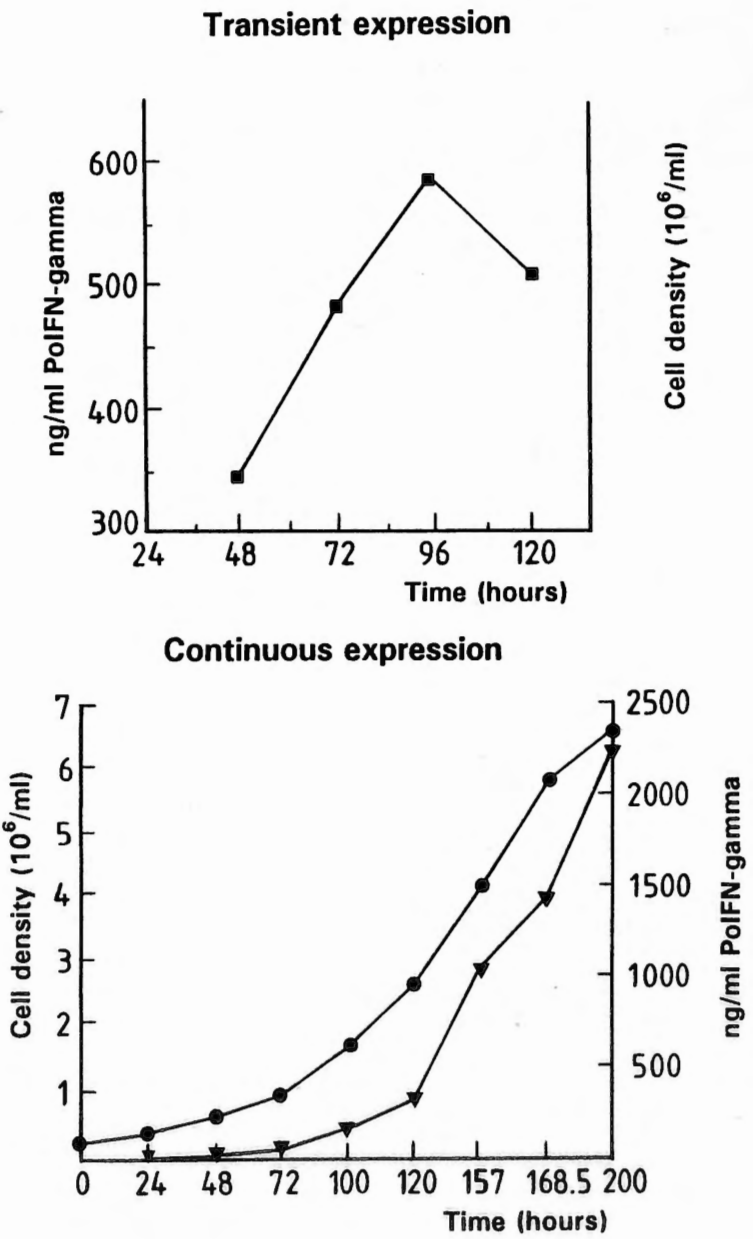

Fig. 5. – Comparison of porcine interferon-gamma production, as determined by a sandwich ELISA (*cfr.* VANDEN BROECK *et al.*, 1994) in a transient recombinant baculovirus based Sf-9 cell system (left panel) and in a continuously expressing, stable transformed S-2 cell system (right panel). In both situations the experiment started from a cell density of $2.5.10^5$ cells /ml. In contrast to the infected cells in which cell division is arrested, the continuously expressing cells (filled dots) continue dividing up to densities of almost 6.10^6 cells/ml without any apparent deleterious effect.

of recombinant protein over a far more extended period is possible without a decline, due to proteolytic damage, in immunologically recognized recombinant protein (LAUWERS, 1996). Comparing promoter activities at transcription level further demonstrated that polyhedrin as well as the early gene promoter results in comparable amounts of transcripts (VANDEN BROECK *et al.*, 1995). This last observation is most probably explained by the extremely high copy numbers of integrated recombinant genes that are usually observed following stable transformation (VULSTEKE, 1995).

CONCLUSIONS

Thanks to the success of baculovirus expression systems, insect cells are recognized as an acceptable environment for the recombinant expression of eukaryotic cDNA and of intron containing genes (IATROU *et al.*, 1988; GOPINATHAN personal communication). Functionality of the expressed proteins is guaranteed and major posttranslational processing events will occur. The original limitation of insect cells having only mannose-type glycosylation properties is now almost circumvented by both selection of cell lines with improved processing characteristics (OGONAH, 1996) as well as by co-expression of genes coding for the necessary enzymes (JARVIS & FINN, 1996). High yields of recombinant protein production and expression in an insect cell environment, both considered as major advantages of the baculovirus expression system, can now be achieved using the continuous S-2 cell and BmNPVIEG promoter based expression system (this paper).

ACKNOWLEDGEMENTS

We would like to thank the team of Prof. A. Billiau (Rega Instituut, K.U.Leuven) for providing the porcine interferon-gamma cDNA as well as the anti-interferon-gamma antibodies.

The «Onderzoeksraad K.U.Leuven (0T90.015), The EC (ERB-C11*-CT94-0092) and the (N)FWO (G.0260.96, G.2169.94) are acknowledged for financially contributing to the realization of this research.

The assistance of Ms. J. Puttemans in the realization of the illustrations is appreciated.

REFERENCES

DAMAK, S., H. SU, N.P. JAY & D.W. BULLOCK (1996) – Improved wool production in transgenic Sheep expressing insulin-like growth factor 1. *Biotechnology*, **14**:185-188.

DAVIES, A.H. (1994) – Current methods for manipulating baculoviruses. *Biotechnology*, **12**: 47-50.

HERSCOVICS, A.O. & P. ORLEAN. (1993) – Glycoprotein biosysnthesis in yeast. *Faseb J.*, **7**: 540-550.

HUYBRECHTS, R., L. GUARINO, M. VAN BRUSSEL & V. VULSTELE (1992) – Nucleotide sequence of a transactivating *Bombyx mori* nuclear polyhedrosis virus immediate early gene. *Biochim. Biophys. Acta*, **1129**: 328-330.

IATROU, K., R.G. MEIDINGER, D.H. SCHMIEL, M.H.M. TRAN, E.M. MOLNAR & A.V.VIEIRA (1988) – Towards the development of a vector for transducing homologous and foreign genes into silkmoth

tissue culture cells and animals. In: *Endocrinological frontiers in physiological insect ecology.* F. SEHNAL, A. ZABZA & D.L. DENLINGER (Eds.): 1055-1074.

JARVIS, D.L., & E.E. FINN (1996) – Modifying the insect cell N-glycosylation pathway with immediate early baculovirus expression vectors. *Nature Biotechnology*, **14**: 1288-1292.

JARVIS, D. & M.D. SUMMERS (1992) – Baculovirus expression vectors In: *Recombinant DNA Vaccines: Rationale and Strategies.* ISAACSON, R.E.(Ed.). Marcel Dekker, New York: 265-291.

JENKINS, N. & E.M. CURLING (1994) – Glycosylation of recombinant proteins, problems and prospects. *Enzyme Microb.Technol.*, **16**: 354-364.

KALSNER, I., F.J. SCHNEIDER, R. GEYER, H. AHORN & I. MAURERFOGY (1992) – Comparison of the carbohydrate moieties of recombinant soluble Fc-epsilon receptor (sFc-e-RII/scd23) expressed in *Saccharomyces cerevisiae* and chinese hamster ovary cells- different O-glycosylation sites are used by yeast and mammalian cells. *Glyconjugate J.*, **9**: 209-216.

LAUWERS, E. (1996) – Expressie van varkensinterferon-gamma in stabiel getransformeerde *Drosophila* S-2 cellen. Licentiaatsverhandeling, K.U.Leuven (English summary).

LUCKOW, V. (1991) – Cloning and expression of heterologous genes in insect cells with baculovirus vectors. In: *Recombinant DNA technology and applications.* PROKOP, A.N, R.K. BAJPAI & C.S. HO (Eds.), McGraw-Hill, Inc., New York: 97-114.

LUCKOW, V.A., S.C. LEE, G.F. BARRY & P.O. OLINS (1993) – Efficient generation of infectious recombinant baculovirus by site specific transposon mediated insertion of foreign genes into a baculovirus genome propagated in *Escherichia coli. J. Virol.*, **67**: 4566- 4579.

OGONAH O.W., R.B. FREEDMAN, N. JENKINS, K. PATEL & B.C. ROONEY (1996) – Isolation and characterization of an insect cell line able to perform complex N-linked glycosylation on recombinant proteins. *Biotechnology*, **14**: 197-202.

POELS, J. (1996) – Productie van recombinant baculovirus gebruikmakend van het bacterieel Tn7 transposon. Licenciaatsverhandeling, K.U.Leuven (English summary).

VANDEN BROECK, J., V. VULSTEKE, R. HUYBRECHTS & A. DE LOOF (1995) Characterization of a cloned locust tyramine receptor cDNA by functional expression in permanently transformed *Drosophila* S-2 cells. *J. Neurochem.*, **64**: 2387-2395.

VANDENBROECK, K., L. WILLEMS, A. BILLIAU, G. OPDENAKKER & R. HUYBRECHTS (1994) – Glycoform heterogeneity of porcine interferon-gamma expressed in Sf9 cells. *Lymphokine and Cytokine research*, **13**: 253-258.

VULSTEKE, V.(1995) – Baculovirus immediate early gene promoter mediated expression in stably transformed insect cells. Doctoral thesis, K.U.Leuven, pp.114.

VULSTEKE, V., I. JANSSEN, J. VANDEN BROECK, A. DE LOOF & R. HUYBRECHTS (1993) – Baculovirus immediate early gene promoter based expression vectors for transient and stable transformation of insect cells. *Insect Molecular Biology*, **2**: 195-204.

Belg. J. Zool. - Volume 127 (1997) - issue 1 - pages 47-55 - Brussels 1997

THE COMPOSITION OF THE FISH AND CRUSTACEAN COMMUNITY OF THE ZEESCHELDE ESTUARY (BELGIUM)

JOACHIM MAES, ARNE TAILLIEU, PAUL A. VAN DAMME AND FRANS OLLEVIER
Katholieke Universiteit Leuven, Zoological Institute,
Laboratory of Ecology and Aquaculture, Naamsestraat 59, B-3000 Leuven, Belgium
e-mail: joachim.maes@bio.kuleuven.ac.be

Abstract. Fykes were used to monitor the fish and crustacean fauna of the mudflats of the Zeeschelde between April 1995 and December 1996. Overall 38 species were recorded; the number of species was greater in the brackish water part than in the fresh water part probably due to reduced oxygen concentrations in the upper reaches of the river. In terms of wet weight, just 6 species accounted for more than 96 % of the total annual catch. These species are shore crab, eel, flounder, common shrimp, sole and bass. Clear seasonal patterns in the community structure were not identified. It is argued that the selectivity of the fishing gear is mainly responsible for the dominance of a few species and the lack of a temporal structure.

Keywords: spatial distribution, fish, Crustacea, fykes, Zeeschelde estuary.

INTRODUCTION

The Zeeschelde is situated in Belgium and stretches from Gent to the Belgian/Dutch border. It is divided in a fresh water part (the Upper Zeeschelde) and a brackish water part (the Lower Zeeschelde) that is connected to the Westerschelde (CLAESSENS, 1988). Although the Zeeschelde is characterised by very poor water quality, a complete salinity gradient is present (HEIP, 1989). In addition, strong tidal incursion creates intertidal areas such as mudflats and salt marshes. These mudflats are important nurseries and feeding grounds for fishes and macrocrustaceans (BOESCH & TURNER, 1984). Field experiments even emphasise the role these mobile epibenthic predators play in determining estuarine mudflat prey densities (GEE *et al.*, 1985; RAFFAELLI *et al.*, 1989).

Most research on the intertidal areas of the Schelde estuary deals with the vegetation (*e.g.* MEIRE & KUIJKEN, 1988) and benthic fauna (*e.g.* YSEBAERT *et al.*, 1993; SOETAERT *et al.*, 1994) or concerns nutrient fluxes between the intertidal and subtidal sectors (*e.g.* HEMMINGA *et al.*, 1993). Little effort has been undertaken to study fish and macrocrustaceans entering these narrow mudflats. Recently CATTRIJSSE *et al.* (1994) investigated the utilisation of a brackish intertidal creek of the Westerschelde by estuarine nekton. They concluded that

Contribution to the 3th Benelux Congress of Zoology, Namur, November 1996.

the marsh is a nursery for juveniles of common shrimp, flounder, common goby, bass and shore crab. Adults of these species possibly use these areas as feeding ground.

This paper presents and discusses results from fyke catches on the intertidal mudflats of the Zeeschelde. These data are the first since POLL (1945) on the spatial distribution of fish and larger crustaceans in the estuary of the Zeeschelde. The aim of this study is to inventory the fish and crustacean species occurring in these mudflats and to evaluate the fishing method as a tool to monitor the Zeeschelde ecosystem.

MATERIAL AND METHODS

Nine sampling sites, all situated in the Zeeschelde, were selected to collect samples of fish and crustaceans. Five stations (A-E) cover the Lower Zeeschelde between Antwerpen and Bath (on the Belgian/Dutch border), four locations (F-I) are situated in the Upper Zeeschelde between Schelle and Antwerpen (Fig. 1). Fish and crustaceans were sampled at each location using double fyke nets containing two fykes both connected by a longitudinal net. The overall length of the entire set-up is 26.4 m; stretched mesh size of the nets is 8 mm. All fyke nets were set at the low-water line and checked for fish and crustaceans every 3 days. Sampling at stations A, B and C was carried out between April 1995 and December 1995. All other stations were sampled in August and November 1995. Minimum and maximum salinity and oxygen concentration as well as temperature recorded in 1995 are given in Table 1. Both salinity and oxygen concentration increase in the downstream direction.

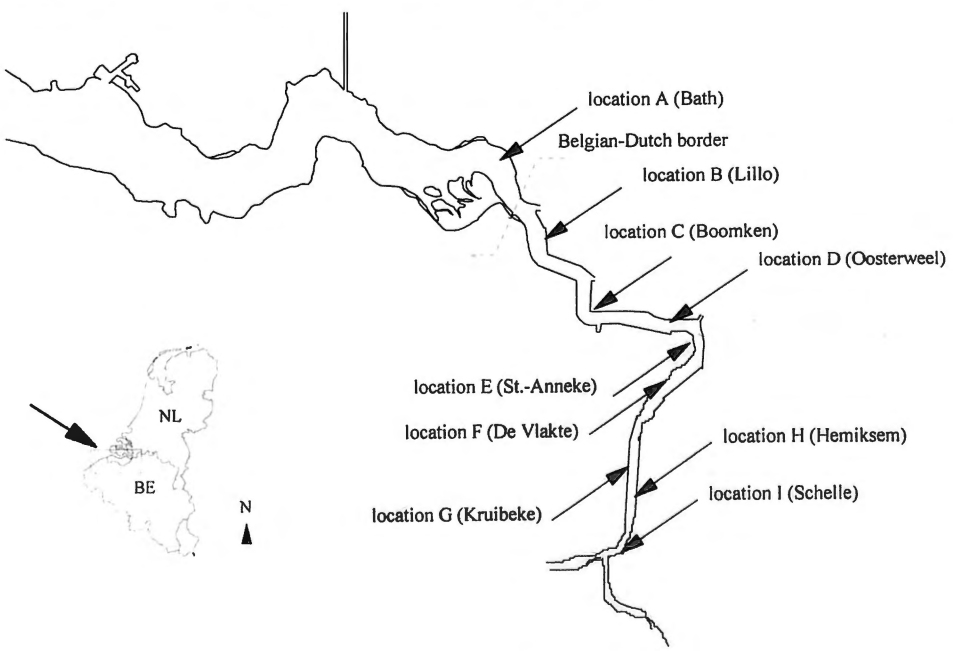

Fig. 1. – Map of the Schelde estuary with indications of the sampling sites. BE = Belgium; NL = the Netherlands.

TABLE 1

Minimum (m) and Maximum (M) salinity (g/l), oxygen concentration (mg/l) and temperature (°C) recorded in 1995 (based on monthly samples) for the sampling locations (the code of the sampling sites is the same as presented in Fig. 1). Data indicated with (*) originate from the environmental database of the Flemish Environment Agency.

sampling sites	salinity (g/l)		O_2 -concentration (mg/l)		temperature (°C)	
	m	M	m	M	m	M
A (*)	2.3	15.9	2.0	7.0	5.3	24.9
B	2.1	15.3	2.2	6.9	5.8	25.0
C	2.0	11.0	0.1	5.8	6.0	24.1
D-E	1.2	8.0	0.2	4.1	5.6	24.7
F	0.3	6.5	0.3	5.5	5.8	24.6
G (*)	0.1	0.6	0.6	6.5	6.0	24.4
H (*)	0.1	1.3	0.9	3.8	4.8	24.6
I	0.1	0.5	0.0	3.1	6.5	25.3

Fish and crustacean species were identified according to WHEELER (1992) and HOLTHUIS & HEEREBOUT (1986) respectively. For each species data are expressed either as densities (monthly average numbers per fyke per day) or as wet weights (monthly average wet weight (g) per fyke per day). Temporal patterns in the community were analysed by means of cluster analysis on densities and on wet weights (Ward's Method, Euclidean distances). This method uses an analysis of variance approach to evaluate distances between clusters and attempts to minimise the sum of squares of any two clusters that can be formed at each step (WARD, 1963). Prior to the statistical analysis the data were log (x + 1) transformed (FIELD *et al.*, 1982).

RESULTS AND DISCUSSION

Fyke netting yielded 38 fish species and 7 crustacean species (Table 2). Of all fish species recorded 23 species are marine (MA) with no strict estuarine requirements; 12 species are identified as fresh water species (FW); eel (*Anguilla anguilla*) is the only catadromous species (CA) and 2 species are anadromous (AN) namely the river lamprey *Lampetra fluviatilis* and the sea trout *Salmo trutta*. All crustacean species are marine species except the noble crayfish *Astacus astacus* which prefers a fresh water habitat. VAN DAMME *et al.* (1994) recently inventoried the fish species occurring in the cooling water of the Nuclear Power Station Doel which is situated near location B. They listed 32 fish species in the Lower Zeeschelde. If the first 3 sampling sites alone are considered, fyke netting recovered 36 fish species. In this case both studies have 26 species in common.

In terms of numbers, 4 species alone represented more than 96 % of the total annual catch. The samples were dominated by the common shrimp *Crangon crangon* (67.6 %)

and the shore crab *Carcinas maenas* (23.7 %). Flounder (*Pleuronectes flesus*) and the palaemonid shrimp *Palaemonetes varians* contributed each 2.7 % of the total numbers. In terms of wet weight 6 species represented more than 92 % of the total annual catch over the 9 sampling sites. Shore crab, eel (*Anguilla anguilla*) and flounder each represented 27.5 % of the total annual catch. The relative proportion of the common shrimp was 4.5 % whereas sole (*Solea solea*) and bass (*Dicentrarchus labrax*) both contributed 4 % and 1.3 % respectively. Other studies confirm indeed the dominant position of a small number of species in estuarine fish and crustacean communities (CLARIDGE *et al.*, 1986; ELLIOT & TAYLOR, 1989; HENDERSON, 1989). The major reason however, that a few species contributed more than 92 % of the annual catch may be the selective catch efficiency of the fishing gear used. Fykes almost only sample benthic or demersal species excluding pelagic species such as clupeids. In addition gobies and pipefish are able to escape through the meshes of the fykes used. These later species as well as clupeids are by contrast regularly sampled in the cooling water system of Nuclear Power Station Doel (VAN DAMME *et al.*, 1994). It is therefore most likely that the relative abundance of shrimps is underestimated. All dominant species recorded in this study were adult individuals of either benthic or demersal species probably using the intertidal as a feeding ground.

TABLE 2

Fish and crustacean species occurring in the intertidal mudflats of the Zeeschelde (the code of the mudflats is the same as presented in Fig. 1). +++ = >1 individuals per fyke per day, ++ = <1 individual per fyke per day, + only 1 record. For abbreviations of ecological type (E.T.) see text.

Fish species	**E. T.**	**brackish water part**					**fresh water part**			
		A	**B**	**C**	**D**	**E**	**F**	**G**	**H**	**I**
Carassius auratus (L.)	FW	+								
Raniceps raninus (L.)	MA	+								
Atherina presbyter Cuvier, 1827	MA	++								
Gymnocephalus cernuus (L.)	FW	++								
Myoxocephalus scorpius (L.)	MA	++								
Pomatoschistus lozanoi (de Buen, 1923)	MA	++								
Zoarces viviparus (L.)	MA	++								
Pomatoschistus microps (Krøyer, 1838)	MA	+++								
Ciliata mustela (L.)	MA	+	+							
Salmo trutta L.	AN	+	+							
Trigla lucerna (L.)	MA	++	+							
Pleuronectes platessa L.	MA	++	++							
Trisopterus luscus (L.)	MA	++	++							
Gadus morhua L.	MA	++	++	+						
Solea solea (L.)	MA	+++	++	+						
Limanda limanda (L.)	MA	+++	++	++						
Dicentrarchus labrax (L.)	MA	+++	++	++						
Merlangius merlangus (L.)	MA	+		+						
Ictalurus nebulosus (Le Sueur, 1819)	FW		+							

Fish species	E. T.	brackish water part					fresh water part			
		A	B	C	D	E	F	G	H	I
Blicca bjoerkna (L.)	FW		+							
Syngnathus acus L.	MA		++	++						
Syngnathus rostellatus Nilsson, 1855	MA		+							
Sprattus sprattus (L.)	MA			+						
Lepomis gibbosus (L.)	FW			+						
Liza ramada (Risso, 1826)	MA	++	+	++	+					
Pomatoschistus minutus (Pallas, 1770)	MA	++	++	++	++	++				
Pleuronectes flesus L.	MA	+++	+++	+++		++				
Osmerus eperlanus (L.)	MA	++	++		+					
Clupea harengus L.	MA	++	++	+++	+++	++				
Gasterosteus aculeatus L.	FW	++	+	+		++				
Lampetra fluviatilis (L.)	AN	+			++	++				
Anguilla anguilla (L.)	CA	+++	+++	+++	+++	++	++	++	++	++
Perca fluviatilis L.	FW	+	++	++	++	++	++	++		
Stizostedion lucioperca (L.)	FW	++	++	++	++	++	++	+		
Rutilus rutilus (L.)	FW	+	++			++	++	++	+	+
Cyprinus carpio L.	FW			++		++	++	++		
Rutilus erypthrophthalmus (L.)	FW					++	++	++	++	
Carassius carassius (L.)	FW						++	++		
Crustacean species										
Callinectes sapidus Rathbun, 1860	MA		+							
Rhithropanopeus harrissi (Gould, 1841)	MA	+	++	+						
Eriocheir sinensis H. Milne Edwards, 1851	MA	++	++	++						
Carcinus maenas (L.)	MA	+++	++	+	+	+				
Crangon crangon (L.)	MA	+++	+++	+++						
Palaemonetes varians (Leach, 1814)	MA	++	+++	+++	+++	+++	++			
Astacus astacus (L.)	FW			+						

It is interesting to note that except for the eel all dominant species are marine. They occur up to station E (Table 2) which can be considered as the final station of the brackish water part. Upstream of station E only fresh water and diadromous species were caught (Table 2). According to REMANE & SCHLIEPER (1971) who defined a relation between salinity and species number one should expect the species number to increase in the fresh water part of the Zeeschelde estuary. But the number of species as well as abundance of fish and crustaceans were probably reduced due to critical oxygen concentrations (<1 mg/l) during most of the year (Table 1). As a result of this hypoxia caused by heavy eutrophication (VAN DAMME *et al.*, 1995) only a few species can be caught. Similar results for the Elbe estuary were found by MÖLLER & SCHOLTZ (1991) who found flounder and smelt (*Osmerus eperlanus*) concentrated downstream from the low-oxygen zone, avoiding

the fresh water reach. Only eel was able to tolerate oxygen concentrations < 1.4 mg/l (MÖLLER & SCHOLZ, 1991). Apart from one record of roach (*Rutilus rutilus*) only eel occurred at station I, the station with the lowest oxygen concentration. Although the sampling effort in the fresh water zone was less than in the first three stations, it does not preclude the possibility that neither fish nor crustaceans can survive the above mentioned low oxygen concentrations.

In polluted systems such as the upper Zeeschelde where the distribution of fresh water species is strongly affected by reduced oxygen levels, these later species profit from the more favourable oxygen conditions in the brackish part of the Zeeschelde. Indeed most fresh water fish were recorded between station A and station E where mean annual salinities approach 10 ‰ and 2 ‰ respectively (CLAESSENS, 1988). These species probably originate from surrounding docks of the Antwerpen Port Area that connect the Lower Zeeschelde with the Albert Channel and the Schelde-Rijn Channel (MAES, unpublished). Sampling in these waterways indeed suggests the presence of important populations of fresh water species and therefore they function as refuges.

Besides the spatial distribution of fish and crustaceans in the Zeeschelde we attempt to describe temporal patterns in the community structure using cluster analysis on densities and on wet weights. Since a monthly sampling regime could not be maintained at all sampling stations only the first 3 locations (A-B-C) are considered (Fig. 2). In both plots the spatial distribution of the community seems to dominate over the temporal pattern. Samples taken at the same location more or less co-occur. In the density plot the first division is made between samples taken at station A between May and October and all other samples including April A, November A and December A. Further clustering however does not result in a seasonal structure with summer samples separated from winter samples. Clustering the wet weight data resulted in the same information. All samples taken at location A except for «December A» are separated from the other samples. Once again no seasonal trends can be detected by the analysis. Many authors nevertheless identify clear seasonal patterns in the composition of estuarine fish and crustacean communities (WHARFE *et al.*, 1984; CLARIDGE *et al.*, 1986; HENDERSON & HOLMES, 1987). In this case the lack of a temporal structure could be once again be the consequence of a selective fishing technique. Because of the exclusion of an important number of species frequently occurring in estuaries such as gobies and clupeids clear seasonal trends were not expressed.

CONCLUSIONS

A major conclusion of this study concerns the fishing gear used. Fyke netting can be most useful to obtain qualitative data in areas where other methods do not succeed because of difficult field conditions. The results show indeed the existence of a stable and permanent community in the brackish part of the Zeeschelde whereas the fish and crustacean community in the Upper Zeeschelde can be described as unstable and temporary. With the prospect of an ecological recovery of the fresh water part of the Zeeschelde as a result of recent waste water treatment programmes fykes could be an appropriate tool to monitor the ecosystem. On the other hand it seems obvious that a complete description of the struc-

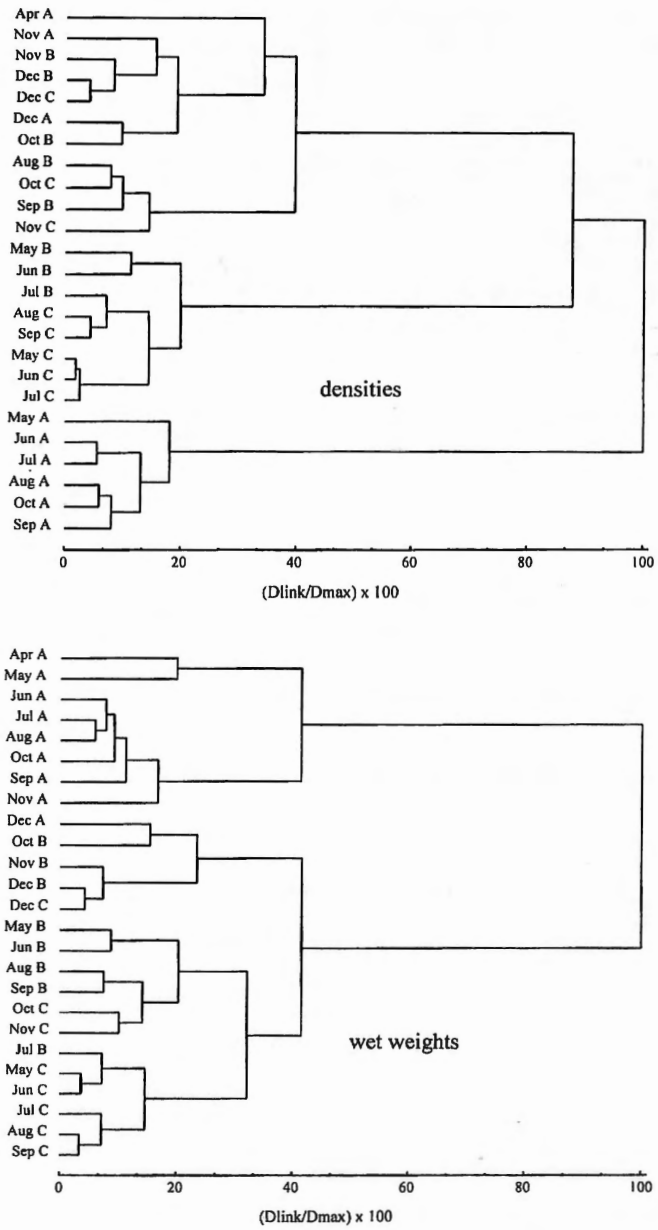

Fig. 2. – Cluster analysis (Ward's Method, Euclidean distances) on the log (x + 1) transformed densities and wet weights of all species recorded between April 1995 and December 1995 on sampling sites A, B and C. The linkage distance (Dlink) is presented as a percentage of the maximum linkage distance (Dmax). The maximum linkage distance is 13.20 for the analysis on densities and 18.29 for the analysis on wet weights.

ture and functioning of an entire fish and crustacean community requires a less selective fishing method such as stow net fisheries or sampling at cooling water intakes, allowing the collection of a fully quantitative and qualitative dataset.

ACKNOWLEDGEMENTS

The authors would like to thank B. Peeters for sampling assistance. Electrabel (Nuclear Power station of Doel) and VIBNA, de Vereniging van de Industriële Bedrijven van Noord-Antwerpen, are acknowledged for financially supporting this study.

REFERENCES

BOESCH, D.F. & R.E. TURNER (1984) – Dependence of fishery species on salt marches: the role of food and refuge. *Estuaries,* **7**: 460-468.

CATTRIJSSE A., E.S. MAKWAIA, H.R. DANKWA, O. HAMERLYNCK & M.A. HEMMINGA (1994) – Nekton communities of an intertidal creek of a European estuarine brackish marsh. *Mar. Ecol. Prog. Ser.*, **109**: 195-208.

CLAESSENS, J. (1988) – Het hydraulisch regime van de Schelde. *Water,* **43**: 163-169.

CLARIDGE, P.N., I.C. POTTER & M.W. HARDISTY (1986) – Seasonal changes in movements, abundance, size composition and diversity on the fish fauna of the Severn Estuary. *J. mar. biol. Ass. U.K.,* **66**: 229-258.

ELLIOTT, M. & C.L.J. TAYLOR (1989) – The structure and functioning of an estuarine/marine fish community in the Forth estuary, Scotland. *Proceedings of the 21st. European Marine Biology Symposium,* Gdansk: 227-240.

FIELD, J.G., K.R. CLARKE & R.M. WARWICK (1982) – A practical strategy for analysing multispecies distribution patterns. *Mar. Ecol. Prog. Ser.,* **8**: 37-52.

GEE, J.M., WARWICK, R.M., DAVEY, J.T. & C.L. GEORGE (1985) – Field experiments on the role of epibenthic predators in determining prey densities in an estuarine mudflat. *Est. Coast. Shelf Sci.*, **21**: 429-448.

HEIP, C. (1989) – The ecology of the rivers Rhine, Meuse and Scheldt in the Netherlands. *Scient. Mar.*, **53**: 457-463.

HEMMINGA, M.A., V.A. KLAP, J. VAN SOELEN & J.J. BOON (1993) – Effect of salt marches inundation on estuarine particulate organic matter characteristics. *Mar. Ecol. Prog. Ser.,* **99**: 153-161.

HENDERSON, P.A. & R.H.A. HOLMES (1987) – On the population biology of the common shrimp *Crangon crangon* (L.) (Crustacea: Caridea) in the Severn estuary and Bristol Channel. *J. mar. biol. Ass. U.K.,* **67**: 825-847.

HENDERSON, P.A. (1989) – On the structure of the inshore fish community of England and Wales. *J. mar. biol. Ass. U.K.,* **69**: 145-163.

HOLTHUIS, L.B. & G.R. HEEREBOUT (1986) – De Nederlandse Decapoda. Wetenschappelijke Mededelingen K.N.N.V. nr. 179, Hoogwoud, 66 pp.

MEIRE, P. & E. KUIJKEN (1988) – Het Land van Saeftinge, slikken en schorren: ecologische betekenis van de intergetijdegebieden langs de Schelde. *Water,* **43**: 214-221.

MÖLLER, H. & U. SCHOLZ (1991) – Avoidance of oxygen-poor zones by fish in the Elbe river. *J. Appl. Ichthyol.*, **7**: 176-182.

POLL, M. (1945) – Contribution à la connaissance de la faune ichthyologique du bas-Escaut. *Bull. Mus. roy. Hist. nat. Belgique*, **21**: 1-32.

RAFFAELLI, D., CONACHER, A., MCLACHLAN, H. & C. EMES (1989) – The role of epibenthic crustacean predators in an estuarine food web. *Est. Coast. Shelf Sci.*, **28**: 149-160.

REMANE, A. & C. SCHLIEPER (1971) – Biology of brackish water. Wiley-Interscience, New York, 372 pp.

SOETAERT, K., M. VINCX, J. WITTOECK, M. TULKENS & D. VAN GANSBEKE (1994) – Spatial patterns of Westerschelde meiobenthos. *Est. Coast. Shelf Sci.*, **39**: 367-388.

VAN DAMME, P.A., HOSTENS, K. & F. OLLEVIER (1994) – Fish species in the Lower Zeeschelde (Belgium): a comparison with historical checklists. *Belg. J. Zool.*, **124**: 93-103.

VAN DAMME, S., P. MEIRE, H. MAECKELBERGHE, M. VERDIEVEL, L. BOUGOING, E. TAVERNIERS, T. YSEBAERT & G. WATTEL (1995) – De waterkwaliteit van de Zeeschelde: evolutie in de voorbije dertig jaar. *Water*, **85**: 244-256.

WARD, J.H. (1963) – Hierarchical grouping to optimise an objective function. *Journal of the American Statistical Association*, **58**: 236-246.

WHARFE, J.R., S.R. WILSON & R.A. DINES (1984) – Observations on the fish populations of an East Coast Estuary. *Marine Pollution Bulletin*, **15**: 133-136.

WHEELER, A.(1992) – A list of common and scientific names of fishes of the British Isles. *J. Fish. Biol.*, **41**, suppl. A: 37 pp.

YSEBAERT, T., P. MEIRE, D. MAES & J. BUIJS (1993) – The benthic macrofauna along the estuarine gradient of the Schelde estuary. *Neth. J. Aquat. Ecol.*, **27**: 327-341.

Belg. J. Zool. - Volume 127 (1997) - issue 1 - pages 57-61 - Brussels 1997

P53 PROTEIN EXPRESSION IN AVIAN OVARIAN FOLLICLES

LUC VAN NASSAUW[1], ANNELEEN SCHREVENS, KOEN VAN DE VIJVER, FREDERIK VAN MIEGHEM, FERNAND HARRISSON AND MARC CALLEBAUT

University of Antwerp (RUCA), Laboratory of Human Anatomy & Embryology, Groenenborgerlaan 171, B-2020 Antwerpen
e-mail: luvanas@ruca.ua.ac.be

Abstract. In the present study, we localized p53 protein in the ovary of the adult Japanese quail using immunohistochemical techniques. The best results were obtained with DO-1 monoclonal antibodies and with a heat-induced epitope retrieval method. Immunostaining was detected in cytoplasm and/or nuclei of granulosa and surface epithelial cells. In atretic follicles, p53 protein was found in a few follicular cells. Immunoreactivity was also detected in leukocytes and in the Balbiani complex of prelampbrush oocytes. It is suggested that p53 protein expression is elevated in proliferating granulosa and surface epithelial cells, and that p53 protein may be involved in granulosa cell differentiation.

Keywords: p53 protein, quail, ovary.

INTRODUCTION

P53 protein, the product of a tumor suppressor gene, is a multifunctional protein (for review see ELLEDGE & LEE, 1995). Previous studies in mammals indicate that p53 protein is an important regulator of granulosa cell fate during folliculogenesis, and that p53 protein is involved in atresia (TILLY *et al.*, 1995; AMSTERDAM *et al.*, 1996). Follicular atresia in mammals and birds is mediated via apoptosis or physiological cell death, and the majority of cells undergoing apoptosis are granulosa cells (TILLY *et al.*, 1991). A recent report on atresia in quail demonstrates that apoptosis is not the exclusive mode of active cell death (D'HERBE *et al.*, 1996). The present study focuses on the distribution of p53 protein during folliculogenesis and atresia in quail ovaries.

MATERIAL AND METHODS

Female adult Japanese quail (*Coturnix coturnix japonica*) were killed by decapitation. Tissue blocks of the ovaries and the pre- and post-ovulatory follicles were fixed in EACH fixative (PERRY-O'KEEFE *et al.*, 1990) or in 4% paraformaldehyde in 10 mM phosphate-

Contribution to the 3th Benelux Congress of Zoology, Namur, November 1996.
[1] Senior Research Assistant of the Belgian National Fund for Scientific Research.

buffered saline at pH 7.2. After fixation, subsamples of tissue were dissected from the walls of the pre- and post-ovulatory follicles and embedded in paraffin. Several commercially available antibodies directed against p53 protein were used (Table 1). P53 protein was localized in paraffin sections using the unlabelled antibody peroxidase-anti-peroxidase technique. Some sections were pre-treated with the pressure cooker heat-induced epitope retrieval method (NORTON *et al.*, 1994). The oocytes and follicles were classified in stages according to CALLEBAUT (1973). Paraffin sections of routinely formalin-fixed human colonic adenocarcinoma (KARAMITOPOULOU *et al.*, 1995) were used as positive controls.

TABLE 1

Antibodies directed against p53 protein

Antibody	*Dilution*	*Source*
CM1[P]	1/200	Novocastra Laboratories Ltd. (Newcastle upon Tyne, U.K.)
DO-1[M]	pd	IMMUNOTECH (Marseille, France)
	pd	DPC (Apeldoorn, The Netherlands)
	1/50	Santa Cruz Biotechnology Inc. (Santa Cruz, CA)
DO-7[M]	pd	DPC
PAb 122[M]	1/40	Boehringer Mannheim GmbH (Mannheim, Germany)
PAb 1801[M]	pd	DPC

[P]: polyclonal antibody; [M]: monoclonal antibody: pd: pre-diluted.

RESULTS

The heat-induced epitope retrieval method enhanced p53 protein immunoreactivity (IR). The best results were obtained using the DO-1 monoclonal antibodies, but the CM1 and PAb 122 antibodies also gave fairly good results. No immunostaining was observed using the DO-7 and PAb 1801 antibodies. Positive staining was found with all antibodies in the adenocarcinoma sections.

IR was detected in cytoplasm and/or nuclei of granulosa cells during each stage of folliculogenesis (Figs 1-3). However, the granulosa cells of the pre-ovulatory follicles were weakly immunostained (Fig. 2). IR was also found in surface epithelial cells (Figs 1, 3), except those in the wall of pre-ovulatory follicles (Fig. 2). In atretic follicles, moderate IR was found in a few follicular cells (Fig. 4). Furthermore, p53 protein was demonstrated in the Balbiani complex of prelampbrush oocytes (Fig. 1) in a few vascular smooth muscle cells, and in leukocytes (Figs 1, 4), predominantly those present in the vicinity of atretic follicles (Fig. 4).

Figs 1-4. – Micrographs of the quail ovary, immunostained with DO-1 antiserum and counterstained with toluidine blue (bar = 10 mm). AF: atretic follicle; B: Balbiani complex of prelampbrush oocyte; g: granulosa; O: oocyte; te: theca externa; ti: theca interna; ts: tunica superficialis; arrowheads: surface epithelium; arrows: leukocytes. – 1. Prelampbrush and developing follicles: IR in granulosa and surface epithelial cells, in leukocytes, and in the Balbiani complex. – 2. Mature pre-ovulatory follicle: weak IR in the granulosa cells. – 3. Post-ovulatory follicle: IR in the granulosa cells. – 4. Atretic follicle: IR predominantly in leukocytes and in surface epithelial cells. A few follicular cells (small arrowheads) were moderately immunostained.

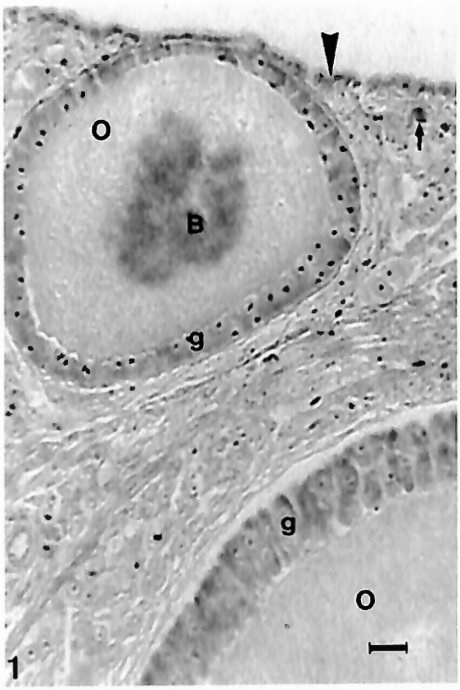
O
B
g
g
O
1

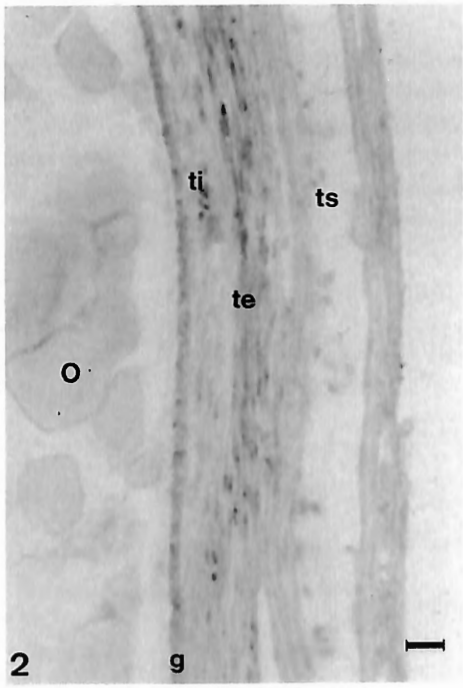
ti
ts
te
O
2
g

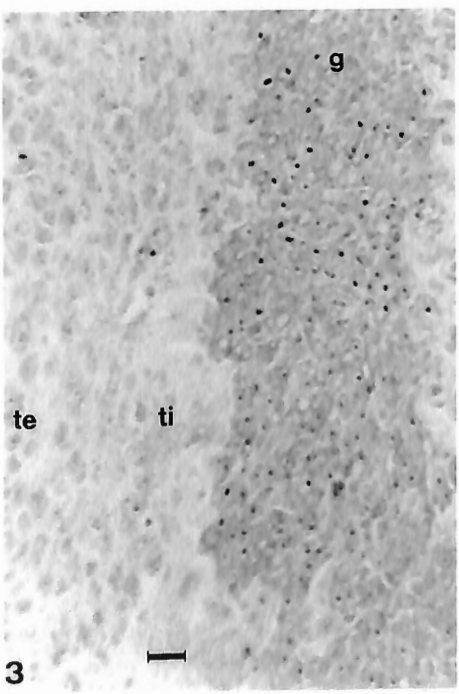
g
te
ti
3

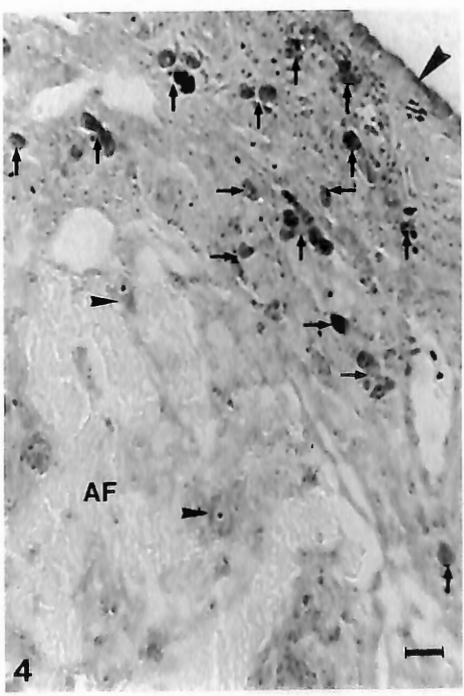
AF
4

DISCUSSION

The results with the different antibodies were probably due to the percentage homology of quail p53 protein with human p53 protein. Chicken p53 protein reveals 47% homology with human p53 protein (SOUSSI *et al.*, 1988).

In the present study, we have shown that p53 protein expression is high in proliferating granulosa and surface epithelial cells. Previous *in vitro* studies reported increased expression of p53 protein in proliferating cells (for review, see KATSUMOTO *et al.*, 1995). P53 protein initially appears in the cytoplasm of mitotic cells, then accumulates in the nucleus before the beginning of DNA synthesis, and thereafter it is no longer found in the nucleus but rather in the cytoplasm.

In the human ovary, p53 protein is detected in the nuclei of granulosa cells of preantral and antral follicles, and in the cytoplasm of surface epithelial cells (BUKOVSKY *et al.*, 1995). However, in the rat ovary, TILLY *et al.* (1995) reported that p53 protein is exclusively localized in nuclei of apoptotic granulosa cells of atretic follicles. In the quail ovary p53 protein has also been found in non-dividing and relatively stable cells: in the cytoplasm of granulosa cells of post-ovulatory and of mature pre-ovulatory follicles, and in the Balbiani complex of prelampbrush oocytes. Nuclear and nucleolar p53 protein expression is demonstrated in human oocytes of resting primary follicles and in luteinized granulosa cells (BUKOVSKY *et al.*, 1995). It is suggested that p53 protein can enhance granulosa cell differentiation and luteinization (AMSTERDAM *et al.*, 1996).

Previous findings suggest the existence of a strong correlation between apoptosis and elevated p53 protein expression in the ovary (TILLY *et al.*, 1995). AMSTERDAM *et al.* (1996) have demonstrated that p53 protein can co-operate with cAMP-generated signals in the induction of apoptosis in granulosa cells. However, we have detected a few immunostained follicular cells in atretic follicles. No clear relation between p53 protein expression and apoptosis is found.

This study supports the hypothesis (AMSTERDAM *et al.*, 1996) that p53 protein is an important regulator of proliferation of granulosa and surface epithelial cells and that p53 protein may be involved in granulosa cell differentiation.

ACKNOWLEDGEMENTS

This study was supported by grant 3.0029.93 of the Belgian National Fund for Scientific Research, and a Matching Fund from the University Centre of Antwerp (RUCA).

REFERENCES

AMSTERDAM, A., I. KEREN-TAL & D. AHARONI (1996) – Cross-talk between cAMP and p53-generated signals in induction of differentiation and apoptosis in steroidogenic granulosa cells. *Steroids*, **61**: 252-256.

BUKOVSKY, A., M.R. CAUDLE, J.A. KEENAN, J. WIMALASENA, J.S. FOSTER, N.B. UPADHYAYA & S.E. VAN METER (1995) – Expression of cell cycle regulatory proteins (p53, pRb) in the human female genital tract. *J. Assist. Reprod. Genet.*, **12**: 123-131.

CALLEBAUT, M. (1973) – Correlation between germinal vesicle and oocyte development in the adult Japanese quail (*Coturnix coturnix japonica*): a cytochemical and autoradiographic study. *J. Embryol. exp. Morph.*, **29**: 145-157.

D'HERDE, K., B. DE PREST & F. ROELS (1996) – Subtypes of active cell death in the granulosa of ovarian atretic follicles in the quail. *Reprod. Nutr. Dev.*, **36**: 175-189.

ELLEDGE, R.M. & W.-H. LEE (1995) – Life and death by p53. *BioEssays*, **17**: 923-930.

KARAMITOPOULOU, E., E. PERENTES, I. DIAMANTIS, U. VOGT & W. WEGMANN (1995) – P53 protein expression in colorectal adenomas: an immunohistochemical study using an antigen retrieval system. *Histopathology*, **27**: 517-523.

KATSUMOTO, T., K. HIGAKI, K. OHNO & K. ONODERA (1995) – Cell-cycle dependent biosynthesis and localization of p53 protein in untransformed human cells. *Biol. Cell*, **84**: 167-173.

NORTON, A.J., S. JORDAN & P. YEOMANS (1994) – Brief, high-temperature heat denaturation (pressure cooking): a simple and effective method of antigen retrieval for routinely processed tissues. *J. Pathol.*, **173**: 371-379.

PERRY-O'KEEFE, H., C.R. KINTNER, J. YISRAELI & D.A. MELTON (1990) – The use of *in situ* hybridisation to study the localisation of maternal mRNAs during *Xenopus* oogenesis. In: HARRIS, N. & D.G. WILKINSON (Eds), *In situ hybridisation: application to developmental biology and medicine.* Cambridge University Press, Cambridge: 115-130.

SOUSSI, T., A. BÈGUE, M. KRESS, D. STEHELIN & P. MAY (1988) – Nucleotide sequence of a cDNA encoding the chicken p53 nuclear protein. *Nucleic Acids Res.*, **16**: 11383.

TILLY, J.L., K.I. KIWALSKI, A.L. JOHNSON & A.J.W. HSUEH (1991) – Involvement of apoptosis in ovarian follicular atresia and postovulatory regression. *Endocrinology*, **129**: 2799-2801.

TILLY, K.I., S. BANERJEE, P.P. BANERJEE & J.L. TILLY (1995) – Expression of the p53 and Wilms' tumor suppressor genes in the rat ovary: gonadotropin repression *in vivo* and immunohistochemical localization of nuclear p53 protein to apoptotic granulosa cells of atretic follicles. *Endocrinology*, **136**: 1394-1402.

Belg. J. Zool. - Volume 127 (1997) - issue 1 - pages 63-73 - Brussels 1997

Received : 18 July, 1996

L'ACÉTYLCHOLINESTÉRASE DU SYSTÈME OLFACTIF DE LA CARPE *CYPRINUS CARPIO* L. (POISSONS, CYPRINIDAE) : FORMES MOLÉCULAIRES ET INHIBITION *IN VIVO* ET *IN VITRO* PAR LE CARBOFURAN

ERIC HAUBRUGE[1] ET JEAN-PIERRE TOUTANT[2]

[1]Unité de Zoologie générale et appliquée, Faculté universitaire des Sciences agronomiques de Gembloux, B-5030 Gembloux, Belgique

[2]Laboratoire de Différenciation Cellulaire et Croissance, INRA, Montpellier, France

e-mail : zoologie@fsagx.ac.be

Résumé. L'utilisation des pesticides en agriculture et principalement dans la lutte contre les insectes est à la base d'importants problèmes écotoxicologiques du fait de leur longue rémanence dans l'environnement et de leur forte toxicité vis-à-vis des organismes aquatiques.

L'acétylcholinestérase (AChE) est utilisée depuis quelques années comme biomarqueur spécifique de l'effet des organophosphorés et des carbamates sur les organismes aquatiques. Ces biocides inhibent l'activité de l'acétylcholinestérase même à de faibles concentrations. L'AChE a été caractérisée dans les rosettes olfactives et le bulbe olfactif de la carpe commune *Cyprinus carpio*. Des formes moléculaires globulaires d'AChE sont présentes dans tout l'organe olfactif et des formes asymétriques ont été mises en évidence dans les rosettes olfactives. Au niveau de cet organe, l'AChE constitue un excellent biomarqueur d'exposition pour détecter la présence d'organophosphorés et de carbamates ; en effet, l'organe olfactif est directement en contact avec les polluants présents dans le milieu aquatique. L'exposition de carpes à des concentrations sublétales de carbofuran montre une inhibition de l'activité AChE de 33,4 ± 5,1 % ; de 49,3 ± 2,7 % et de 45,8 ± 2,6 % respectivement pour les rosettes, le bulbe olfactif et le cerveau après 48 heures.

Acetylcholinesterase, in the olfactory organ of the common carp *Cyprinus carpio* (Teleost, Cyprinidae) : characterization of molecular forms *in vitro* and *in vivo* inhibition by carbofuran

Abstract. The use of pesticides in agriculture and in insect control has been creating a potential danger to aquatic life and human health. Acetylcholinesterase, an enzyme regulating nerve-impulse transmission, is reported to be inhibited by carbamates and organophosphates in many living systems including aquatic organisms. AChE is also present in the entire olfactory organ of the common carp *Cyprinus carpio*. The native molecular forms of AChE present in olfactory organ have been characterized by sedimentation analysis in sucrose gradients. AChE exists as gobular and asymmetric forms. The reduction of olfactory organ AChE activity is already perceptible at sublethal concentrations of carbofuran. The results show an inhibition of olfactory organ AChE ranging from 33,4% to 49,3% after 48 hours. This makes the AChE activity a potential biochemical indicator of toxic stress in fishes and a sensitive test for the presence of carbamates and organophosphates in water.

Mots-clés : acétylcholinestérases, système olfactif, carbofuran, biomarqueur d'exposition, *Cyprinus carpio.*

INTRODUCTION

Abréviations:
acétylcholinestérase(s) = AChE(s);
cholinestérase(s) = ChE(s);
acide 5,5'-dithio-bis-2-nitrobenzoïque = DTNB;
Phosphate Buffer = PB.

Ces deux dernières décennies, le développement des biotechnologies a permis de préciser l'origine et le rôle comportemental des substances chimiques chez les poissons (SCHERER, 1975; SCHUMACHER & NEY, 1980; SAGLIO, 1986). Ce domaine de recherches présente un grand intérêt pour l'aquaculture, la mise au point de méthodes de pêche plus sélectives et le contrôle des déplacements des populations de poissons en milieu naturel.

Ces perspectives d'avenir se heurtent toutefois aux problèmes soulevés par les concentrations élevées en micropolluants dans le milieu aquatique (GALGANI *et al.*, 1992; ADMIRAAL *et al.*, 1993). Les métaux lourds peuvent, à faibles doses, provoquer des altérations olfactives, gustatives et comportementales chez les poissons. Une brève exposition au mercure ($HgCl_2$) à la concentration 10^{-4} M pendant 10 secondes suffit pour inhiber la sensibilité olfactive de *Oncorhynchus gorbuscha* Walbaum, aux acides aminés pendant plus d'une heure (SUTTERLIN, 1974).

L'organe olfactif, présent sur le bord antérieur de l'oeil de la carpe, est directement en contact avec le milieu aquatique et ne possède pas de barrière de protection contre les substances xénobiotiques (SUTTERLIN,1974).

Parmi les biomarqueurs, l'acétylcholinestérase (AChE; EC 3.1.17.) a été largement étudiée et utilisée pour mesurer l'impact des organophosphorés et des carbamates sur le milieu aquatique (HABIG & DI GIULIO, 1991; SZABO *et al.*, 1992; BOCQUENÉ *et al.*, 1993). L'AChE, l'enzyme responsable de l'hydrolyse de l'ACh au niveau des synapses cholinergiques, est présente dans le système nerveux de tous les vertébrés (MASSOULIÉ & BON, 1982) et des invertébrés, à l'exception des formes très primitives (WÄCHTLER,1988). Les organophosphorés et carbamates inhibent ces AChEs et perturbent ainsi la transmission cholinergique.

Le but du présent travail a été la mise en évidence et la caractérisation de l'AChE dans les rosettes, les bulbes olfactifs de la carpe commune ainsi que l'étude des formes moléculaires et de l'impact de micropolluants à action anticholinergique.

MATÉRIEL ET MÉTHODES

Prélèvement des rosettes, des bulbes olfactifs et du cerveau

Les carpes (*Cyprinus carpio* L.) ont été élevées à la station expérimentale de pisciculture de la Faculté universitaire des Sciences agronomiques de Gembloux. Pour les expérimentations, nous avons choisi des poissons âgés de deux ans.

Le poisson, ramené vivant au laboratoire, est tué en sectionnant la moelle épinière à l'arrière de la tête. La peau située sur la face antérieure de la tête entre les deux narines est incisée au moyen d'un scalpel sur une longueur d'environ 2 à 3 cm. Deux autres incisions sont pratiquées perpendiculairement de part et d'autre des orifices olfactifs. La peau est alors retirée latéralement au moyen de pinces brucelles et les rosettes tapissant les deux cavités olfactives sont prélevées. La boîte crânienne est alors ouverte afin de prélever les bulbes olfactifs ainsi que la totalité du cerveau. Des échantillons de la peau située à proximité directe des cavités olfactives sont également prélevés. Le dosage de l'activité AChE des tissus cutanés proches des fosses nasales trouve sa justification dans le souci de vérifier si l'activité AChE mesurée dans la rosette olfactive provient uniquement du tissu olfactif.

Pour comparer l'activité acétylcholinestérasique des rosettes de la carpe avec celle observée chez la truite (*Oncorhynchus mykiss* Walbaum), nous avons extrait des rosettes olfactives sur des truites âgées de 2 années.

Préparation des extraits

Pour le dosage des AChEs, les tissus prélevés sont broyés dans un tampon HST (Tris HCl pH 8,0 0,01 M; 1M NaCl; 50 mM $MgCl_2$; 0,5 % Triton X-100; EDTA 1mM; 0,1 mg/ml bacitracine) au moyen d'un Potter Elvehjem. Après une centrifugation de 15 mn à 18.000 *g* et à 4°C, le surnageant est récolté afin d'effectuer les dosages de protéines et des acétylcholinestérases.

Dosage des protéines

La teneur en protéines est évaluée au moyen du «Protein Standard Test» (Bio-Rad) basé sur la méthode de BRADFORD (1976).

Dosage des acétylcholinestérases

Les acétylcholinestérases ont été dosées selon la méthode de ELLMAN *et al.* (1961) modifiée par nos soins. Cent microlitres de surnageant sont mélangés à un milieu d'incubation composé de tampon phosphate PB pH 8,0 (0,1 *M*) et de DTNB (0,01 *M*). Après une incubation d'une minute, 10 µl d'iodure d'acétylthiocholine (AcSCh) sont ajoutés pour obtenir une concentration finale de 100 m*M*. La lecture spectrophotométrique continue de l'absorbance est réalisée pendant 1 minute à 412 nm. L'activité spécifique est ensuite calculée selon la méthode de ZINKL, *et al.* (1991).

Inhibition *in vitro* de l'activité des cholinestérases

L'effet de trois inhibiteurs: le diisopropyl fluorophosphate (DFP), le BW (Burrows Wellcome) 284C51 (bis [4-allyldimethyl-ammoniumphenyl]pentan-3-one, un inhibiteur spécifique de l'AChE), et le carbofuran (2,3-dihydro-2,2-diméthylbenzofuran-7,yl méthylcarbamate) a été testé vis-à-vis de l'activité de l'AChE. Pour chaque inhibiteur, une

série de concentrations allant de 10^{-3} à 10^{-9} M ont été préparées. Dans le milieu d'incubation, 10 µl de l'inhibiteur choisi ont été ajoutés après le DTNB et le tampon phosphate PB.

Centrifugation au moyen de gradients de saccharose

Pour l'analyse précise du polymorphisme moléculaire de l'AChE et l'identification de certaines formes minoritaires, des extractions successives ont été réalisées (Massoulié & Bon, 1980): l'échantillon est tout d'abord homogénéisé dans un milieu LS (pour «Low-Salt»; 50 mM $MgCl_2$; EDTA 1mM; 10 mM Tris-HCl pH 7,0; 0,1 mg/ml bacitracine). Après une centrifugation de 15 mn à 18.000 *g* et à 4°C, le culot est repris dans un tampon LST (pour «Low-Salt Triton»; 50 mM $MgCl_2$; EDTA 1mM; 10 mM Tris-HCl pH 7,0; 1% de Triton X-100; 0,1 mg/ml bacitracine) et après une nouvelle centrifugation dans le milieu HS (pour «High Salt»; 1M NaCl; 50 mM $MgCl^2$; EDTA 1mM; 10 mM Tris-HCl pH 7,0; 0,1 mg/ml bacitracine). Les extraits obtenus sont, dans l'ordre, les fractions LSS («Low-Salt Soluble» dans le milieu LS), DS («Detergent Soluble» dans le tampon LST) et HSS («High Soluble Soluble» dans le milieu HS). Cent cinquante microlitres d'extrait sont déposés au sommet d'une solution de gradient de saccharose (5%-20%) dans un tampon HST (1M NaCl; 50 mM $MgCl_2$; EDTA 1mM; 10 mM Tris-HCl pH 7,0; 1% de Triton X-100; 0,1 mg/ml bacitracine) ou dans un tampon HS. La centrifugation est réalisée à 6°C sur un rotor Beckman SW41 pendant 16 h à 200.000 *g*. La phosphatase alcaline (6,1 S) et la b-galactosidase (16S) sont incorporées dans la solution de gradient de saccharose comme standards du point de sédimentation. L'activité des cholinestérases totales de chacune des fractions collectées est ensuite mesurée. Dans certains cas, nous avons procédé à une extraction unique dans HST (les trois fractions des extractions séquentielles sont solubilisées en même temps). Les extraits sont analysés sur des gradients HST ou HS comme précédemment. De telles extractions donnent une idée des proportions de chacune des formes moléculaires dans le tissu.

Inhibition *in vivo* des acétylcholinestérases par le carbofuran

Les expérimentations ont été réalisées à la pisciculture expérimentale de la Faculté universitaire des Sciences agronomiques de Gembloux. Un système semi-statique dans des bassins de polyéthylène d'une contenance de 400 l a été utilisé. A la température de 12 ± 2 °C, la charge moyenne en carpes est d'environ 1 kg pour 400 l d'eau renouvelée tous les 2 jours. Le carbofuran utilisé est une formulation commerciale de 200 g/l (Curater 200 SC).

Un bassin contient 400 l d'eau traitée au moyen de carbofuran à la dose de 50 ppb tandis qu'un autre d'une même contenance d'eau sert de témoin. Quinze carpes sont placées dans chaque bassin. Tous les deux jours, l'eau est renouvelée. Après une semaine, les carpes sont sacrifiées et disséquées. L'activité des acétylcholinestérases présentes dans le système olfactif est ensuite mesurée.

Un lot de 15 carpes a également été mis en balnéation à la dose de 10 ppb en carbofuran. Quinze autres carpes ont été placées dans un autre bac ne contenant pas de carbofuran. Après 48 heures, les poissons sont sacrifiés pour extraire les rosettes, les bulbes olfactifs et le cerveau. L'activité des acétylcholinestérases présentes dans le système olfactif est ensuite mesurée.

RÉSULTATS

Activité acétylcholinestérasique dans le système olfactif

L'activité acétylcholinestérasique présente dans les différentes parties du système olfactif de la carpe est montrée à la Fig. 1 en comparaison avec la peau et le cerveau.

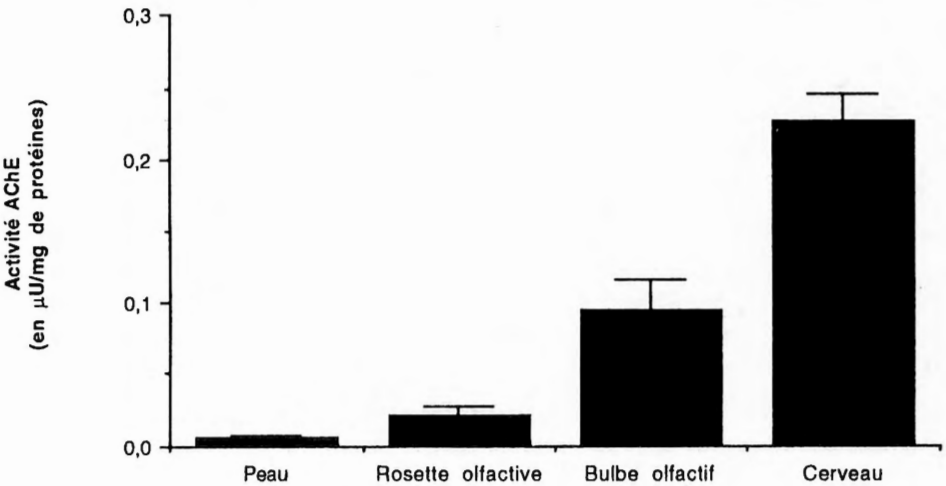

Fig. 1. – Activité acétylcholinestérasique (moyenne ± écart-type) présente dans l'organe olfactif et le cerveau de la carpe commune *Cyprinus carpio* à 25 °C pendant une minute. Vingt poissons ont été utilisés pour l'expérimentation.

Les rosettes olfactives présentent une activité AChE de $2{,}2.10^{-5}$ mU/mg de protéines alors que l'activité AChE dans le cerveau est de $22{,}8.10^{-5}$ mU/mg de protéines. Les bulbes possèdent une activité AChE de $9{,}5.10^{-5}$ mU/mg de protéines. Une activité AChE plus faible de $0{,}6.10^{-5}$ mU/mg de protéines a été observée au niveau de la peau avoisinant les fosses nasales.

Ayant mis en évidence l'activité AChE de la rosette olfactive de la carpe, nous avons voulu savoir si celle-ci existait également chez la truite et de manière aussi importante. Nous avons effectivement trouvé de l'acétylcholinestérase dans les rosettes olfactives de la truite, mais l'activité spécifique y était plus faible que chez la carpe. Elle s'élève en effet à $3{,}5 \pm 0{,}5\ 10^{-6}$ mU/mg de protéines.

Inhibition *in vitro* de l'activité AChE

L'activité des AChEs a été inhibée *in vitro* par le DFP, le BW 284C51 et le carbofuran. L'observation des résultats concernant l'inhibition par le diisopropyl fluorophosphate a permis de montrer que les cholinestérases présentes dans tout le système olfactif sont

semblables. On observe en effet une concentration inhibitrice de 50% de l'activité acétylcholinestérasique (CI_{50}) de $5{,}0.10^{-5}$ M, de $3{,}4.10^{-5}$ M et de $3{,}8.10^{-5}$ M respectivement pour les rosettes, le bulbe et le cerveau (Fig. 2).

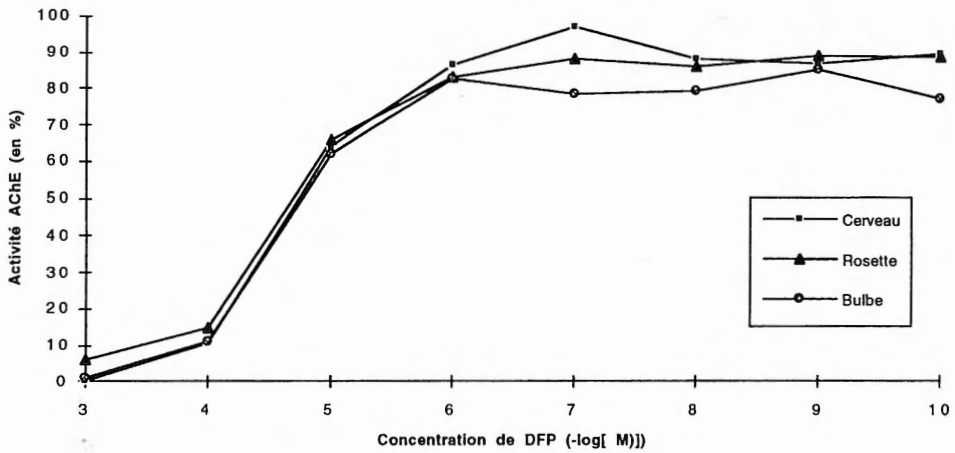

Fig. 2. – Inhibition de l'activité acétylcholinestérasique présente dans l'organe olfactif de la carpe commune *Cyprinus carpio* par le DFP. L'inhibition de l'AChE extraite du cerveau est montrée par comparaison.

L'utilisation du BW284C51, inhibiteur spécifique des AChEs, confirme ces résultats. On remarque que la CI_{50} est de $7{,}5.10^{-7}$M et de $7{,}8.10^{-7}$M respectivement pour le cerveau et les rosettes olfactives. Les courbes d'inhibition par le DFP et le BW284C51 sont monophasiques, ce qui indique que dans les échantillons de cerveau et de rosettes olfactives, l'activité mesurée est due exclusivement à une acétylcholinestérase sans participation de butyrylcholinestérase (EC 3.1.1.8.). Le carbofuran provoque également une diminution de l'activité des acétylcholinestérases du système olfactif. La CI_{50} est de $1{,}6.10^{-6}$M et de $1{,}8.10^{-6}$M respectivement pour le cerveau et les rosettes.

Les formes moléculaires de l'AChE du système olfactif

La Fig. 3a montre les profils de sédimentation d'un extrait direct de rosettes effectué dans un tampon HST centrifugé soit sur un gradient HST soit sur un gradient HS. Par analogie aux résultats obtenus sur l'AChE d'autres vertébrés, on identifie les deux formes globulaires prédominantes comme les formes G1 (monomériques) et G4 (tétramériques) avec un épaulement vers 7S correspondant aux formes G2 (dimériques). Une failble quantité de formes asymétriques A12 est détectable vers 17-18S.

L'analyse des fractions successives LSS, DS et HSS (Fig. 3 b et c) confirme les résultats obtenus avec l'extrait direct: formes G1, G2 et G4 dans les fractions LSS et DS. Ce

type d'extractions successives permet la détection plus facile des formes A12 dans la fraction HSS seulement (Fig. 3c). Les profils obtenus sont très comparables à ceux des bulbes olfactifs et du reste du cerveau.

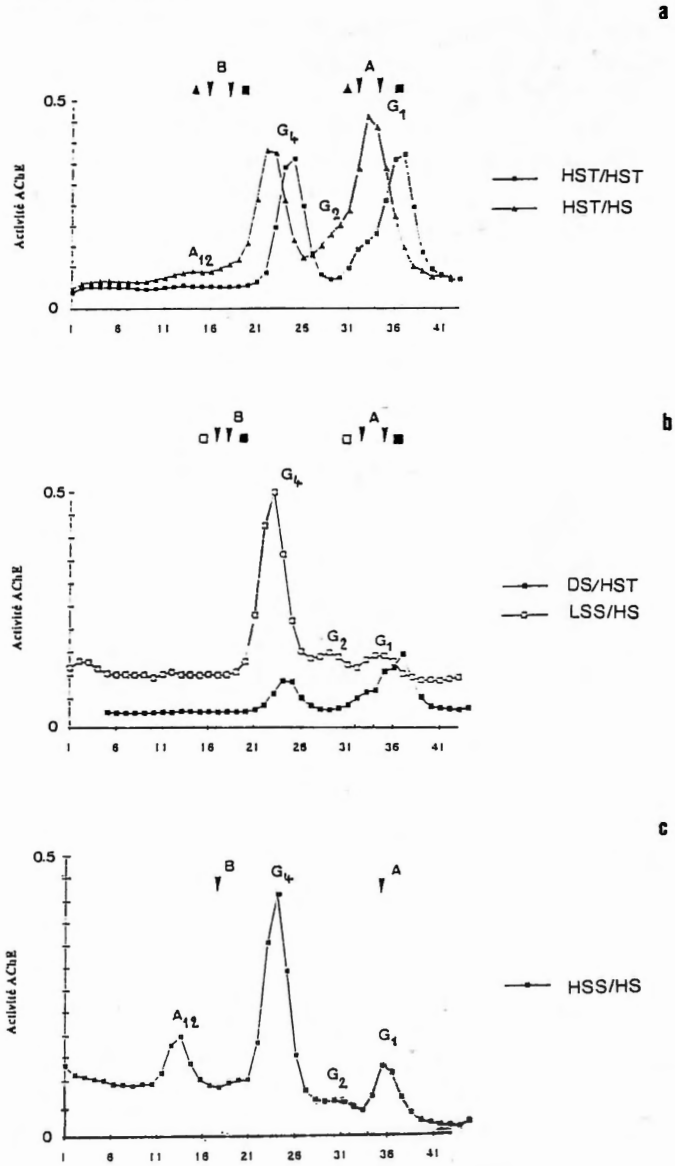

Fig. 3. – Analyse des formes moléculaires de l'acétylcholinestérase présente dans les rosettes olfactives de la carpe commune *Cyprinus carpio*. Les formes moléculaires ont été extraites au moyen de tampon HST (a, extrait direct), ou de façon séquentielle dans des tampons LS puis LST (en b), puis HS (en c) donnant les fractions LSS, DS et HSS. L'activité acétylcholinestérasique est exprimée en ΔA_{412}min.$^{-1}$ml^{-1}.A=phosphatase alcaline (6,1 S); B=E. coli ß-galactosidase (16 S).

Inhibition *in vivo* de l'AChE du système olfactif par le carbofuran

Balnéation de carpes à la dose de 50 ppb en carbofuran

Un premier essai a été entrepris. Il visait à mettre en évidence l'effet d'inhibition d'un micropolluant anticholinestérasique sur l'organe olfactif de la carpe. Le choix s'est porté sur une dose relativement élevée en toxique de façon à être certain que la concentration en inhibiteur soit suffisante pour provoquer une inhibition importante de l'AChE.

Il est important de signaler que la mortalité s'élève à 4 individus dans le bassin contenant le carbofuran et que les autres poissons souffraient de troubles moteurs graves comme des convulsions ou de la tétanie. Le taux d'inhibition de l'activité AChE dans le cerveau (83,1 ± 1,3 %), peut expliquer la mortalité observée (Fig. 4).

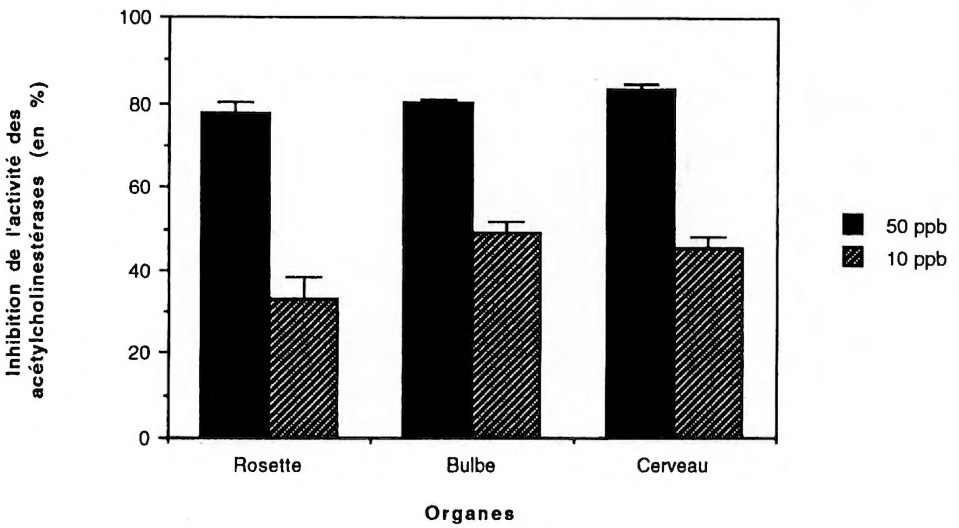

Fig. 4. – Effet du carbofuran aux doses de 10 et 50 ppb sur l'activité de l'acétylcholinestérase de l'organe olfactif et du cerveau de la carpe commune *Cyprinus carpio* après 48 heures.

On observe également un taux d'inhibition de 77,7 ± 2,8 % et de 80,5 ± 0,4 % respectivement dans les rosettes et le bulbe olfactif (Fig. 4). Les différents organes du système olfactif sont aussi sensibles aux anticholinestérases que le cerveau. Puisque la rosette est en contact direct et permanent avec le milieu extérieur, celle-ci subirait davantage l'effet des pesticides et serait un meilleur indicateur de la présence d'une pollution.

Balnéation de carpes à la dose de 10 ppb en carbofuran

Après 48 heures de balnéation en présence du carbofuran à la dose de 10 ppb, une diminution de l'activité AChE a été observée dans tous les organes olfactifs. En effet, les

taux d'inhibition de 33,4 ± 5,1 %; 49,3 ± 2,7 % et 45,8 ± 2,6 % ont été observés respectivement pour les rosettes, le bulbe olfactif et le cerveau (Fig. 4).

DISCUSSION

Dans le présent travail, nous avons caractérisé l'AChE présente en forte concentration dans le système olfactif de la carpe. Dans les rosettes olfactives, cette activité est cinq fois plus forte chez la carpe que chez la truite par exemple. Ces différences pourraient avoir un rapport avec le mode de vie.

La présence d'acétylcholinestérases au sein de la rosette olfactive serait liée à la perception des odeurs. L'olfaction serait moins développée chez les espèces vivant dans les eaux à courant rapide et utilisant préférentiellement la vue pour la recherche de nourriture que chez celles vivant dans les eaux calmes où la luminosité est plus faible. Selon KOTRSCHAL *et al.* (1991), la structure du cerveau des Téléostéens reflète leur style de vie. En comparant la morphologie des cerveaux de Cyprinidés, il est possible de distinguer le type de comportement alimentaire et notamment le style de recherche de nourriture: par la vue («sight feeders»), par le goût et l'olfaction («mouth tasters») ou par un sens chimique lié à la peau («skin tasters»).

Les inhibitions *in vitro* et *in vivo* par le carbofuran ont montré que l'AChE des rosettes, des bulbes olfactifs et du cerveau de la carpe sont sensibles à l'action des carbamates. Cette sensibilité de l'AChE au carbofuran rend certainement compte des troubles de comportement observés aux plus fortes doses. CHAKRABORTY *et al.* (1989) ont observé une diminution de l'activité acétylcholinestérasique de 95,39% au niveau de l'organe olfactif de *Heteropneustes fossilis* (Bloch) après une balnéation de deux heures avec du parathion-méthyle. Ils ont remarqué que les poissons présentaient de nombreuses anomalies comportementales, des mouvements rapides suivis d'une immobilité tétanique et un retard de l'ouverture des opercules. DUTTA *et al.* (1992) ont étudié la relation entre le comportement de la carpe indienne *Labeo rohita* (Haming Buchen) et la concentration en malathion. Ils ont montré que cet insecticide anticholinergique à la dose de 1 ppm perturbe également les mouvements du poisson.

Les formes moléculaires de l'AChE des rosettes olfactives ont été étudiées en comparaison avec celles détectées dans les bulbes olfactifs ou dans le reste du cerveau. Nous avons identifié les formes majoritaires G1 et G4 ainsi que des quantités plus faibles de formes dimériques G2. Des expériences préliminaires d'interaction avec les détergents non dénaturants nous ont montré qu'une partie au moins de ces formes est sans doute amphiphile indiquant qu'elles sont associées, *in situ*, à la membrane plasmique. Des études complémentaires sont toutefois encore nécessaires pour déterminer la nature exacte du domaine hydrophobe des molécules amphiphiles. Les formes globulaires représentent la très grande majorité de l'activité AChE des rosettes puisque les formes asymétriques sont à peine détectables dans un extrait direct (HST, Fig. 3a). Le recours aux extractions séquentielles permet cependant d'identifier sans ambiguité la forme A12 dans l'extrait HS (Fig. 3c).

Le rôle de l'AChE dans les rosettes olfactives reste énigmatique. En effet, il n'a jamais été décrit de synapses cholinergiques au niveau des récepteurs sensoriels ou des terminaisons efférentes de la muqueuse olfactive. La présence de formes globulaires d'AChE en dehors de tout contexte cholinergique n'est pas nouvelle y compris dans le système nerveux central (TOUTANT & MASSOULIÉ, 1988). Le rôle de ces formes d'AChE pourrait être un rôle d'hydrolyse de peptides auxquels le système olfactif est très sensible. En effet, l'hydrolyse des peptides neuroactifs par l'AChE a déjà été mentionnée (TOUTANT & MASSOULIÉ, 1988) et le système olfactif est très sensible aux acides aminés L- (CAPRIO, 1988). En revanche, la présence de formes asymétriques est considérée jusqu'à présent comme l'indice d'une innervation cholinergique si l'on excepte le cas des cellules musculaires différenciées *in vivo* et *in vitro* (Toutant, 1988). La présence de formes asymétriques dans les rosettes olfactives pose donc un problème intéressant; la contamination lors de la dissection des rosettes olfactives par des débris de bulbes (comportant des voies cholinergiques et apportant les formes asymétriques) pouvant être exclue. Il est à noter que les Téléostéens possèdent souvent des proportions très élevées de formes asymétriques (plus de 50% de l'activité totale AChE chez *Danio renio* ou *Esox lucius*, observations non publiées) sans que l'on sache pour l'instant si celles-ci sont toujours localisées aux voies cholinergiques.

Nous essayerons, dans l'avenir, de préciser la localisation de l'AChE des rosettes olfactives par histochimie ou immunohistochimie et des lieux de synthèse par hybridation *in situ*.

REMERCIEMENTS

Nos remerciements vont à Messieurs B. De Bast et B. Domange pour l'aide apportée dans la réalisation scientifique de ce travail ainsi que Messieurs J.-C. Gilson et C. Wonville pour la lecture du manuscrit. Les recherches sont subsidiées par le Ministère de la Région Wallonne (convention n° 21253).

RÉFÉRENCES BIBLIOGRAPHIQUES

ADMIRAAL, W., G. VAN DER VELDE , H. SMIT & W. G. CAZEMIER (1993) – The rivers Rhine and Meuse in the Netherlands: present state and signs of ecological recovery. *Hydrobiologia*, **265**:97-128.

BOCQUENÉ, G., F. GALGANI, T. BURGEOT, L. LE DEAN & P. TRUQUET (1993) – Acetylcholinesterase levels in marine organisms along french coasts. *Baseline*, **26**(2):101-106.

BRADFORD (1976) – A rapid and sensitive method for the quantitation of microgram quantities of protein using the principle of protein dye binding. *Anal. Biochem*, **22**: 248-258.

CAPRIO J. (1988) – Peripheral filters and chemoreceptor cells in fishes. *In*: *Sensory biology of aquatic animals*, ATEMA R., A.N. FAY, A.N. POPPER & W.N. TAVOLGA (eds). Springer Verlag, New York, 248 pp.

CHAKRABORTY, P.S., A. MALLIK, D.K. DINGAL & S. BANERJEE (1989) – Effect of methyl parathion on brain and olfactory organ acetylcholinesterase activity of the fish Heteropneustes fossilis. *Environment & Ecology*, 7: 310-314.

DUTTA, H.M., S.S.T. NASAR, J.S.D. MUNSHI & C.R. RICHMONDS (1992) – Malathion induced changes in the optomotor behavior of an indian carp, Laheo rohita. *Bull. Environ. Contam. Toxicol,* **49**: 562-568.

ELLMAN, G.L., K.D. COURTNEY, V. ANDRES & R.M. FEATHERSTONE (1961) – A new and rapid colorimetric determination of acetylcholinesterase activity. *Biochem. Pharmacol*, **7**: 88-95.

GALGANI, F., G. BOCQUENE, P. TRUQUET, T. BURGEOT, J.-F. CHIFFOLEAU & D. CLAISSE (1992) – Monitoring of pollutant biochemical effects on marine organisms of French Coasts. *Oceanologica Acta*, **15**: 355-364.

HABIG, C. & R.T. DI GIULIO (1991) – Biochemical characteristics of cholinesterases in aquatic organisms. *In*: *Cholinesterase-inhibiting insecticides. Their impact on widlife and the environment.* MINEAU P. (ed). Elsevier, Amsterdam: 19-34.

HARA T.J. (1986) – Role of olfaction in fish behaviour. *In*: *The behaviour of teleost fishes.* PITCHER T.J. (ed). Croom Helm, London & Sidney: 185-197.

KOTRSCHAL, K., R. BRANDSTÄTTER, A. GOMAHR, H. JUNGER, M. PALZENBERGER & M. ZAUNREITER (1991) – Brain and sensory systems. *In*: *Cyprinid Fishes. Systematics, biology and exploitation.* WINFIELD I.J. and NELSON J.S. (eds). Chapman & Hall, London: 45-63.

MASSOULIÉ, J. & S. BON (1982) – The molecular forms of cholinesterase and acetylcholinesterase in vertebrates. *Ann. Rev. Neurosci*, **5**: 57-106.

MASSOULIÉ, J. & J.-P. TOUTANT (1988) – Vertebrates cholinesterases: structures and types of interaction. *In*: *Handbook of Experimental Pharmacology Vol. 86.* V.P. WHITTAKER (ed). Springer Verlag, Berlin: 225-265.

SAGLIO, P. (1986) – Considérations sur le mécanisme chémosensoriel de la migration reproductrice chez les Salmonidés. *Bull. Fr. Pêche Piscic.*, **301**: 35-55.

SCHERER, E. (1975). – Avoidance of fenitrothion by goldfish. *Bull. Environ. Contam. Toxicol.*, **13**: 492-496.

SCHUMACHER, P.D. & J.J. NEY, (1980) – Avoidance response of rainbow trout to single dose chlorination in a power plant discharge canal. *Water Res.*, **14**: 651-655.

SUTTERLIN, A.M. (1974). – Pollutants and the chemical senses of aquatic animals - perspective and review. *Chem. Senses Flavor,* **1**: 167-178.

SZABO, A., J. NEMCSOK, B. ASZTALOS, Z. RAKONCZAY, P. KASA & LE HUU HIEU (1992) – The effects of pesticides on Carp (*Cyprinus carpio* L.). Acetycholinesterase and its biochemical characterization. *Ecotoxicology and Environmental Safety*, **23**: 39-45.

TOUTANT, J.-P. (1988) – Expression of asymmetric forms of acetylcholinesterase during myogenesis in vitro. *Reprod. Nutr. Develop.*, **28**: 693-702.

TOUTANT, J.-P. & J. MASSOULIÉ (1988) – Vertebrates cholinesterases: tissues and cellular distribution of molecular forms and their physiological regulation. *In*: *Handbook of Experimental Pharmacology* Vol. 86. WHITTAKER V. (ed). Springer Verlag, Berlin, 355 p.

WÄCHTLER, K. (1988) – Phylogeny of cholinergic synapse. *In*: *Handbook of Experimental Pharmacology* Vol. 86. WHITTAKER V.P. (ed.). Springer Verlag, Berlin: 57-80.

ZINKL, J.G., W.L. LOCKHART, S.A. KENNY & F.L. WARD (1991) – The effects of cholinesterase inhibiting insecticides on fish. *In*: *Cholinesterase-inhibiting insecticides. Their impact on wildlife and the environment.* MINEAU (ed.) Elsevier, Amsterdam: 233-254.

Belg. J. Zool. - Volume 127 (1997) - issue 1 - pages 75-97 - Brussels 1997

Received : 21 January 1997

LES CLUPÉOMORPHES (PISCES, TELEOSTEI) DU CÉNOMANIEN (CRÉTACE) DE KIPALA (KWANGO, ZAIRE): OSTÉOLOGIE ET PHYLOGÉNIE

LOUIS TAVERNE

Université Libre de Bruxelles (U.L.B.), Faculté des Sciences,
Département de Biologie animale, Laboratoire de Morphologie
fonctionnelle (C.P. 160/11), avenue F.D. Roosevelt, 50, B-1050 Bruxelles, Belgique

Résumé. «*Diplomystus*» *dartevellei*, *Eoknightia caheni* et *Nolfia kwangoensis*, les trois Téléostéens Clupéomorphes du Cénomanien de Kipala (Kwango, Zaïre) sont réétudiés. Leur position systématique dans la phylogénie des Clupéomorphes est discutée et un cladogramme phylogénétique proposé. Un nouveau genre, *Kwangoclupea*, est érigé pour «*D.*» *dartevellei* qui est le groupe-frère immédiatement apomorphe des Ellimmichthyiformes. *Eoknightia* est plus apomorphe que *Kwangoclupea* et représente le groupe-frère plésiomorphe d'un clade incluant *Spratticeps*, *Santanaclupea* et les Clupéiformes. *Nolfia* se révèle être un Clupéoïde.

Mots clefs: «*Diplomystus*» *dartevellei*, *Eoknightia caheni*, *Nolfia kwangoensis*, *Kwangoclupea* nov. gen., Clupéomorphes, Téléostéens, Cénomanien, Kipala, Kwango, Zaïre.

The clupeomorphs (Pisces, Teleostei) from the Cenomanian (Cretaceous) of Kipala (Kwango, Zaire): osteology and phylogeny

Abstract. «*Diplomystus*» *dartevellei*, *Eoknightia caheni* and *Nolfia kwangoensis*, the three Cenomanian clupeomorph teleosts from Kipala (Kwango, Zaire), are restudied. Their systematic position within the clupeomorph phylogeny is discussed and a phylogenetic cladogram proposed. A new genus, *Kwangoclupea*, is erected for «*D.*» *dartevellei* which is the immediate apomorphic sister-group of the Ellimmichthyiformes. *Eoknightia* is more apomorphic than *Kwangoclupea* and represents the plesiomorphic sister-group of a clade including *Spratticeps*, *Santanaclupea* and the Clupeiformes. *Nolfia* appears to be a clupeoid.

Key words: «*Diplomystus*» *dartevellei*, *Eoknightia caheni*, *Nolfia kwangoensis*, *Kwangoclupea* nov. gen., clupeomorphs, teleosts, Cenomanian, Kipala, Kwango, Zaire.

INTRODUCTION

Les Clupéiformes ou Isospondyles n'ont été durant des décennies qu'un vaste regroupement paraphylétique où se rangeaient la plupart des familles téléostéennes primitives. GREENWOOD *et al.* (1966) furent les premiers à scinder de façon cohérente cet ensemble en une série d'ordres et de super-ordres bien définis par leurs caractères spécialisés. Ils ont ainsi proposé un super-ordre des Clupéomorphes sur la base de quelques synapomorphies

remarquables dont la présence d'un *recessus lateralis* et de diverticules vésicaux intracrâniens abrités dans des bulles osseuses du prootique et du ptérotique (*ibid.*: 350). Tel que défini par ces auteurs, ce super-ordre ne comprenait qu'un seul ordre, les Clupéiformes, très restreint par rapport à son acception ancienne, et deux sous-ordres, les Denticipitoidei et les Clupeoidei.

La connaissance des Clupéomorphes s'est affinée par la suite. On a ainsi montré que certains représentants fossiles primitifs du super-ordre ne possédaient pas encore tous les caractères invoqués pour définir le groupe et que, par exemple, le *recessus lateralis* n'était pas encore réalisé chez les formes les plus archaïques (PATTERSON, 1967, 1970; GRANDE, 1982a). Un nouvel ordre, les Ellimmichthyiformes, et divers autres clades ont ainsi été fondés (PATTERSON, 1970; FOREY, 1973, 1975; GRANDE, 1982a, b, 1985; MAISEY, 1993). La phylogénie des Clupéomorphes a également été étudiée et les ordres, sous-ordres et familles qui composent ce super-ordre ont été définis de manière cladistique (GRANDE, 1982a, b, 1985; GRANDE & NELSON, 1985).

Rappelons aussi que le plus ancien représentant avéré des Clupéomorphes remonte au Barrémien (milieu du Crétacé inférieur). Il s'agit de «*Clupea*» *antiqua* Pictet, 1858 de Voirons, en Suisse (PATTERSON, 1993: 627). Son ostéologie demeure trop mal connue pour qu'une attribution générique précise puisse être proposée pour lui mais sa serrature ventrale (PICTET, 1858: pl. IV, fig. 7, 8, 12, 13) est typique du super-ordre.

L'ichtyofaune cénomanienne (début du Crétacé supérieur) marine lagunaire de Kipala, au Kwango, Zaïre, renferme trois espèces, «*Diplomystus*» *dartevellei* Casier, 1965, *Eoknightia caheni* Taverne, 1976 et *Nolfia kwangoensis* Taverne, 1976, dont la serrature ventrale et le complexe urophore attestent qu'elles appartiennent aux Clupéomorphes (CASIER, 1965; TAVERNE, 1976). Lors de leur description, ces trois poissons ont été rapportés à la famille des Clupeidae.

Cependant, PATTERSON (1967) et surtout GRANDE (1982a, b) ont apporté une meilleure connaissance du genre fossile *Diplomystus* Cope, 1877. Cela a conduit à la création du genre *Armigatus* Grande, 1982 pour l'espèce «*Diplomystus*» *brevissimus* de Blainville, 1818, du Crétacé supérieur du Liban, et a restreint *Diplomystus* à quatre espèces seulement dont *Diplomystus dentatus* Cope, 1877, de l'Eocène des Etats-Unis, est l'espèce-type. Les autres espèces du genre, y compris «*Diplomystus*» *dartevellei*, en ont été exclues et laissées en position *incertae sedis* (GRANDE, 1985: 315). D'autre part, certains des critères anatomiques utilisés par GRANDE (1982a, b, 1985) pour classifier les Clupéomorphes n'étaient pas ou étaient incomplètement connus chez les deux autres espèces de Kipala qui ont, dès lors, elles aussi, été laissées *incertae sedis* (GRANDE, 1985: 316, 319).

Il était donc nécessaire de réétudier ces trois Clupéomorphes du Kwango pour préciser davantage leur position systématique au sein du super-ordre et cela d'autant plus que, pour «*Diplomystus*» *dartevellei* et *Eoknightia caheni*, les spécimens disponibles permettent une description du crâne plus détaillée que celles qui ont été faites antérieurement (CASIER, 1965; TAVERNE, 1976). C'est là le but du présent travail.

Notons encore que la stratigraphie, les conditions de dépôts, la paléoécologie, la zoogéographie et la biodiversité du gisement de Kipala ont déjà fait l'objet de multiples études (GREKOFF, 1960; CASIER, 1965, 1969; TAVERNE, 1976; LEPERSONNE, 1977). J'y renvoie le lecteur intéressé.

Remarquons aussi que les trois Clupéomorphes de Kipala ne sont pas les seuls représentants de ce super-ordre dans le Crétacé marin du Zaïre. Une quatrième espèce, *Audenaerdia casieri* (Taverne, 1969) est connue dans le Santonien (milieu du Crétacé supérieur) de Vonso, au Bas-Zaïre. Elle vient de faire l'objet d'une toute récente révision (TAVERNE, sous presse).

MATÉRIEL ET MÉTHODE

L'ensemble du matériel concerné, déposé dans les collections du Musée Royal de l'Afrique Centrale, à Tervuren, Belgique, a été revu: les exemplaires R.G. 10.982 (holotype), 10.983 (paratype), 10.979, 10.980, 10.981 et 11.079 de «*Diplomystus*» *dartevellei*, 11.129 (holotype) d'*Eoknightia caheni* et 10.978 (holotype) de *Nolfia kwangoensis*.

Le matériel a été étudié au moyen d'un stéréomicroscope WILD M8 et dessiné par l'auteur à la chambre claire (camera lucida).

RÉSULTATS

Ostéologie de «*Diplomystus*» *dartevellei* (Fig. 1A, 2, 3A, B, C, 4)

«*Diplomystus*» *dartevellei* est un très petit téléostéen qui ne dépasse pas une trentaine de millimètres de longueur totale. La tête est à peu près aussi longue que haute. Le corps est court, élevé et offre un abdomen très saillant.

C'est le paratype R.G. 10.983 qui possède la tête la mieux conservée. Elle y est présentée par sa face latérale droite. Le même échantillon renferme aussi un spécimen fragmentaire où l'on distingue la moitié gauche du toit crânien. La tête de l'holotype R.G. 10.982 est très abimée et ne montre guère plus que le contour général. Les informations sur le squelette crânien proviennent donc du paratype uniquement.

Le mésethmoïde et le vomer manquent. L'ethmoïde latéral est bien développé et descend du frontal jusqu'au parasphénoïde.

La voûte crânienne est formée par les vastes frontaux, les petits pariétaux et le supraoccipital. Le crâne est médio-pariétal, avec des pariétaux traversés par la commissure sensorielle extrascapulaire. Le canal sensoriel supraorbitaire suit le bord externe du frontal et se rabat postéro-latéralement vers la région du ptérotique. Le canal émet une fine commissure sensorielle pariétale toute entière comprise dans le frontal et qui ne pénètre donc pas sur le pariétal. Le frontal et le pariétal sont ornés de fortes rides longitudinales. Le supraoccipital porte une crête médio-postérieure bien marquée et n'est pas traversé par la commissure sensorielle extrascapulaire.

Le ptérotique est haut et traversé près de sa base par le canal sensoriel postorbitaire (=otique) qui prolonge le canal supraorbitaire venu du frontal. L'absence de *recessus lateralis* s'observe aisément. Un petit épiotique (=épioccipital) surplombe l'arrière du ptérotique. Un étroit renfoncement entre ces deux os marque l'emplacement de la petite fosse préépiotique. Le substrat géologique apparaît dans une lacune osseuse entre le frontal, le

pariétal et le ptérotique. C'est la trace d'une fenêtre temporale bien développée. Un petit sphénotique triangulaire se remarque sous la région antérieure du ptérotique.

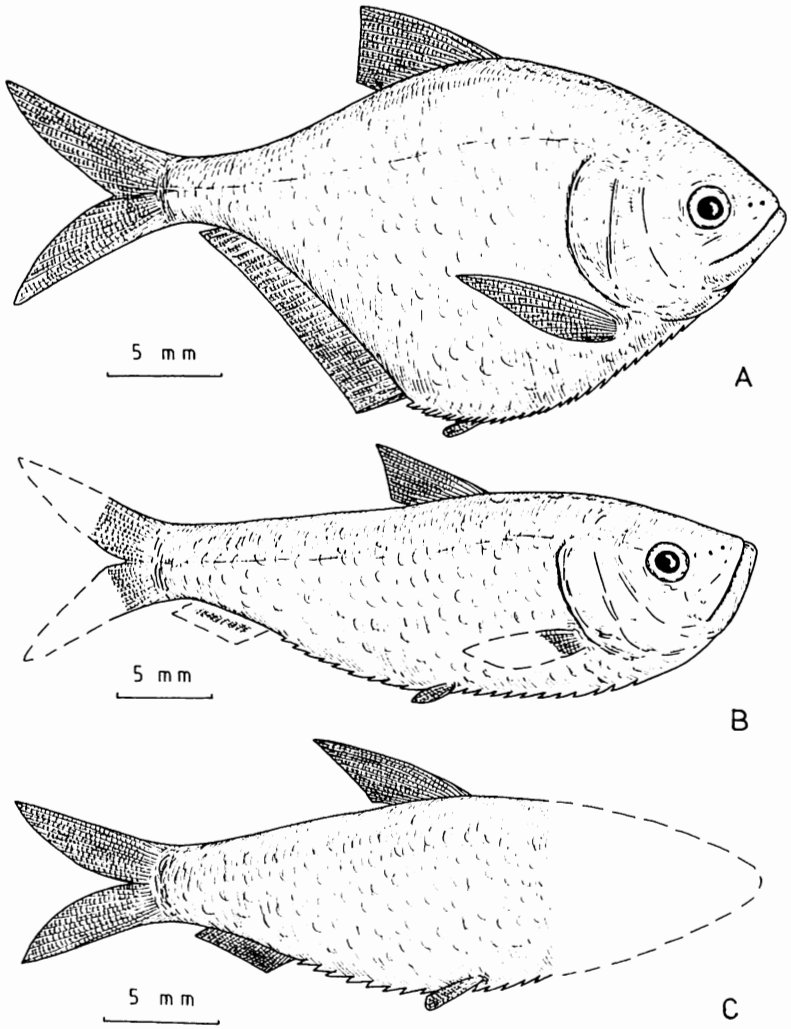

Fig. 1. – Reconstitutions de «*Diplomystus*» *dartevellei* (A), d'après l'holotype R.G. N° 10.982 (retourné), d'*Eoknightia caheni* (B), d'après l'holotype R. G. N° 11.129, et de *Nolfia kwangoensis* (C), d'après l'holotype R. G. N° 10.978.

Les os sphénoïdes sont grands. L'orbitosphénoïde impair est vaste et en position très antérieure puisqu'il s'applique contre le bord postérieur de l'ethmoïde latéral. Il est suivi par le pleurosphénoïde bien visible sous le frontal et, plus ventro-postérieurement, par le basisphénoïde muni d'un large bélophragme. Le parasphénoïde est fin, allongé, garni d'un fort processus basiptérygoïde et paraît édenté.

Le basioccipital est situé beaucoup plus haut sur le crâne que la portion sous-orbitaire du parasphénoïde. Cela indique que les parties parachordale et trabéculaire du plancher neurocrânien formaient entre elles un angle presque droit. Le prootique, l'intercalaire et l'exoccipital ne sont pas connus.

Chaque hémi-mâchoire supérieure comporte le prémaxillaire, le maxillaire et deux supramaxillaires. Le prémaxillaire est grand, denté, élevé dans sa région symphysaire et étroit dans sa partie post-symphysaire. Le maxillaire est incomplet mais semble avoir été de forme allongée, étroit au-dessus du prémaxillaire, élargi en arrière. Il forme la plus grande partie du bord buccal supérieur. Les deux supramaxillaires sont énormes et le postérieur encore un peu plus que l'antérieur. Le supramaxillaire postérieur s'étire en une forte pointe antérieure qui surplombe le premier supramaxillaire.

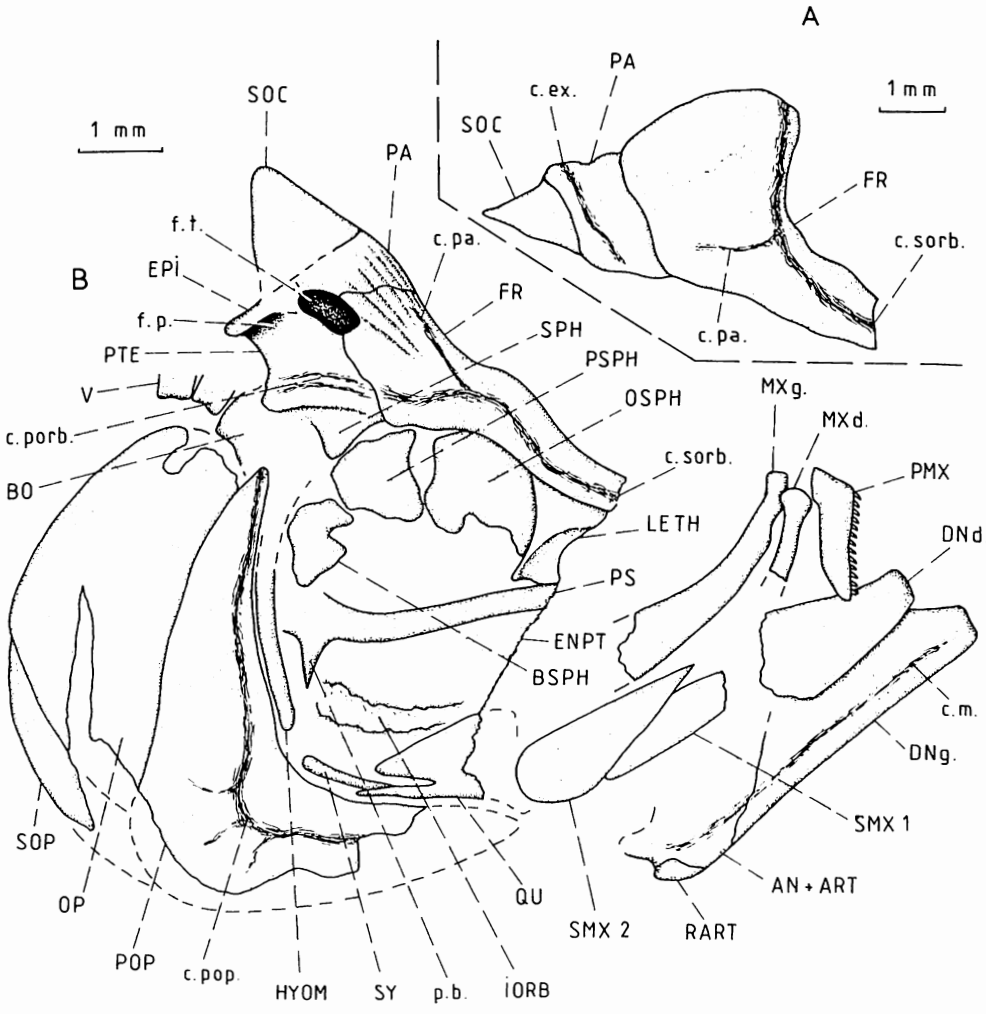

Fig. 2. – Le crâne de «*Diplomystus*» *dartevellei*: (A) la moitié gauche du toit crânien d'après le paratype R. G. N° 10.983 (spécimen incomplet); (B) en vue latérale droite d'après le paratype R.G. N° 10.983 (spécimen complet).

La mandibule est mal préservée. Sa longueur fait un peu moins de la moitié de la longueur de la tête. Son articulation avec le carré se réalise au niveau du bord antérieur de l'orbite. Le bord symphysaire est étroit mais, plus en arrière, le bord oral du dentaire s'élève de façon régulière. On ne distingue pas de dents sur le dentaire mais cela est probablement dû au mauvais état de conservation. Sous l'extrémité postérieure de l'angulo-articulaire, on distingue un petit rétroarticulaire exclu de la fossette d'articulation avec le carré.

Rien n'est connu des os de la série orbitaire si ce n'est les restes partiels d'un infraorbitaire allongé et étroit (le deuxième?) qui chevauche l'entoptérygoïde.

Le carré est partiellement conservé. Il paraît avoir été triangulaire. Il s'orne d'un processus quadrato-jugal que prolonge un étroit symplectique. L'entoptérygoïde est très large et semble édenté. Le palatin, l'ectoptérygoïde et le métaptérygoïde sont inconnus. La fine tige ventrale de l'hyomandibulaire se distingue devant le préoperculaire.

Les os de la série operculaire sont très développés. Le préoperculaire est grand, large, avec de longues branches dorsale et ventrale formant entre elles un angle droit. Le canal sensoriel préoperculaire émet quelques diverticules dans sa partie basale. L'interoperculaire n'est pas visible. L'operculaire est vaste, beaucoup plus haut que large. Le sous-operculaire est étroit et sa ligne de suture avec l'operculaire est très oblique. Quelques faibles traces de rayons branchiostèges s'aperçoivent sur l'holotype mais il est impossible de les dénombrer.

De la ceinture scapulaire, seul le cleithrum est visible. Deux postcleithra au moins, en forme d'écaille, lui sont accolés. La nageoire pectorale est longue, insérée haut sur les flancs et compte au moins 12 rayons. L'holotype a conservé quelques traces de très courtes nageoires pelviennes, situées à mi-longueur de l'abdomen et débutant un peu en arrière du niveau de l'origine de la nageoire dorsale.

C'est à nouveau le paratype qui permet le compte le plus exact des vertèbres. Il y en a 32, y compris les vertèbres urales I et II, dont 13 ou 14 sont abdominales et les autres caudales. Toutes les vertèbres portent des arcs neuraux et des neurépines, sauf les deux dernières. Les vertèbres abdominales portent de petites hémapophyses. Un arc hémal normal prolongé d'une courte hémépine apparaît dès l'avant-dernière vertèbre abdominale. Les vertèbres caudales possèdent des arcs hémaux prolongés par de longues hémépines. Il y a des épineuraux associés aux vertèbres abdominales et aux premières vertèbres caudales ainsi que des épipleuraux associés aux premières vertèbres caudales. TAVERNE (1976: 8) signale cinq supraneuraux. Cela s'observe, en effet, chez l'holotype. Cependant, l'exemplaire R.G. 10.981 (face gauche) montre l'empreinte de trois supraneuraux antérieurs suivis des restes de quatre supraneuraux plus grands, soit sept supraneuraux au total. Ces supraneuraux sont larges, nettement plus larges à leur sommet qu'à leur base et orientés à peu près verticalement. Le premier supraneural est situé derrière l'occiput et le dernier devant le premier ptérygophore dorsal. On compte 10 ou 11 paires de longues côtes étroites attachées aux vertèbres depuis la troisième jusqu'à l'avant-dernière abdominale. La dernière vertèbre abdominale ne porte qu'une paire de courtes côtes.

La nageoire dorsale est courte, débute aux environs du niveau de la huitième vertèbre, soit un peu en avant de l'origine des nageoires pelviennes, et compte 2 petits rayons épineux suivis de 11 à 13 rayons segmentés allongés. Le premier ptérygophore dorsal est plus développé que les suivants. La nageoire anale occupe une position reculée sur le corps.

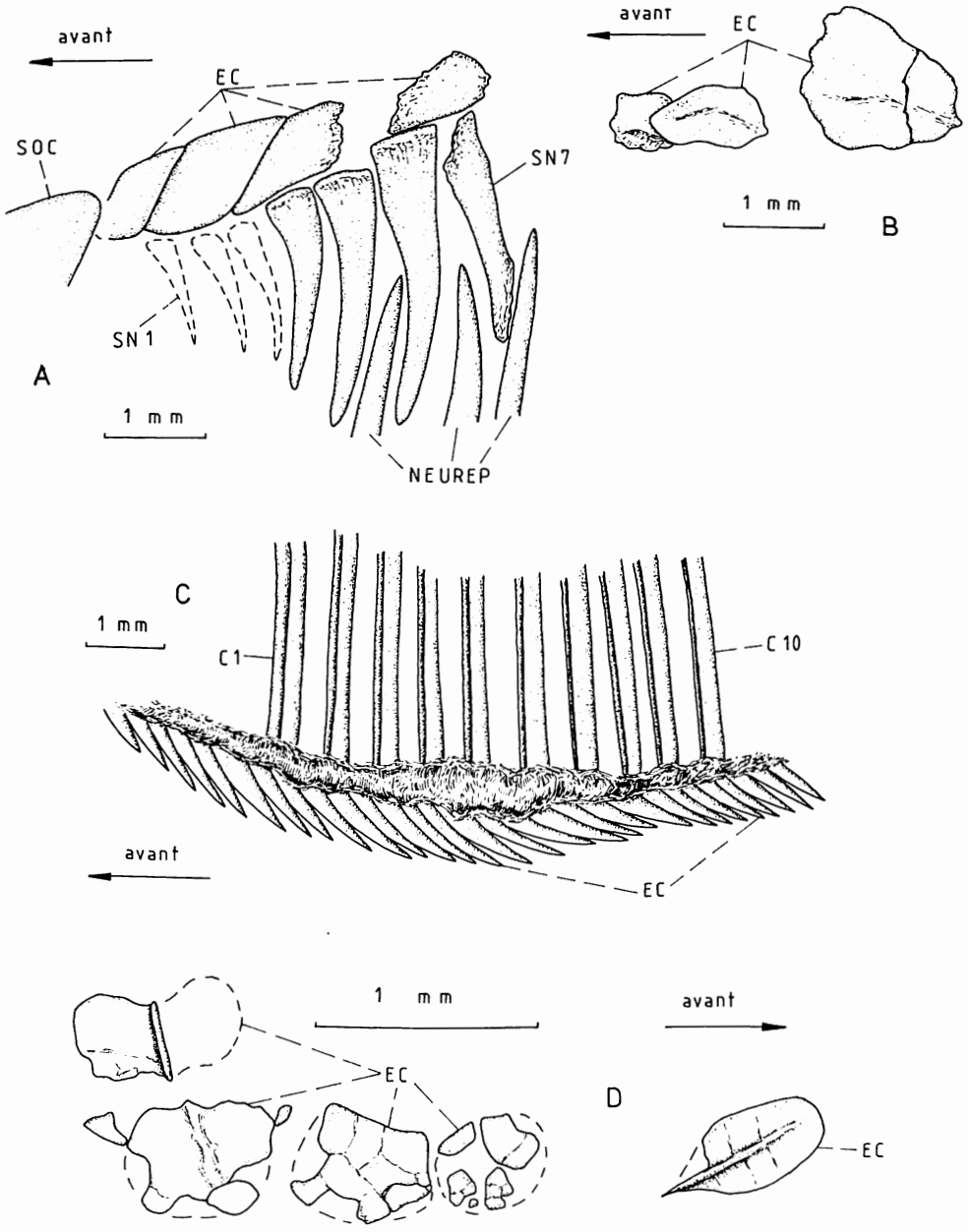

Fig. 3. – «*Diplomystus*» *dartevellei*: (A) le début de la serrature dorsale, derrière le crâne, d'après la face gauche du spécimen R. G. N° 10.981; (B) l'extrémité postérieure de la serrature dorsale, juste en avant de la nageoire dorsale, d'après la face droite de l'holotype R. G. N° 10.982 (retourné); (C) la serrature ventrale d'après l'holotype R. G. N° 10.982. *Eoknightia caheni*: (D) la serrature dorsale d'après l'holotype R. G. N° 11.129, avec les dernières écailles, juste devant la nageoire dorsale (à gauche) et une des écailles antérieures (à droite).

Elle est longue, compte au moins 1 petit rayon épineux et 27 à 29 rayons segmentés de plus grande taille. Elle se termine très près de la nageoire caudale. Les premiers ptérygophores anaux sont très allongés et le premier d'entre eux qui se positionne dans le prolongement de l'hémépine de la première vertèbre caudale, est aussi quelque peu élargi.

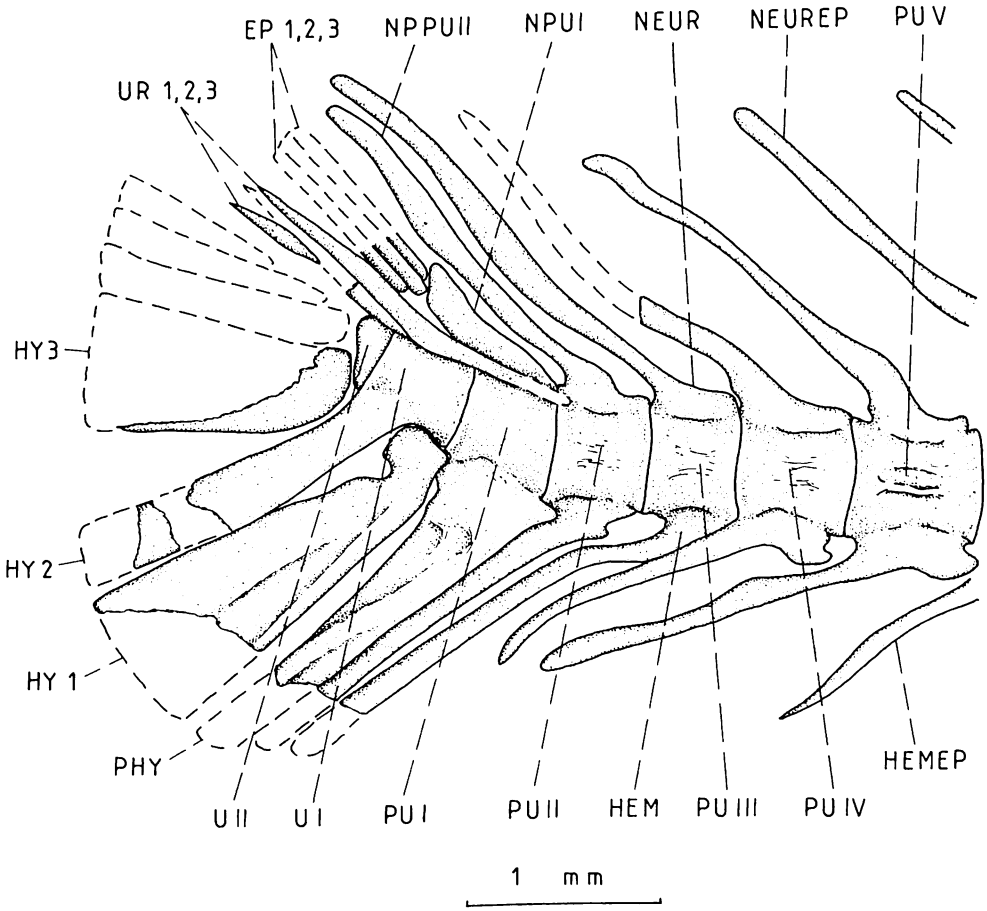

Fig. 4. – Le squelette caudal de «*Diplomystus*» *dartevellei*, d'après le paratype R.G. N° 10.983 (spécimen complet).

C'est sur le paratype que le complexe urophore est le mieux conservé. Les vertèbres préurale I, urale I et urale II sont indépendantes les unes des autres. Le centre ural II est réduit. Par contre, la vertèbre urale I est pratiquement aussi développée que la vertèbre préurale I. La neurépine préurale II est complète. La vertèbre préurale I porte un long arc neural mais il n'y a plus de neurépine complète. On observe trois épuraux. Il y a également trois paires d'uroneuraux. Le premier uroneural est autogène et s'étend jusqu'au niveau de la vertèbre préurale II. Le deuxième uroneural, plus court, ne s'étend que jusqu'au bord postérieur de la vertèbre urale I. Le troisième uroneural est très petit et rejeté

postérieurement entre les bases des lépidotriches caudaux. Le parhypural est très large et soudé à la vertèbre préurale I. Le premier hypural, très large, possède une tête proximale bien développée et qui s'articule avec la face ventrale de la vertèbre urale I. Le deuxième hypural, massif mais plus étroit, est soudé à la vertèbre urale I. On distingue un fragment d'un très large troisième hypural derrière le petit centre ural II. Les autres hypuraux ne sont pas visibles mais il y en avait fort probablement six au total comme chez les autres Clupéomorphes primitifs. Un espace sépare les deuxième et troisième hypuraux.

La queue est bifide mais aucun exemplaire ne permet le décompte exact des rayons caudaux. Il y en avait probablement 19 principaux dont 17 branchus comme chez la plupart des Clupéomorphes. Il ne paraît y avoir ni plaques précaudales ou fulcres frangeants ni urodermaux.

TAVERNE (1976: fig. 3) décrit les écailles comme petites et couvertes de fins *circuli* concentriques. De telles écailles existent mais sont confinées dans la région du bord dorsal du poisson, entre les nageoires dorsale et caudale. Sur le corps, on remarque des écailles plus grandes où les fins *circuli* sont légèrement arqués mais gardent néanmoins une disposition à peu près verticale et non pas concentrique. Il y a une serrature dorsale entre l'occiput et le début de la nageoire dorsale. Ce sont des écailles de forme grossièrement triangulaire. Le début de cette serrature dorsale s'observe sur le spécimen R. G. 10.981 et la fin sur l'holotype 10.982. D'après la taille de ces écailles, il ne devait pas y en avoir plus de six ou sept pour toute la serrature dorsale. La dernière de ces écailles est plus vaste que les précédentes et précède directement l'origine de la nageoire dorsale. Une forte serrature ventrale occupe toute la ligne médio-ventrale du poisson depuis l'isthme de la gorge jusqu'à l'origine de la nageoire anale. Elle comprend une trentaine d'écailles pointues très serrées les unes contre les autres. Dans la région des côtes ventrales, il y a correspondance de deux écailles par paire de côtes. Cela tranche d'avec *Armigatus*, *Diplomystus* et les autres Ellimmichthyidae où cette correspondance est d'à peu près une écaille par paire de côtes (observations personnelles).

Ostéologie d'*Eoknightia caheni* (Fig. 1B, 3D, 5, 6)

Eoknightia caheni n'est connu que par l'holotype R.G. 11.129, un exemplaire très mal conservé de 38 mm de longueur totale et 32 mm de longueur standard. Le corps est moyennement élevé, avec un hauteur maximale qui entre 3 fois dans la longueur standard. Le dos est plat et le ventre arrondi mais sans hypertrophie. La tête est grande, un peu plus longue que haute et sa longueur va 2,66 fois dans la longueur standard. La forme générale du poisson évoque beaucoup celle de *Diplomystus dentatus*.

Certains détails du crâne sont discernables malgré la médiocre conservation. La voûte crânienne est formée par de grands frontaux sur lesquels on discerne le trajet du canal sensoriel supraorbitaire, des petits pariétaux jointifs et déterminant donc un crâne de type médio-pariétal, ainsi que par le supraoccipital qui a laissé une profonde empreinte sur le substrat. Certains fragments du mésethmoïde sont visibles mais la forme précise de l'os n'est pas déterminable. L'ethmoïde latéral est bien développé. Plus en arrière, on observe un vaste orbitosphénoïde creusé d'une fenêtre médiane pour le passage des nerfs optiques (II) gauche et droit. L'orbitosphénoïde est proche de l'ethmoïde latéral mais il n'y a cepen-

dant pas contact entre les deux os. Derrière l'orbitosphénoïde, on remarque une masse osseuse concassée, le pleurosphénoïde. La portion sous-orbitaire du parasphénoïde, seule visible, est édentée et dépourvue de processus basiptérygoïde. Il y a une vaste fenêtre interoculaire entre l'orbitosphénoïde et le pleurosphénoïde, d'une part, et le parasphénoïde, d'autre part. Des fragments du sphénotique, de l'épiotique, du ptérotique et du basioccipital sont visibles, sans qu'on puisse cependant définir la forme de ces os. Le basioccipital occupe sur le crâne une position nettement plus élevée que la portion sous-orbitaire du parasphénoïde, ce qui indique l'existence d'un angle marqué entre les parties parachordale et trabéculaire du plancher neurocrânien. Toutefois, ce caractère est moins prononcé que chez «*Diplomystus*» *dartevellei*. Le basisphénoïde, le prootique, l'exoccipital et l'intercalaire ne sont pas connus. Il en va de même des os de la série orbitaire dont seuls quelques petits fragments s'observent dans la fenêtre interoculaire.

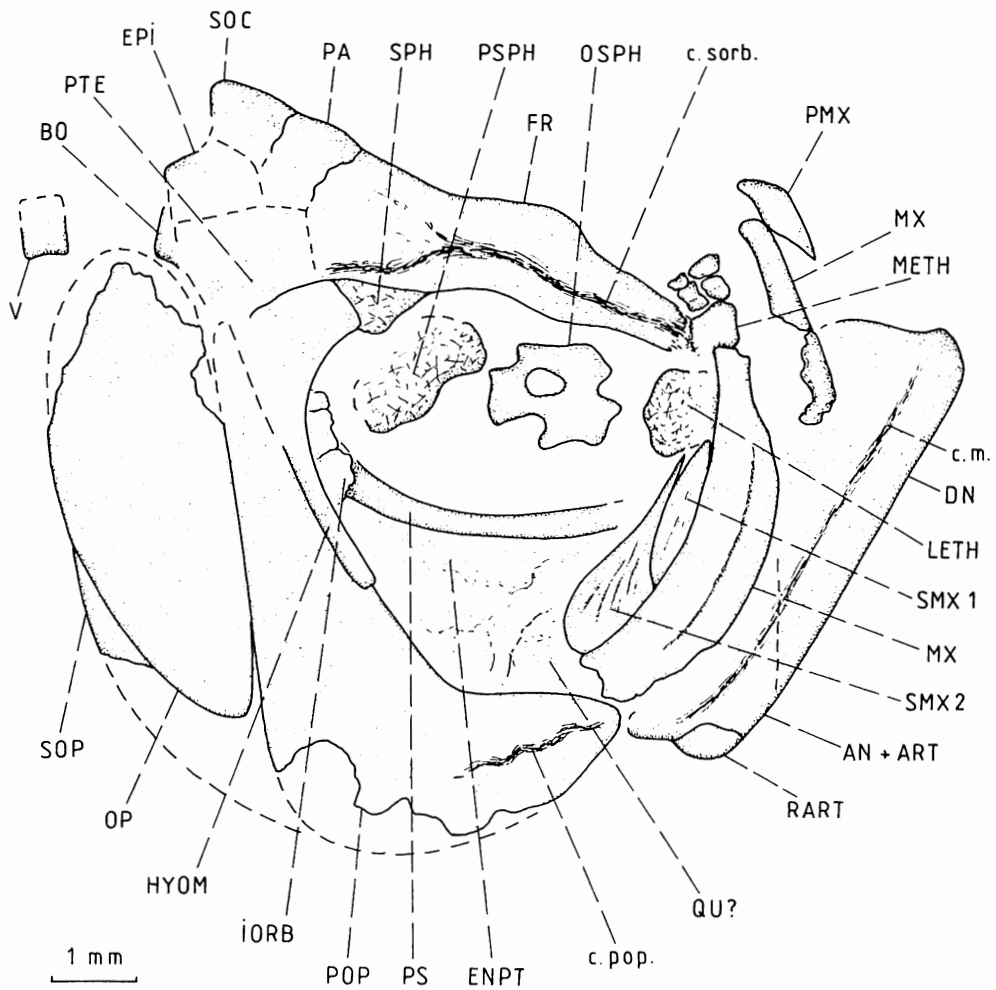

Fig. 5. – Le crâne d'*Eoknightia caheni* en vue latérale droite, d'après l'holotype R. G. N° 11.129.

Chaque hémi-mâchoire supérieure comprend un prémaxillaire, un maxillaire et deux supramaxillaires. Le prémaxillaire a laissé une empreinte très profonde; c'est un petit os, pointu vers l'arrière, un peu plus haut dans la région symphysaire. Le maxillaire est long, étroit dans la région supra-premaxillaire, fort large dans la région où il borde la bouche. Le premier supramaxillaire est plus petit que le second qui s'étire en une fine pointe antérieure. La mâchoire supérieure est édentée.

La mandibule est grande puisqu'elle représente près de la moitié de la longueur du crâne; elle paraît haute et son articulation avec le carré se situe au niveau du bord antérieur de l'orbite. Le prognathisme est très prononcé. Le bord symphysaire est étroit mais le bord oral s'élève vers l'arrière de façon très marquée. La limite entre le dentaire et l'angulo-articulaire n'est pas discernable. Par contre, on voit très clairement le petit rétroarticulaire exclu de la fossette d'articulation pour le carré. La mandibule est édentée.

L'ectoptérygoïde, le métaptérygoïde et le palatin ne sont pas connus. L'entoptérygoïde est large et semble dépourvu de denticules. L'hyomandibulaire est allongé, élargi dorsalement et prolongé ventralement par une fine tigelle qui longe le bord antérieur du préoperculaire.

L'operculaire est très haut mais aussi très étroit. Le préoperculaire est très large, avec une branche dorsale plus longue que la ventrale. Les deux branches forment entre elles un angle obtus. Le sous-operculaire est long, très étroit et sa suture avec l'operculaire est très oblique. L'interoperculaire et les rayons branchiostèges ne sont pas connus.

Un morceau de la nageoire pectorale est conservé. On peut y compter 8 rayons. Les nageoires pelviennes sont petites, insérées à mi-longueur de la région abdominale du poisson, soit un peu en arrière du niveau de l'origine de la nageoire dorsale. Le nombre des rayons pelviens n'est pas déterminable.

Du squelette axial, seuls les moules internes des quatorze dernières vertèbres sont conservés. En comparant la longueur de ce segment de quatorze vertèbres et celle du squelette axial au complet, on peut extrapoler que le nombre total des vertèbres devait être d'approximativement 35. Derrière la tête, on observe les restes concassés de quelques neurépines et supraneuraux.

L'origine de la nageoire dorsale se situe au niveau du premier quart de la longueur du dos. Cette nageoire comporte 2 petits rayons épineux initiaux suivis de 10 rayons plus grands et segmentés. La nageoire anale occupe une position reculée sur le corps mais elle est trop partiellement conservée pour qu'on puisse en dénombrer les rayons ou juger de sa longueur.

Le squelette caudal a laissé une empreinte à peu près complète, recouverte ça et là de fragments osseux. C'est un complexe urophore fondamentalement du même type que celui de «*Diplomystus*» *dartevellei*, avec les vertèbres préurale I, urale I et urale II indépendantes les unes des autres, une neurépine préurale II complète, un grand arc neural préural I dépourvu de neurépine et un premier uroneural autogène. Il y a au moins un épural. Cette apparente réduction du nombre des épuraux est vraisemblablement due à l'état de conservation défectueux du spécimen. Seul le premier uroneural est partiellement conservé. Il s'étend jusqu'à la vertèbre préurale I dont il reste indépendant. Il y avait probablement deux autres uroneuraux comme chez beaucoup de Clupéomorphes. La vertèbre urale I est

un peu plus petite que la vertèbre préurale I. Le parhypural est soudé à la vertèbre préurale I et le deuxième hypural à la vertèbre urale I. Le large premier hypural s'articule sur la vertèbre urale I mais son extrémité proximale est assez fine. Le troisième hypural est large et le quatrième étroit. Seule l'extrémité proximale du cinquième hypural est visible. Un éventuel sixième hypural n'est pas observable mais pourrait être caché sous les bases des lépidotriches caudaux. Il n'y a pas d'espace entre les deuxième et troisième hypuraux.

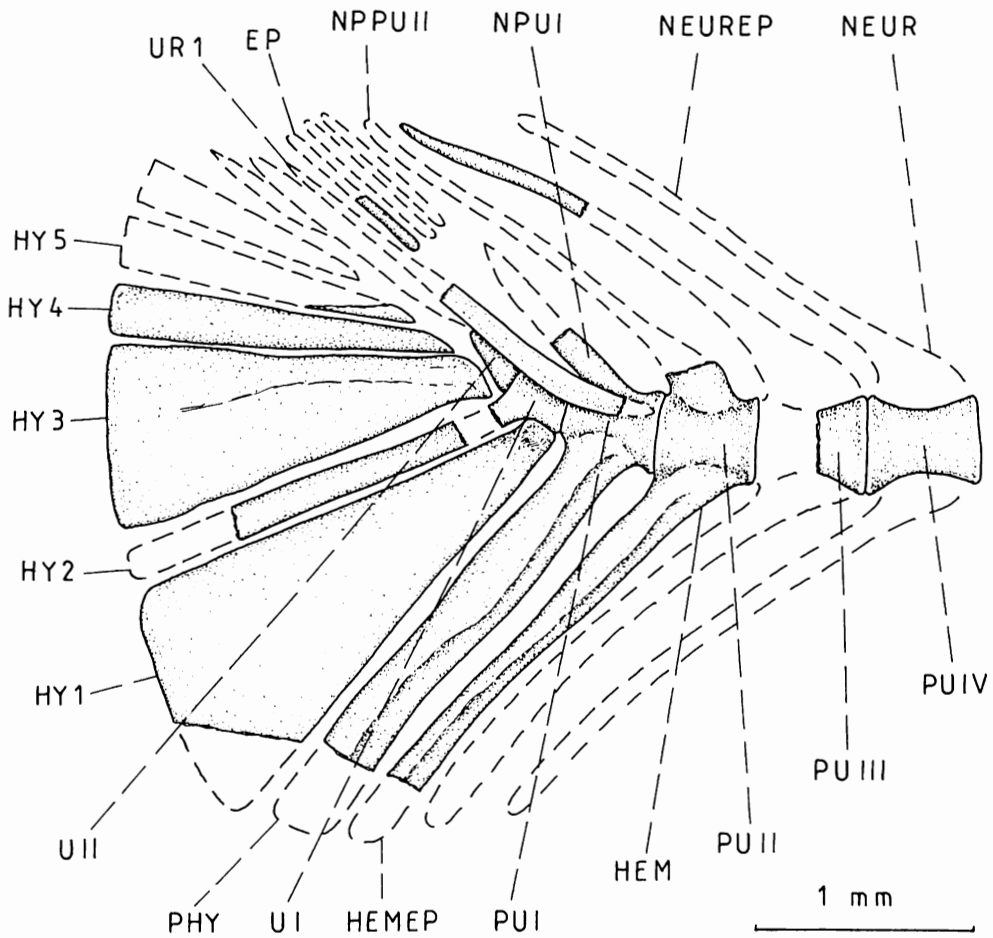

Fig. 6. – Le squelette caudal d'*Eoknightia caheni*, d'après l'holotype R. G. N° 11.129.

La queue est bifide. On ne peut guère en compter les rayons. Il y avait sans doute 19 rayons principaux dont 17 branchus comme chez la plupart des Clupéomorphes.

Les écailles sont grandes et couvertes de *circuli* légèrement arqués mais à disposition générale plus ou moins verticale. La serrature ventrale est complète depuis l'isthme de la gorge jusqu'à la région anale. Les grandes écailles qui la composent ont une densité nettement moindre que chez «*Diplomystus*» *dartevellei*. La serrature dorsale est incomplète-

ment conservée. L'une des écailles antérieures est clairement visible. Elle est ovale et porte une carène médiane dont la pointe dépasse de l'écaille proprement dite. Juste devant la nageoire dorsale, les écailles de la serrature deviennent plus larges et plus longues.

Ostéologie de *Nolfia kwangoensis* (Fig. 1C, 7)

Nolfia kwangoensis est représenté uniquement par les deux faces de l'holotype. Il s'agit d'un exemplaire long d'une vingtaine de millimètres et auquel manquent la tête et le début du corps. Ce corps est moyennement élevé, avec un abdomen arrondi mais sans hypertrophie.

La partie conservée du squelette axial comporte 35 vertèbres dont 18 caudales, y compris les centres uraux I et II. Les premières vertèbres abdominales font défaut. Les arcs neuraux et les neurépines sont bien développés tout au long du squelette axial. Les premières vertèbres abdominales conservées possèdent de petites hémapophyses sur lesquelles s'articulent de longues côtes. Les dernières vertèbres abdominales montrent des arcs hémaux prolongés par des hémépines qui supportent des côtes plus courtes. Les vertèbres caudales sont garnies d'arcs hémaux et d'hémépines normaux. Il y a des épineuraux tout au long du squelette axial et quelques épipleuraux associés aux premières vertèbres caudales.

Les nageoires pectorales ne sont pas conservées. Les nageoires pelviennes sont bien développées et leur origine se situe légèrement en avant de celle de la nageoire dorsale. Cette dernière est haute mais à base courte. La nageoire dorsale débute par 1 ou 2 petits rayons épineux courts et compte 11 grands rayons segmentés. Les premiers de ces rayons sont très allongés. Le premier ptérygophore dorsal est très long et composé de deux branches, l'une antérieure large mais plus courte, l'autre postérieure plus fine mais plus allongée. La nageoire anale occupe une position reculée sur le corps, près de la queue. Elle débute par 1 ou 2 petits rayons épineux et se poursuit par près de 20 rayons segmentés. Les quatorze premiers rayons segmentés anaux sont bien conservés. Les suivants sont disloqués et l'on ne peut guère les compter de façon précise. Il est sûr cependant que leur nombre ne dépassait pas vingt.

Le squelette caudal est plus évolué que chez «*Diplomystus*» *dartevellei* et *Eoknightia caheni*. Les vertèbres préurale I, urale I et urale II sont indépendantes les unes des autres mais le centre ural I est très réduit par rapport à la vertèbre préurale I. La neurépine préurale II est complète. L'arc neural préural I est très allongé et son sommet atteint le niveau des trois quarts de la longueur de la neurépine précédante. Le large parhypural est articulé mais pas soudé à la vertèbre préurale I. Le premier hypural est large mais est dépourvu de tête articulaire et d'articulation avec le centre ural I. Le deuxième hypural est étroit et soudé au petit centre ural I. L'extrémité proximale du troisième hypural est visible derrière le minuscule centre ural II. Les autres hypuraux ne sont pas conservés. Il y a deux épuraux qui ont laissé des traces très fragmentaires. On trouve trois paires d'uroneuraux. La première de ces paires est soudée en un pleurostyle à la vertèbre préurale I. Le deuxième uroneural atteint vers l'avant le niveau du bord arrière de la vertèbre urale I. Le troisième uroneural est réduit et rejeté entre les bases des lépidotriches caudaux.

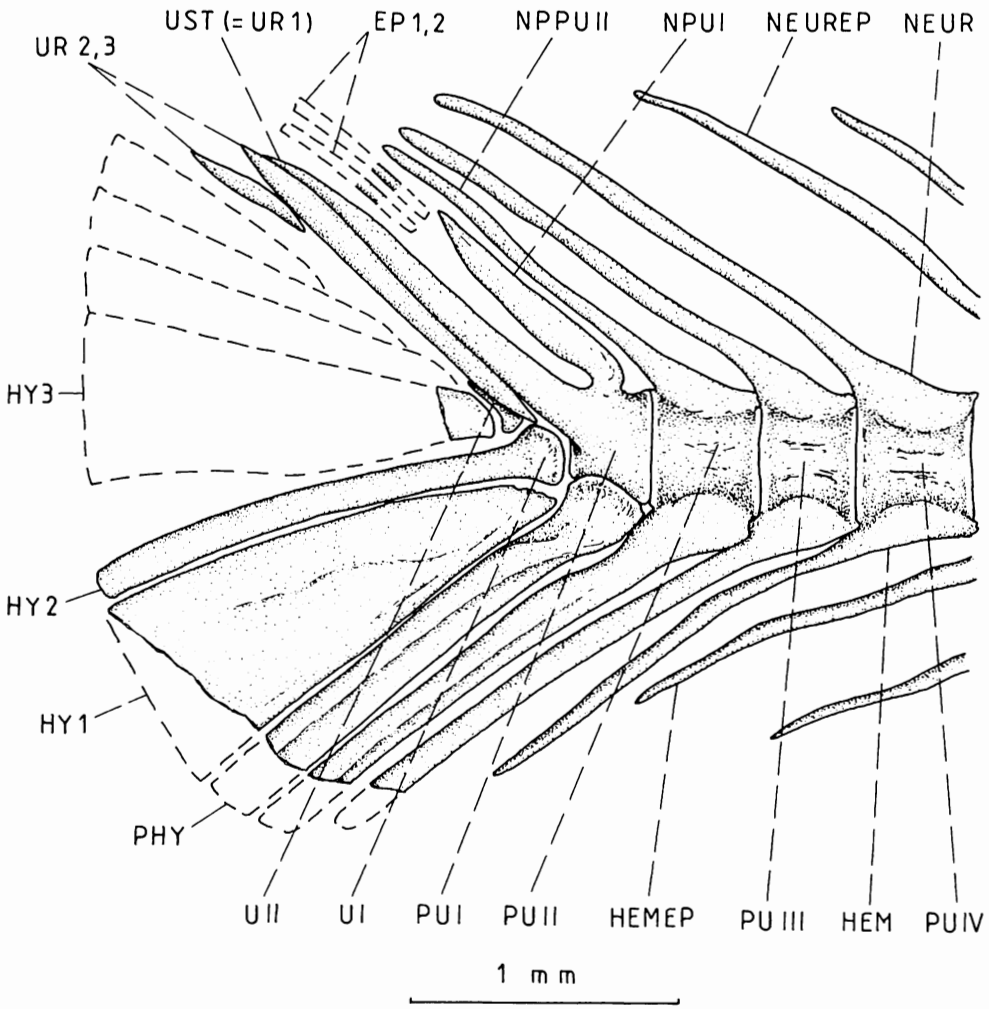

Fig. 7. – Le squelette caudal de *Nolfia kwangoensis*, d'après l'holotype R. G. N° 10.978.

La queue est bifide mais trop abimée pour dénombrer les rayons caudaux. Il y en avait très probablement 19 principaux dont 17 branchus, comme chez la plupart des Clupéomorphes.

Les écailles sont grandes et ornées de *circuli* à disposition quasi verticale. L'éventuelle serrature dorsale n'est pas conservée. La serrature ventrale est complète et s'étend jusqu'à la nageoire anale. Il y a à peu près une écaille de cette serrature par paire de côtes.

DISCUSSION

Position systématique de «*Diplomystus*» *dartevellei*

La serrature dorsale de «*Diplomystus*» *dartevellei* ne comporte pas les très nombreuses petites écailles subrectangulaires et à bord postérieur denticulé par lesquelles GRANDE (1982a) a redéfini *Diplomystus*. Il est donc clair que l'espèce de Kipala n'appartient pas à ce genre ni d'ailleurs à l'ordre des Ellimmichthyiformes puisque toutes les formes qui le composent montrent une serrature dorsale faite d'un grand nombre de petites écailles subrectangulaires (GRANDE, 1982a: 5, 22).

Par ailleurs, le poisson de Kipala partage avec les Ellimmichthyiformes et les Clupéomorphes plus évolués deux apomorphies: la serrature dorsale complète entre la nageoire dorsale et le crâne ainsi que la présence d'une fenêtre temporale entre le frontal, le pariétal et le ptérotique (observations personnelles chez *Diplomystus dentatus*). *Armigatus brevissimus*, au contraire, n'offre encore qu'une serrature dorsale incomplète (GRANDE, 1982a: 4) et est dépourvu de fenêtre temporale (PATTERSON, 1967: fig. 7). Notre espèce est donc apomorphe pour ces caractères par rapport à *Armigatus*.

D'autre part, la séparation du premier uroneural et de la vertèbre préurale I indique que «*Diplomystus*» *dartevellei* est plus primitif que les Clupeoidei (GRANDE, 1985: 258). L'absence de *recessus lateralis* en fait une forme plus primitive que les Clupéiformes et que *Santanaclupea silvasantosi* Maisey, 1993 de l'Albien du Brésil (GRANDE, 1985: 255; MAISEY, 1993: 9). Ses pariétaux jointifs indiquent qu'il est également plus primitif que *Spratticeps gaultinus* Patterson, 1970 de l'Albien d'Angleterre (PATTERSON, 1970: 163). La présence d'un fort processus basiptérygoïde sur son parasphénoïde confirme le fait qu'il est moins évolué que *Santanaclupea silvasantosi* et les Clupéiformes (GRANDE, 1982a: 8; MAISEY, 1993: 9).

Les quelques éléments exposés ci-avant situent «*Diplomystus*» *dartevellei* au même endroit que les Ellimmichthyiformes dans la phylogénie des Clupéomorphes, entre *Armigatus brevissimus* et *Spratticeps gaultinus*. Toutefois, cette dichotomie peut être aisément résolue. En effet, l'espèce zaïroise partage avec les Clupéomorphes plus évolués deux apomorphies, la perte des dents du parasphénoïde et celle des dents des os ptérygoïdes, qui font défaut chez *Armigatus brevissimus* et les Ellimmichthyiformes (PATTERSON, 1967: fig. 7; GRANDE, 1982a: fig. 6). Notre poisson représente donc le groupe-frère directement apomorphe des Ellimmichthyiformes.

Il convient encore de donner un nouveau statut générique à notre poisson puisqu'il n'appartient pas au genre *Diplomystus* et qu'il se différencie aussi des autres Ellimmichthyiformes ainsi que d'*Armigatus*:

Kwangoclupea nov. gen.

Derivatio nominis: de Kwango, province du Zaïre, et de *Clupea*, nom du genre-type de la famille des Clupeidae.

Espèce-type: *Kwangoclupea dartevellei* (Casier, 1965).

Diagnose: Petit Clupéomorphe archaïque. Crâne médio-pariétal. Commissure sensorielle extrascapulaire comprise dans les pariétaux mais pas dans le supraoccipital. Très forte crête supraoccipitale. Grand orbitosphénoïde en contact étroit avec l'ethmoïde latéral. Mâchoires dentées. Deux supramaxillaires. Articulation mandibulo-carrée située au niveau du bord antérieur de l'orbite. Fort processus basiptérygoïde du parasphénoïde. Os ptérygoïdes et parasphénoïde édentés. Fosse préépiotique présente mais petite. Fenêtre temporale présente. Angle très marqué entre les parties trabéculaire et parachordale du plancher neurocrânien. Operculaire haut et étroit. Les deux branches du préoperculaire bien développées et formant entre elles un angle droit. 32 vertèbres dont 13 ou 14 abdominales et 18 ou 19 caudales. 11 à 12 paires de côtes. Epineuraux et épipleuraux présents. 7 larges supraneuraux verticaux. Nageoire dorsale proche du crâne, débutant un peu en avant des pelviennes et comptant de 11 à 13 rayons segmentés. Nageoire anale longue, proche de la queue, comptant 27 à 29 rayons segmentés. Très large parhypural soudé à la vertèbre préurale I. Vertèbre urale I très développée et soudée au deuxième hypural. Premier hypural large, avec une forte tête articulaire pour la vertèbre urale I. Présence d'un espace entre les régions distales des deuxième et troisième hypuraux. Trois uroneuraux dont le premier autogène. Trois épuraux. Serrature dorsale complète entre la nageoire dorsale et le crâne, composée de quelques écailles plus ou moins triangulaires. Serrature ventrale complète, avec les écailles nombreuses et très serrées (deux écailles par paire de côtes). Corps court et élevé. Abdomen arrondi et hypertrophié.

Kwangoclupea dartevellei (CASIER, 1965)

Citations antérieures:

Diplomystus dartevellei n. sp. – *in*: CASIER (1965: 13).

Diplomystus dartevellei Casier, E., 1965 – *in*: TAVERNE (1976: 7).

Diagnose: Cf. celle du genre (genre monospécifique).

Position systématique d'*Eoknightia caheni*

Son premier uroneural autogène atteste qu'*Eoknightia caheni* est plus primitif que les Clupeoidei et son crâne médio-pariétal le situe en position plésiomorphe par rapport à *Spratticeps gaultinus*, à *Santanaclupea silvasantosi* et aux Clupéiformes.

Par contre, *Eoknightia caheni* est plus évolué qu'*Armigatus brevissimus*, les Ellimmichthyiformes et *Kwangoclupea dartevellei* par la perte du processus basiptérygoïde du parasphénoïde ainsi que par la légère réduction de la vertèbre urale I par rapport à la vertèbre préurale I.

Eoknightia caheni se situe donc entre *Kwangoclupea dartevellei* et *Spratticeps gaultinus* dans la phylogénie des Clupéomorphes.

Nous pouvons également améliorer la définition de notre poisson:

Eoknightia (TAVERNE, 1976)

Espèce-type: Eoknightia caheni (TAVERNE, 1976)

Diagnose émendée: Petit Clupéomorphe archaïque. Crâne médio-pariétal. Faible crête supraoccipitale. Mâchoires édentées. Deux supramaxillaires. Articulation mandibulo-carrée située au niveau du bord antérieur de l'orbite. Parasphénoïde dépourvu de processus basiptérygoïde. Os ptérygoïdes et parasphénoïde édentés. Angle marqué entre les parties trabéculaire et parachordale du plancher neurocrânien. Branches du préoperculaire très larges, avec la branche dorsale plus longue que la ventrale et les deux branches formant entre elles un angle obtus. Operculaire haut et très étroit. Environ 35 vertèbres. Nageoire dorsale débutant au premier quart de la longueur du dos, un peu en avant de l'origine des pelviennes et comptant environ 10 rayons segmentés. Nageoire anale reculée vers l'arrière du corps, près de la queue. Vertèbre urale I réduite par rapport à la vertèbre préurale I et soudée au deuxième hypural. Parhypural soudé à la vertèbre préurale I. Premier hypural large, à extrémité proximale étroite mais toujours articulée sur la vertèbre urale I. Premier uroneural autogène. Au moins un épural. Serrature dorsale complète, avec des écailles ovales, allongées et carénées derrière la tête et des écailles plus larges que longues près de la nageoire dorsale. Serrature ventrale complète, avec des écailles peu serrées les unes sur les autres (correspondance probable: une écaille par paire de côtes). Corps moyennement allongé et élevé. Dos assez plat. Abdomen arrondi mais sans hypertrophie.

Position systématique de *Nolfia kwangoensis*

Sa première paire d'uroneuraux soudée à la vertèbre préurale I en un pleurostyle, son parhypural articulé et non pas soudé à la vertèbre préurale I et sa vertèbre urale I très réduite font de *Nolfia kwangoensis* un indéniable représentant du sous-ordre des Clupeoidei (GRANDE, 1985: 258-259).

L'absence de la tête et du début du corps ne permet pas de pousser plus avant les investigations relatives à la position systématique de ce poisson qui doit donc être laissé Clupeoidei *incertae sedis*.

Remarquons aussi que *Nolfia kwangoensis* du Cénomanien devient ainsi le plus ancien représentant avéré du sous-ordre des Clupeoidei, une position occupée jusqu'ici par *Gasteroclupea branisai* Signeux, 1964 du Maastrichtien (fin du Crétacé supérieur) de Bolivie (PATTERSON, 1993: 628).

Phylogénie des Clupéomorphes

Les caractères de *Kwangoclupea* et d'*Eoknightia* permettent d'affiner notablement notre compréhension de la phylogénie des Clupéomorphes telle que GRANDE (1982a, b, 1985) et GRANDE et NELSON (1985) l'ont proposée. Cette phylogénie peut dorénavant être tracée de la manière exposée ci-après.

Erichalcis arcta et les autres Clupéomorphes partagent deux apomorphies:

(1) il y a une serrature ventrale faite d'au moins une mais généralement de nombreuses écailles impaires à processus latéraux ascendants.
(2) un diverticule vésical pair pénètre dans le neurocrâne par un orifice de l'exoccipital et se loge dans une bulle creusée dans le prootique.

Une troisième apomorphie est parfois invoquée: la capture par le pariétal d'une portion de la commissure sensorielle extrascapulaire (GRANDE, 1985: 253). En fait, il s'agit là d'un caractère spécialisé que les Clupéomorphes partagent avec les Ostariophysi dont ils sont très proches parents ainsi que l'ont révélé des recherches génétiques récentes (LE *et al.*, 1993; MÜLLER-SCHMID *et al.*, 1993). La signification de ce caractère dans la phylogénie des Téléostéens paraît d'ailleurs assez faible puisqu'on le retrouve aussi chez certains Ostéoglossomorphes et divers Eutéléostéens.

Erichalcis arcta offre quelques autapomorphies (FOREY, 1975):

(3) la perte des dents du parasphénoïde et de la série palato-ptérygoïdienne. Ces dents font défaut chez la plupart des Clupéomorphes mais existent chez *Armigatus* (PATTERSON, 1967: fig. 7) et les Ellimmichthyiformes (GRANDE, 1982a: fig. 6) qui sont pourtant plus évolués qu'*Erichalcis arcta*. La parcimonie implique donc que cette perte s'est réalisée indépendamment chez cette espèce.
(4) l'arc neural préural I a disparu et une expansion aliforme postérieure de l'arc neural préural II rejoint le stégural. Les Clupéomorphes possèdent, au contraire, presque toujours un arc neural préural I très développé.
(5) le sixième hypural manque. Cet os est généralement présent chez les Clupéomorphes.

Armigatus brevissimus et les Clupéomorphes plus évolués partagent de nouvelles synapomorphies:

(6) le parhypural se soude à la vertèbre préurale I (PATTERSON, 1967: fig. 8; TAVERNE, 1976: fig. 7; GRANDE, 1982a: fig. 10, 12, 17). Cette fusion disparaît chez les Clupeoidei.
(7) le deuxième hypural se soude à la vertèbre urale I (GRANDE, 1985: 254; etc.).
(8) la fosse préépiotique apparaît (PATTERSON, 1967: fig. 7, 1970: 176).
(9) un début de serrature dorsale se développe en avant de la nageoire dorsale, faite de quelques écailles subtriangulaires, mais n'atteint pas l'arrière du crâne (GRANDE, 1982a: 4).

Les Ellimmichthyiformes et les Clupéomorphes plus avancés montrent de nouvelles synapomorphies:

(10) la fenêtre temporale apparaît (observations personnelles chez *Diplomystus dentatus*).
(11) la serrature dorsale dorsale devient complète entre le crâne et la nageoire dorsale.

Les Ellimmichthyiformes qui comprennent les deux genres *Diplomystus* et *Ellimmichthys* Jordan, 1919, offrent une autapomorphie:

(12) les écailles de la serrature dorsale s'élargissent considérablement et deviennent subrectangulaires.

Kwangoclupea dartevellei et le reste des Clupéomorphes se montrent plus évolués par:

(13) la perte des dents du parasphénoïde.

(14) la perte des dents sur les os ptérygoïdes. Ce caractère connaît une réversion chez les Denticipitoidei où quelques dents sont connues sur l'entoptérygoïde (GREENWOOD, 1968: fig. 17) et dans de très rares cas chez les Clupeoidei (RIDEWOOD, 1904: 458).

Kwangoclupea dartevellei offre deux autapomorphies:

(15) l'orbitosphénoïde est très développé et situé derrière l'ethmoïde latéral avec lequel il entre en contact.

(16) la serrature ventrale est faite d'un grand nombre d'écailles très serrées les unes contre les autres (environ deux écailles par paire de côtes).

Eoknightia caheni et les autres Clupéomorphes présentent en plus:

(17) la perte du processus basiptérygoïde du parasphénoïde.

(18) une légère réduction de la vertèbre urale I par rapport à la vertèbre préurale I.

Spratticeps gaultinus et les Clupéomorphes plus évolués partagent d'autres synapomorphies:

(19) le crâne devient latéro-pariétal (PATTERSON, 1970: fig. 1)

(20) outre les pariétaux, la commissure sensorielle extrascapulaire passe aussi dans ou au-dessus du supraoccipital (PATTERSON, 1970: fig. 1).

Spratticeps gaultinus possède une autapomorphie:

(21) la fenêtre temporale est couverte par le frontal et le pariétal et s'ouvre plus postérieurement dans une petite fosse posttemporale (PATTERSON, 1970: fig. 2).

Santanaclupea silvasantosi et les espèces plus spécialisées montrent:

(22) un *recessus lateralis* (MAISEY, 1993: fig. 5).

(23) outre le prootique, le ptérotique abrite aussi, dans une cavité osseuse, un diverticule vésical intracrânien (MAISEY, 1993: 9).

(24) une fenêtre auditive entre le prootique, l'exoccipital et le basioccipital (MAISEY, 1993: fig. 5A).

Santanaclupea silvasantosi se caractérise aussi par quelques autapomorphies:

(25) la fenêtre temporale s'ouvre entre le frontal et le sphénotique (MAISEY, 1993: fig. 5). Normalement, la fenêtre temporale s'ouvre entre le frontal, le pariétal et parfois aussi le ptérotique mais n'intéresse pas le sphénotique (RIDEWOOD, 1904: fig. 118B, 122B, 126B, 130B, 133, 136b; TRACY, 1920: pl. 1, fig. 1; WOHLFAHRT, 1937: fig. 2; TAVERNE, 1977: fig. 4; GRANDE, 1985: fig. 31, 44; etc.).

(26) la perte de la serrature dorsale (MAISEY, 1993: fig. 7). Ce caractère se réalise à plusieurs reprises et de manière indépendante chez les Clupéomorphes.

Les Clupéiformes montrent une nouvelle synapomorphie:

(27) la perte du foramen béryciforme du cératohyal antérieur (GRANDE, 1985: 256-257).

Les Denticipitoidei se caractérisent par une grande quantité d'autapomorphies dont GREENWOOD (1968) donne le détail.

Les Clupeoidei, y compris *Nolfia kwangoensis*, présentent plusieurs autres synapomorphies:

(28) la ligne latérale n'est plus enclose dans des écailles, sauf parfois à son début (GRANDE, 1985: 259).

(29) la vertèbre urale I est très réduite par rapport à la vertèbre préurale I (GRANDE, 1985: 258-259).
(30) le parhypural n'est plus fusionné mais simplement articulé sur la vertèbre préurale I (GRANDE, 1985: 259-260).
(31) la première paire d'uroneuraux se fusionnent en un pleurostyle à la vertèbre préurale I (GRANDE, 1985: 258).
(32) le premier hypural perd son articulation avec la vertèbre urale I et se décroche légèrement de l'axe vertébral.

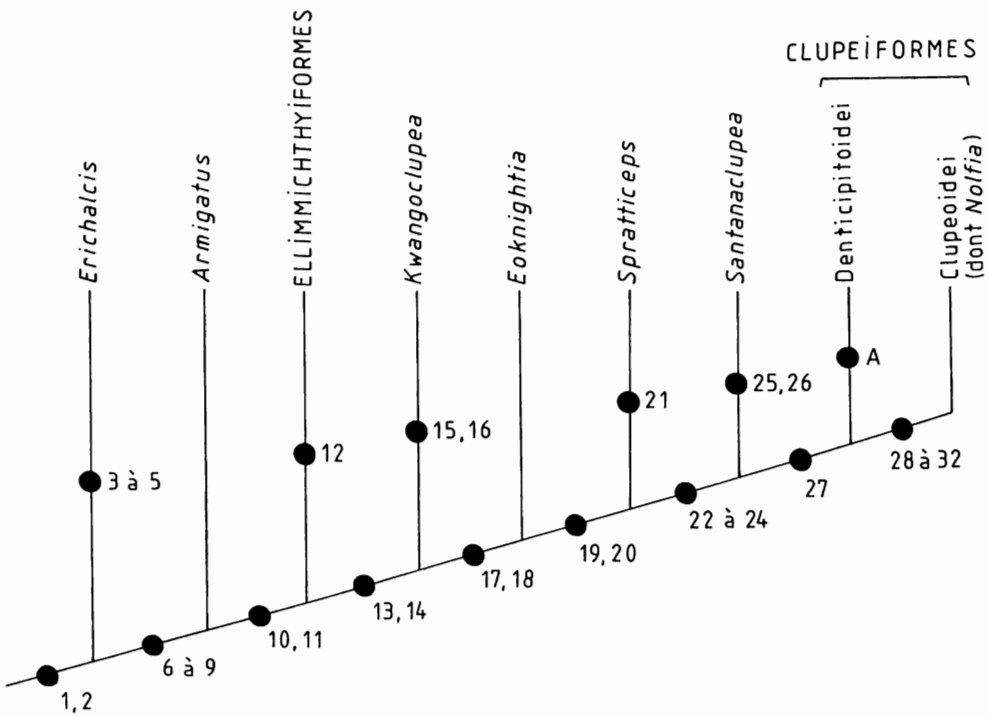

Fig. 8. – La phylogénie des Clupéomorphes, incluant les trois genres du Cénomanien de Kipala (Kwango, Zaïre). Les chiffres font référence aux apomorphies discutées dans le texte et la lettre «A» aux nombreux caractères spécialisés des Denticipitoidei tels qu'ils sont exposés dans GREENWOOD (1968).

Le cladogramme de la figure 8 résume la phylogénie des Clupéomorphes telle que ci-dessus exposée.

REMERCIEMENTS

Je tiens à dire ma gratitude au Dr. Luc Tack du Département de Géologie du Musée Royal de l'Afrique Centrale (Tervuren, Belgique) pour m'avoir permis de réétudier les Clupéomorphes fossiles

de Kipala. Le Prof. Dr. Michel Chardon de l'Université de Liège (Belgique) et le Dr. Mireille Gayet de l'Université de Lyon (France) ont bien voulu lire et commenter le présent article. Je les en remercie tous deux très vivement.

LISTE DES ABRÉVIATIONS DES FIGURES

AN + ART:	angulo-articulaire (= angulosplénio-articulaire)
BO:	basioccipital
BSPH :	basisphénoïde
C 1 à 10 :	côtes (de la 1ère à la 10^{e} paire)
DN (d., g.) :	dentaire (= dento-splénial, dentalo-splénial) (droit, gauche)
EC :	écailles (des serratures dorsale et ventrale)
ENPT:	entoptérygoïde (= endoptérygoïde, mésoptérygoïde)
EP 1, 2, 3:	épuraux
EPI:	épiotique (= épioccipital)
FR:	frontal
HEM:	arc hémal (= hémarcual)
HEMEP:	hémépine (= hémacanthe)
HY 1 à 5:	hypuraux
HYOM:	hyomandibulaire
IORB:	infraorbitaire
LETH:	ethmoïde latéral
METH:	mésethmoïde
MX (d., g.):	maxillaire (droit, gauche)
NEUR:	arc neural (= neurarcual)
NEUREP:	neurépine (= neuracanthe)
NPPUII:	neurépine préurale II
NPUI:	arc neural préural I
OP:	operculaire
OSPH:	orbitosphénoïde
PA:	pariétal
PHY:	parhypural
PMX:	prémaxillaire
POP:	préoperculaire
PS:	parasphénoïde
PSPH:	pleurosphénoïde (= ptérosphénoïde)
PTE:	ptérotique
PU I à V:	vertèbres préurales I à V
QU:	carré (= quadratique)
RART:	rétroarticulaire
SMX 1, 2:	supramaxillaires 1, 2
SN 1 à 7:	supraneuraux 1 à 7
SOC:	supraoccipital
SOP:	sous-operculaire
SPH:	sphénotique
SY:	symplectique
U I, II:	vertèbres urales I, II
UR 1, 2, 3:	uroneuraux 1, 2, 3
UST:	pleurostyle (= urostyle)
V:	corps vertébral
c. ex.:	commissure sensorielle extrascapulaire
c. m.:	canal sensoriel mandibulaire
c. pa.:	commissure sensorielle pariétale
c. pop.:	canal sensoriel préoperculaire
c. porb.:	canal sensoriel postorbitaire (=otique)
c. sorb.:	canal sensoriel supraorbitaire
f. p.:	fosse préépiotique
f. t.:	fenêtre (= fosse) temporale
p. b.:	processus basiptérygoïde du parasphénoïde

BIBLIOGRAPHIE

CASIER, E. (1965) – Poissons fossiles de la Série du Kwango (Congo). *Ann. Mus. Roy. Afr. Centr., Sci. Géol.*, Tervuren, **50**: 64 p.

CASIER, E. (1969) – Sur les conditions de dépôt de quelques-unes des Formations mésozoïques du Bassin du Congo. *Ann. Mus. Roy. Afr. Centr., Sci. Géol.*, Tervuren, **62**: 27-47.

FOREY, P. L. (1973) – A primitive Clupeomorph Fish from the Middle Cenomanian of Hakel, Lebanon. *Canad. Journ. Earth Sci.*, **10** (8): 1302-1318.

FOREY, P. L. (1975) – A fossil clupeomorph fish from the Albian of the Northwest Territories of Canada, with notes on cladistic relationships of clupeomorphs. *Journ. Zool.*, London, **175**: 151-177.

GRANDE, L. (1982a) – A Revision of the Fossil Genus *Diplomystus*, With Comments on the Interrelationships of Clupeomorph Fishes. *Amer. Mus. Novit.*, New York, **2728**: 1-38.

GRANDE, L. (1982b) – A Revision of the Fossil Genus *Knightia*, With a Description of a New Genus from the Green River Formation (Teleostei, Clupeidae). *Amer. Mus. Novit.*, New York, **2731**: 1-22.

GRANDE, L. (1985) – Recent and fossil clupeomorph fishes with materials for a revision of the subgroups of clupeoids. *Bull. Amer. Mus. Nat. Hist.*, New York, **181** (2): 231-372.

GRANDE, L. & NELSON, G. J. (1985) – Interrelationships of Fossil and Recent Anchovies (Teleostei, Engrauloidea) and Description of a New Species from the Miocene of Cyprus. *Amer. Mus. Novit.*, New York, **2826**: 1-16.

GREENWOOD, P. H. (1968) – The osteology and relationships of the Denticipitidae, a family of clupeomorph fishes. *Bull. Brit. Mus. (Nat. Hist.), Zool.*, London, **16** (6): 213-273.

GREENWOOD, P. H., D. E. ROSEN, S. H. WEITZMAN & G. S. MYERS (1966) – Phyletic studies of teleostean fishes, with a provisional classification of living forms. *Bull. Amer. Mus. Nat. Hist.*, New York, **131**(4): 339-456.

GREKOFF, N. (1960) – Ostracodes du Bassin du Congo. II Crétacé. *Ann. Mus. Roy. Congo Belge, Sci. Géol.*, Tervuren, **35**: 70 p.

LE, H.L.V., G. LECOINTRE, & R. PERASSO (1993) – A 28S rRNA-Based Phylogeny of Gnathostomes: First Steps in the Analysis of Conflict and Congruence with Morphologically Based Cladograms. *Molec. Phylog. Evol.*, **2** (1): 31-51.

LEPERSONNE J. (1977) – Structure géologique du bassin intérieur du Zaïre. *Acad. Roy. Belg., Bull. Cl. Sci.*, Bruxelles, 5e sér., **63** (12): 941-965.

MAISEY, J. G. (1993) – A New Clupeomorph Fish from the Santana Formation (Albian) of NE Brazil. *Amer. Mus. Novit.*, New York, **3076**: 1-15.

MÜLLER-SCHMID, A., B. GANSS, Th. GORR & W. HOFFMANN (1993) – Molecular Analysis of Ependymins from the Cerebrospinal Fluid of the Orders Clupeiformes and Salmoniformes: No Indication for the Existence of an Euteleost Infradivision. *Journ. Molec. Evol.*, **36**: 578-585.

PATTERSON, C. (1967) – Are the teleosts a polyphyletic group?. In: *Coll. Intern. C. N. R. S.*, 163, *Problèmes actuels de Paléontologie (Evolution des Vertébrés), Paris, 6-11 juin 1966*, Edit. C. N. R. S., Paris: 93-109.

PATTERSON, C. (1970) – A clupeomorph fish from the Gault (Lower Cretaceous). *Zool. Journ. Linn. Soc.*, London, **49** (3): 161-182.

PATTERSON, C. (1993) – Osteichthyes: Teleostei. In: *The Fossil Record* 2. BENTON, M. J. (Ed.). Chapman & Hall, London: 621-656.

PICTET, F. J. (1858) – Description des poissons fossiles du terrain néocomien des Voirons. In: *Matér. Paléont. Suisse*, Libr. J. KESSMANN, Genève, sér. 2, **1**: 54 p.

RIDEWOOD, W. G. (1904) – On the Cranial Osteology of the Clupeoid Fishes. *Proceed. Zool. Soc.*, London, 1904, II, 29: 448-493.

TAVERNE, L. (1976) – Les téléostéens fossiles du Crétacé moyen de Kipala (Kwango, Zaïre). *Ann. Mus. Roy. Afr. Centr., Sci. Géol.*, Tervuren, **79**: 50 p.

TAVERNE, L. (1977) – Ostéologie de *Clupavus maroccanus* (Crétacé supérieur du Maroc) et considérations sur la position systématique et les relations des *Clupavidae* au sein de l'ordre des Clupéiformes *sensu stricto* (Pisces, Teleostei). *Geobios*, Lyon, **10** (5): 697-722.

TAVERNE, L. (sous presse) – Ostéologie et position systématique d'*Audenaerdia casieri*, téléostéen clupéomorphe (Pisces) du Santonien (Crétacé) de Vonso, Bas-Zaïre. *Mus. Roy. Afr. Centr., Dép. Géol., Rapp. Ann. 1996*, Tervuren.

TRACY, H. C. (1920) – The clupeoid cranium in its relation to the swimbladder diverticulum and the membranous labyrinth. *Journ. Morphol.*, **33**: 439-483.

Belg. J. Zool. - Volume 127 (1997) - issue 1 - pages 99-102 - Brussels 1997

SHORT NOTE

STATISTICAL COMMENTS ON A BIOMETRICAL STUDY

ROBBY STOKS

Evolutionary Biology Group, Department of Biology, University of Antwerp (RUCA), Groenenborgerlaan 171, 2020 Antwerpen and Laboratory for Animal Ecology, Department of Biology, University of Antwerp (UIA), Universiteitsplein 1, 2610 Wilrijk. e-mail: stoks@ruca.ua.ac.be

Key-words: Biometry, multicollinearity, type II-regression.

SKOUFAS *et al.* (1) presented biometrical data on Anthozoa. My concern is in the statistical analysis and interpretation of these data. Many statistical incorrectnesses will probably not lead to interpretation errors due to the robustness of the used techniques or to the strength of the analysed effects, others however certainly will do so. This study gives the opportunity to discuss a number of statistical errors of which some occur regularly in the literature.

SKOUFAS *et al.* (1) provide the first biometrical data on the gorgonian *Eunicella singularis*. There are several problems with the tests for normality in (1). The frequency distribution of for example S (Fig. 2 in [1]) shows significant skewness, although their test shows no deviation from normality. Probably this is due to the low power of their normality tests. One tends to accept normality and use normality-based methods when samples are small. Yet, with small samples many normality-based methods have limited value (2). The authors report a single t-test statistic for the normality test for the distribution. To the best of my knowledge there are no tests for normality using a single t-value. The preferred test for normality is the Shapiro-Wilks'W test because of its good power properties as compared to a wide range of alternative tests (3).

In addition to the dubious validity of the normality tests, the p-values are misinterpreted. The authors conclude from the non-significant t-values of the normality tests for variables H and S (1 : p. 87) that the corresponding distributions are respectively not normal and normal (1 : p. 90). On the other hand it is rather strange that after acceptance of the normality of, for example the distribution of P.S., and while explicitly stating that the distributions are unimodal (1 : p. 85), the authors continue with the detection of several groups based on the «normal» frequency distribution of the character.

SKOUFAS *et al.* (1) correctly argued that a multiple regression procedure should be used to determine the relative contribution of the variables height/length (H/L), number of dichotomies (nb. dich.) and surface (S) in explaining the variance in dry weight (P.S.). It follows from the name «multiple regression» that there have to be linear relationships between each independent variable (i.c. H/L, nb. dich. and S) and the dependent variable (P.S.) (4). The relationship between H/L (S) and P.S. however is only linear in the log scale (Fig. 4A in [1]) while this transformation was not used in the multiple regression procedure. Furthermore, the dependent variable has to be normally distributed (3), which is not the case (see above). The authors report the F-statistic of the overall significance test of the multiple regression as 58.903 with 52 df. The shape of the F- distribution is however only fully determined by two values for degrees of freedom, in this case (k, n-k-1) with k the number of independent variables (i.c. 3), and n the number of observations (i.c. 55) (5). The correct significance test should therefore be based on F (3,51).

Finally, perhaps the most serious complication is the existence of correlations among the independent variables, the so-called multicollinearity problem (6). Multicollinearity implies that part of the variation in the dependent variable may be attributed to more than one independent variable (6) and therefore one can not exactly determine the unique contribution of each independent variable to the variance of P.S. (the goal of the multiple regression in this study). Multicollinearity is severe when independent variables are more related to each other than they are to the dependent variable (7). Statistically this means that the coefficient of determination of the regression when the ith independent variable is regressed against all other independent variables (r^2_i) is greater than the coefficient of multiple determination for the total model (r^2_{tot}). A log transformation of the variables (to induce linear relationships between independent and dependent variables, see higher) would not solve the problem of multicollinearity. For example the r^2 of logS with only one of the two other independent variables (nb. dich.) is already 0.8 (see Fig. 5 in [1]). The value of r^2_i for logS will be even greater because it will also include the unique variance of logS explained by H/L. As a result r^2_i will almost certainly be greater than r^2_{tot} (model with untransformed data: $r^2_{tot}=0.72$) indicating severe multicollinearity. The problem of multicollinearity can be solved by combining independent variables into principal components or by using biased estimation methods such as ridge regression (6). In addition, there is another problem in the determination of the variance explained by the independent variables. To assess the fraction of variance explained by a single factor, one compares r^2_{tot} to r^2 for the model with all except the factor of interest: the difference (r^2_i) is the variance uniquely explained by that single factor (6). As a logical result the coefficient of determination of the total model should equal the sum of the r^2_is. The r-square for the total model they report is 0.72 while the sum of the r-squares associated with each independent variable sums to 1.86 (this is also theoretically impossible because > 1.00). This means that the given r-squares do not answer the purpose of the analysis, namely to show «de quelle manière interviennent les trois paramètres... dans la détermination de la variance de P.S.» (1). Therefore the explaining capacity of the independent variables will be smaller than reported.

The allometric relationships between the measured variables were determined with ordinary least squares linear regressions on log-transformed data (1, 8). However, when both variables are subject to measurement error, as is the case, a critical assumption of ordinary least squares regression has been violated and the estimates of slopes are biased (5, 9, for some examples of bias introduced in the context of allometry see 10). This is especially important if one attempts to compare scaling exponents with values expected under the null hypothesis of isometry. In such cases one should use type II regression (5, 9). In morphometric work logarithmically transformed variables are often employed, and their functional relationship should be estimated by the slope of the major axis of the bivariate sample (5). The differences between slopes estimated by both techniques decrease as the correlation coefficients increase (9). Therefore especially the slope of log H/L against log P.S. will be biased.

Even after ignoring the bias in the calculated scaling exponents, there are some problems with their interpretation. Isometry is specified by the ratio of the dimensions of the variables (9). Allometry is the departure from isometry. SKOUFAS *et al.* (1) found a scaling exponent of 0.7 between P.S. and S (after log transformation). Because this value is smaller than three, they conclude that there is a positive allometric relationship between both variables. The calculated scaling exponent should however be tested against the appropriate null hypothesis of isometry. The expected slope of a plot of log area versus log dry weight is $L^2/L^3=2/3$ (11) and not three. Therefore it is highly probable that the claimed positive allometric relationship is in fact a purely isometric one. Also the allometry of P.S. against H/L and nb. dich. against S is checked by comparing the scaling exponents at sight (and not statistically) with values generated by a wrong null hypothesis (respectively with a scaling exponent under isometry of three and two).

I would like to thank Thierry Backeljau, Luc De Bruyn and Stefan Van Dongen for useful discussions and an anonymous referee for comments on the manuscript. Wim Jacobs and Solange Goethals provided me with some key articles. The author is a Research Assistant of the Fund for Scientific Research – Flanders (Belgium FWO).

REFERENCES

1. SKOUFAS, G., M. POULICEK & C.CH. CHINTIROGLOU (1996) – Etude préliminaire de la biométrie d'*Eunicella singularis* (Esper, 1974) (Gorgonacea, Anthozoa) à la mer Egée. *Belg. J. Zool.*, **126** (2) : 85-92.
2. STEWART-OATEN, A. (1995) – Rules and judgements in statistics: three examples. Ecology, **76** (6) : 2001-2009.
3. STATSOFT (1994) – Statistica. Volume I: general conventions & statistics I. Statsoft, Tulsa.
4. MANLY, B.F.J. (1992) – The design and analysis of research studies. Cambridge University Press, Cambridge, 353 pp.
5. SOKAL, R.R. & F.J. ROHLF (1995) – Biometry. W.H. FREEMAN and Co., New York, 887 pp.
6. PHILIPPI, T.E. (1994) – Multiple regression: herbivory. In: SCHEINER, S.M. & GUREVITCH, J. (eds.) – *Design and analysis of ecological experiments*. Chapman and Hall, London: 183-210.
7. FREUND, R.J. and LITTELL, R.C. (1986) – SAS system for regression, 1986 Edition. SAS Institute Inc., Cary.

8. GOULD, S.J. (1966) – Allometry and size in ontogeny and phylogeny. *Biol. Rev.*, **41**: 587- 640.
9. LABARBERA, M. (1989) – Analyzing body size as a factor in ecology and evolution. *Annu. Rev. Ecol. Syst.*, **20** : 97-117.
10. GREENE, A.J. (1992) – Positive allometry is likely with mate choice, competitive display and other functions. *Anim. Behav.*, **43**: 170-172.
11. MCNEILL, A.R. (1971) – Size and shape. Arnold, London, 51 pp.

NEW GUIDE FOR AUTHORS

1. The Belgian Journal of Zoology publishes, in English or French, original papers and notes in all fields of zoology. Reviews on topics of general interest or current importance may be considered after invitation by or agreement with the editors. Manuscripts must contain significant new findings and must not have been published elsewhere nor be simultaneously under consideration by any other journal. Single-species descriptions will not be accepted unless they have broader relevance such as implications for phylogeny or biogeography. Papers submitted in French must include English translations of the title and of the abstract.
2. Members of the Society, as well as non-members benefit from a waiver of page charges up to 15 printed pages. This waiver is subject to annual consideration of the Council of the Society. Additional pages are charged to authors at cost price (1300 BEF per page, incl. illustrations). Authors will receive 50 reprints free of charge. To order additional reprints, the completed order form must be returned together with the galley proofs.
3. Each manuscript is reviewed by at least two referees, usually one Belgian and one non-Belgian referee. After acceptance, authors remain fully responsible for their article.
4. Authors are requested to follow rigorously the lay-out as shown in the articles in this issue, paying particularly attention to the format of references. Papers should be written in clear, concise language and consist of an abstract (summarising the essential results and conclusions), introduction, material and methods, results and discussion. Sections and sub-sections should not be numbered but authors may suggest a printing format to provide structure to the article. Author names in text citations should be in SMALL CAPITALS and in the following format: PERRIN & KOKKINN (1985) for two authors (with ampersand (&) and not «and» as previously used) or WILSON *et al.* (1987) for more than two authors. Consecutive references must be separated by a semicolon (;). Figures in the text are referred to by «Fig. n» or «Figs n-m». Names of species (and names of higher taxa in axonomic papers) should be followed, on the first occasion of use, by the name of the author who described the species or introduced the taxon name (in lower case) and the year. Latin expressions (*species names*, *e.g.*, *et al.* etc.) should be in italics.
5. Short notes not exceeding 4 printed pages (incl. figures) with new findings of temporary importance, comments on papers published in the journal, new records for (*e.g.*) the Belgian fauna, curiosa, etc. will be published in the next issue whenever possible. They should be written as continuous text without the various divisions of regular papers. References for Notes must be indicated in the text by numbers and listed and numbered in the order of their appearance in the text. Short notes will be reviewed as normal papers. Reviews of books of interest to the members (max. 1 p.) are welcome.
6. All parts of the manuscript including text, references, tables and legends for illustrations should be type-written, double spaced (on one side of the page only) and all pages numbered. Figures, tables and legends should remain separated from the text. Scale bars should be drawn on figures where appropriate and size indicated in the legend. Three copies of text and three quality copies of figures (not exceeding the journal page size must be provided. In addition, authors are requested to provide a computer diskette with the manuscript (in WP, MSWord or RTF file, DOS or Macintosh) to allow electronic transmission with referees and authors. Please indicate on the manuscript the author e mail address for correspondence where available). Whenever possible, authors are asked to also include on the diskette(s) computer generated or scanned figures and photographs (as PICT or TIFF files with an indication of the program and system used). Indicate on the hard copy where figures and tables are to be inserted, and provide a short running title and keywords (separated by commas).
7. Following acceptance of the manuscript, authors must provide the originals of the figures together with the final version of the text. Photographs should be mounted and clearly labelled. Hand made drawing should be in black ink (clearly readable after reduction). All figures should be labelled in pencil on the reverse side with the number of the figure, the name of the author(s), title of the paper, number of the MS and intended degree of reduction. Photocopies of photographs or figures are not acceptable.

The royal Belgian zoological Society organizes meetings by invitation of the members.
The contribution for members is 800 BEF. annually. For members living outside Belgium, the contribution is 900 BEF. Belgian students benifit from a contribution of 300 BEF. (foreign students, 400 BEF.). Familial contributions, comprising one subscription to the journal, are 900 BEF. Members receive the journal (two issues per year, resp. in June and December and the occasional special issues) free of charge.

The price for one volume (two issues) is 1.500 BEF.

C.C.P. 000-0049113-31, Société Royale Zoologique de Belgique, Bruxelles.

P.R. 000-0049113-31, Koninklijke Belgische Vereniging voor Dierkunde, Brussel

Requests for exchange and other library matter: Prof. Dr. J. Delinge (library administrator), ULB-CP 160/11, Av. Roosevelt, 50, B-1050 Brussels (Belgium).

CONTENTS

The **BELGIAN JOURNAL OF ZOOLOGY** is covered in **Current Contents** and in Science Citation index.

ISSN: 0777-6276